

August 2014

A Decision Support System to Analyze, Predict, and Evaluate Solar Energy System Performance: PVSysCO (photovoltaic System Comparison)

Lisa Bosman
University of Wisconsin-Milwaukee

Follow this and additional works at: <https://dc.uwm.edu/etd>

 Part of the [Industrial Engineering Commons](#), [Natural Resource Economics Commons](#), and the [Oil, Gas, and Energy Commons](#)

Recommended Citation

Bosman, Lisa, "A Decision Support System to Analyze, Predict, and Evaluate Solar Energy System Performance: PVSysCO (photovoltaic System Comparison)" (2014). *Theses and Dissertations*. 666.
<https://dc.uwm.edu/etd/666>

This Dissertation is brought to you for free and open access by UWM Digital Commons. It has been accepted for inclusion in Theses and Dissertations by an authorized administrator of UWM Digital Commons. For more information, please contact open-access@uwm.edu.

A DECISION SUPPORT SYSTEM TO ANALYZE, PREDICT, AND EVALUATE
SOLAR ENERGY SYSTEM PERFORMANCE: PVSYS (PHOTOVOLTAIC
SYSTEM COMPARISON)

by

Lisa Bosman

A Dissertation Submitted in

Partial Fulfillment of the

Requirements for the Degree of

Doctor of Philosophy

in Engineering

at

The University of Wisconsin-Milwaukee

August 2014

ABSTRACT
A DECISION SUPPORT SYSTEM TO ANALYZE, PREDICT, AND EVALUATE
SOLAR ENERGY SYSTEM PERFORMANCE: PVSYS/CO (PHOTOVOLTAIC
SYSTEM COMPARISON)

by

Lisa Bosman

The University of Wisconsin-Milwaukee, 2014
Under the Supervision of Professor Wilkistar Otieno

In 2010, the U.S. Department of Energy announced the SunShot Initiative, which aims to reduce the total installation cost of solar technologies by 75% between 2010 and 2020. This implies that solar energy is a top priority in the U.S. and many other countries. The purpose of this dissertation research is focused on creating a model to better understand the performance and reliability of photovoltaic (PV) energy systems over time. The model will be used to analyze, predict, and evaluate the performance of PV systems, taking into consideration technological and geographical location attributes. The overall research goal is to build a “Solar Energy Blue Book,” conceptually similar to the Kelley Blue Book, which allows consumers to estimate the value of a used car. The Solar Energy Blue Book, a solar energy system evaluation tool, will allow consumers to estimate the value of a used solar energy system, taking into consideration many factors, such as latitude (which determines the quantity of incoming sunlight) and zip code (which determines the approximate cost of electricity). The Solar Blue Book will allow potential solar energy system consumers the opportunity to understand the return on investment for new and in particular, used solar energy systems.

© Copyright by Lisa Bosman, 2014
All Rights Reserved

DEDICATION

To my family, for always keeping me grounded.

TABLE OF CONTENTS

Chapter 1 1

 1.0 Background on Solar Energy 1

 1.1 Research Motivation 3

 1.2 Research Plan 4

Chapter 2 7

 2.0 Introduction to Performance and Evaluation Models 7

 2.1 Literature Review 7

 2.1.1 5-Parameter Array Performance Model 7

 2.1.2 Sandia Array Performance Model 9

 2.1.3 Sandia Inverter Performance Model 9

 2.1.4 PV Watts 10

 2.1.5 Solar Estimate 11

 2.1.6 PV Value 12

 2.1.7 Solar Advisor Model 14

 2.1.8 RETScreen Photovoltaic Project Model 15

 2.2 Proposed Contributions 17

 2.2.1 System Configuration 18

 2.2.2 Monthly Derate Factor 22

 2.2.3 Annual Degradation by Component 23

2.2.4 PV Module Specific Characteristics	23
2.2.5 Albedo Coefficient.....	26
2.2.6 Inverter Selection.....	27
2.2.7 Multiple PV Comparison	30
2.2.8 Differing Valuation Techniques	30
Chapter 3.....	31
3.0 Introduction to Factors Affecting Return on Investment.....	31
3.1 PV Array	31
3.1.1 Sun Tracking.....	31
3.1.2 Module Specific Information.....	47
3.2 DC and AC Wiring Losses	61
3.2.1 Wiring Considerations	62
3.2.2 Insulation Resistance Testing	63
3.3 DC-AC Inverter	64
3.4.1 Inverter Specific Information.....	64
3.4.2 Inverter Efficiency	65
3.4.3 Inverter Warranty.....	67
3.4 Utility Grid Availability.....	68
3.5 System Costs.....	69
3.5.1 PV Modules	70

3.5.2 Balance of System.....	72
3.6 Grid-Tied Electricity Rates	72
3.7 U.S. Federal and State Incentives for Investing in PV System.....	76
Chapter 4.....	80
4.0 Introduction to Data Collection	80
4.1 Motivation for U.S. Midwest	80
4.2 Argonne National Laboratory’s Midwest PV Analysis Facility.....	82
4.2.1 Solar Modules	83
4.2.2 Inverter	85
4.2.3 Weather Stations	86
4.2.4 Monitoring, Data Collection, and Data Processing	87
4.3 College of Menominee Nation’s Solar Initiative	88
4.3.1 Solar Modules	89
4.3.2 Inverter	90
4.3.3 Weather Stations	91
4.3.4 Monitoring, Data Collection, and Data Processing	92
Chapter 5.....	94
5.0 Introduction to PVSysCo	94
5.1 Input	95
5.1.1 System Characteristics	95

5.1.2 Irradiance and Weather Data Files.....	95
5.2 Processing	97
5.2.1 Sun Position	97
5.2.2 Module Irradiance	97
5.2.3 Module Temperature.....	101
5.2.4 Module Performance.....	103
5.2.5 System Degradation	111
5.2.6 System Derate	113
5.2.7 System Performance	115
5.3 Output	115
5.3.1 Module Irradiance	115
5.3.2 Derate Values.....	116
5.3.3 AC Energy Value.....	116
5.3.4 Hourly Expectations.....	116
5.3.5 Valuation.....	116
5.3.6 Comparison	118
5.4 Feedback	118
5.4.1 Verification	118
5.5 Novel PVSysCo Decision Support System.....	119
Chapter 6.....	126

6.0 Conclusion	126
6.1 Contributions.....	126
6.1.1 Contribution 1: System Configuration.....	128
6.1.2 Contribution 2: Monthly Derate Factor	128
6.1.3 Contribution 3: Annual Degradation by Component.....	129
6.1.4 Contribution 4: PV Module Specific Characteristics.....	129
6.1.5 Contribution 5: Albedo Coefficient	131
6.1.6 Contribution 6: Inverter Selection	131
6.1.7 Contribution 7: Comparison	132
6.1.8 Contribution 8: Differing Valuation Techniques.....	132
6.2 Assumptions and Limitations of Research	133
6.3 Future Research	134
Chapter 7.....	135
7.0 References.....	135

LIST OF FIGURES

Figure 1: History of Best Research Cell Efficiencies	2
Figure 2: High Level Solar Energy System Performance I-P-O Model	5
Figure 3: Equivalent circuit for 5-Parameter model (DeSoto, Klein et al. 2006).....	9
Figure 4: PV Watts System Info	10
Figure 5: Solar Estimate sample output	12
Figure 6: PV Value example of input	13
Figure 7: System Advisor Model report generator	15
Figure 8: RETScreen Five Step Standard Analysis	16
Figure 9: Example of Off-Grid DC Direct PV Systems (U.S. Department of Energy: Energy Efficiency & Renewable Energy Last Updated 06/18/2013).....	18
Figure 10: Example of Off-Grid DC Direct with Battery PV Systems (U.S. Department of Energy: Energy Efficiency & Renewable Energy Last Updated 06/18/2013)	19
Figure 11: Example of Off-Grid AC PV Systems (U.S. Department of Energy: Energy Efficiency & Renewable Energy Last Updated 06/18/2013)	20
Figure 12: Grid-Direct System (U.S. Department of Energy: Energy Efficiency & Renewable Energy Last Updated 06/18/2013)	21
Figure 13: Major PV Technologies.....	24
Figure 14: Comparison of Flat Panel to Cylindrical Tubes (Koshel, Smestad et al. 2012)	26
Figure 15: String Inverter vs Microinverter (Enecsys Micro Inverters Retrieved 06/28/2013).....	29

Figure 16: Quantity of Daylight as Function of Month and Earth’s Rotation (solarenergyfallacies.com Retrieved 06/28/2013)	32
Figure 17: Solar Irradiation through the World (solarenergyfallacies.com Retrieved 06/28/2013).....	33
Figure 18: Example of PV Array in Northern Hemisphere	34
Figure 19: Recommended PV Array Tilt for Roof Pitch.....	34
Figure 20: Optimal PV Array Tilt Angle (RS Components 2005)	35
Figure 21: Recommended PV Array Tilt for Green Alchemy Solar Power Farm (Green Alchemy Retrieved 07/06/2013).....	35
Figure 22: Solar Radiation on Tilted Surface (Honsberg and Bowden Obtained 01/21/2014).....	36
Figure 23: Green Outline of First Triangle Calculation.....	36
Figure 24: Green Outline of Second Triangle Calculation	37
Figure 25: Examples of Single-Axis and Dual-Axis PV Array Tracking Designs (Juda 2013)	39
Figure 26: Comparison of Fixed and Tracked PV Arrays (Home Power 2013)	40
Figure 27: Wattsun AZ-225 Solar Tracker for 12 Kyocera 200 Modules (Infinigi Infinite Energy Solutions 2013).....	41
Figure 28: Shading Site Assessment Tools.....	43
Figure 29: Solar Pathfinder Example.....	44
Figure 30: Examples of Different Types of Mounting Options.....	45
Figure 31: Typical Testing Sequence for Crystalline Silicon Modules (Osterwald and McMahon 2009).....	48

Figure 32: Typical information required for a PV module nameplate label.....	51
Figure 33: Typical Manufacturer's Technical Datasheet (Hren 2011)	52
Figure 34: Module Technical Datasheet Aleo 225W (Aleo Solar AG 2011).....	57
Figure 35: Aleo 225W PV Module I-V Curve.....	58
Figure 36: Example portraying the influence of temperature on the I-V curve.....	58
Figure 37: Example results for change in temperature	60
Figure 38: Example Warranty Degradation Derate Factors	61
Figure 39: Series vs Parallel (Schwartz 2002).....	63
Figure 40: Megger Megohmmeter	64
Figure 41: Centralized Inverter vs Micro inverter (CPS Solar Retrieved 07/01/14)	65
Figure 42: Example String Inverter Specification Data Sheet (PV Powered 2009)	66
Figure 43: Typical PV System Costs (Schwartz, Woofenden et al. 2013).....	70
Figure 44: Solar Module Price Trends 2007-2013 (SNE Research 2009).....	71
Figure 45: Cost breakdown of conventional U.S. PV system (Browning 2011).....	72
Figure 46: Net-metering vs. Feed-in tariffs (Austech Forums Jan 2008).....	73
Figure 47: Example Time-of-Use Rate Strategy (Bartholomew County REMC Obtained 07/01/2013).....	74
Figure 48: Visual Illustration Depicting Tiered Electricity Rate Plans	75
Figure 49: U.S. Net Metering Policies.....	76
Figure 50: U.S. Grant Programs for Renewable Energy	77
Figure 51: U.S. Property Tax Credits for Renewable Energy	77
Figure 52: U.S. Sales Tax Incentives for Renewable Energy.....	78
Figure 53: U.S. Rebate Programs for Renewable Energy	78

Figure 54: U.S. Tax Credits for Renewable Energy	79
Figure 55: U.S. Loan Programs for Renewable Energy http://www.dsireusa.org/	79
Figure 56: Photovoltaic Solar Resources of the United States	82
Figure 57: Midwest PV Analysis Facility.....	83
Figure 58: Five different Solar Modules at the Midwest PV Analysis Facility.....	84
Figure 59: SMA’s Sunny Boy 5000-US DC-to-AC Inverter.....	85
Figure 60: WeatherHawk 520 Weather Station	86
Figure 61: Apogee Instruments SP-110 Pyranometer Sensor.....	87
Figure 62: Two different PV technologies within CMN’s Solar Initiative	90
Figure 63: Enphase M215 Microinverter.....	91
Figure 64: SMA Sunny SensorBox.....	91
Figure 65: Enphase communication and monitoring	92
Figure 66: SMA weather communication and monitoring	93
Figure 67: Solar Energy System Performance I-P-O Model	94
Figure 68: Cylindrical Panel Characteristics (Koshel, Smestad et al. 2012).....	107
Figure 69: PVSysCo Example Screen 1 of 2	120
Figure 70: PVSysCo Example Screen 2 of 2	121

LIST OF TABLES

Table 1: Literature Review for PV Performance and Evaluation Tools.....	8
Table 2: Limitations of current PV performance and evaluation tools.....	17
Table 3: Components vs Configurations.....	22
Table 4: Albedo Coefficient Values (Mermoud and Wittmer 2014).....	27
Table 5: Comparison of Solar Evaluation Tools (Duluk, Nelson et al. 2013).....	42
Table 6: Sample list of modules and attributes.....	53
Table 7: Typical Module Efficiencies.....	54
Table 8: Example Inverter Warranties.....	67
Table 9: Comparative Data Sheet Information for Five Different Solar Modules.....	84
Table 10: MPAF Data Collection Devices.....	88
Table 11: Comparative Data Sheet Information for CMN’s Solar Initiative.....	90
Table 12: CMN’s Solar Initiative Communication and Monitoring Devices.....	92
Table 13: List of TMY2 Data Parameters.....	96
Table 14: Albedo values.....	99
Table 15: Perez f coefficients.....	101
Table 16: Parameters associated with each module temperature model.....	102
Table 17: Module Temperature (Actual versus Model) Results of Pearson Correlation.....	103
Table 18: Coefficients for NREL 3-Parameter Model.....	103
Table 19: Crystalline Silicon Flat-Plate Panels: Expected vs Actual Power.....	105
Table 20: Thin-Film Flat-Plate Panels: Expected vs Actual Power.....	106
Table 21: CIGS Cylindrical Panel: Expected vs Actual Power.....	111
Table 22: Results of comparing actual to predicted for Days 1-50.....	122

Table 23: Data comparison for Days 1-25	124
Table 24: Data comparison for Days 26-50	125
Table 25: Limitations of current PV performance and evaluation tools.....	127

ACKNOWLEDGEMENTS

I wish to thank my major advisor, Dr. Wilkistar Otieno, and committee members, Dr. Seth Darling, Dr. Vishnu Nanduri, Dr. Hamid Seifoddini, and Dr. Chris Yuan, for their expertise, continued guidance, reading over drafts, challenging my ideas, making suggestions, and providing moral support.

Chapter 1

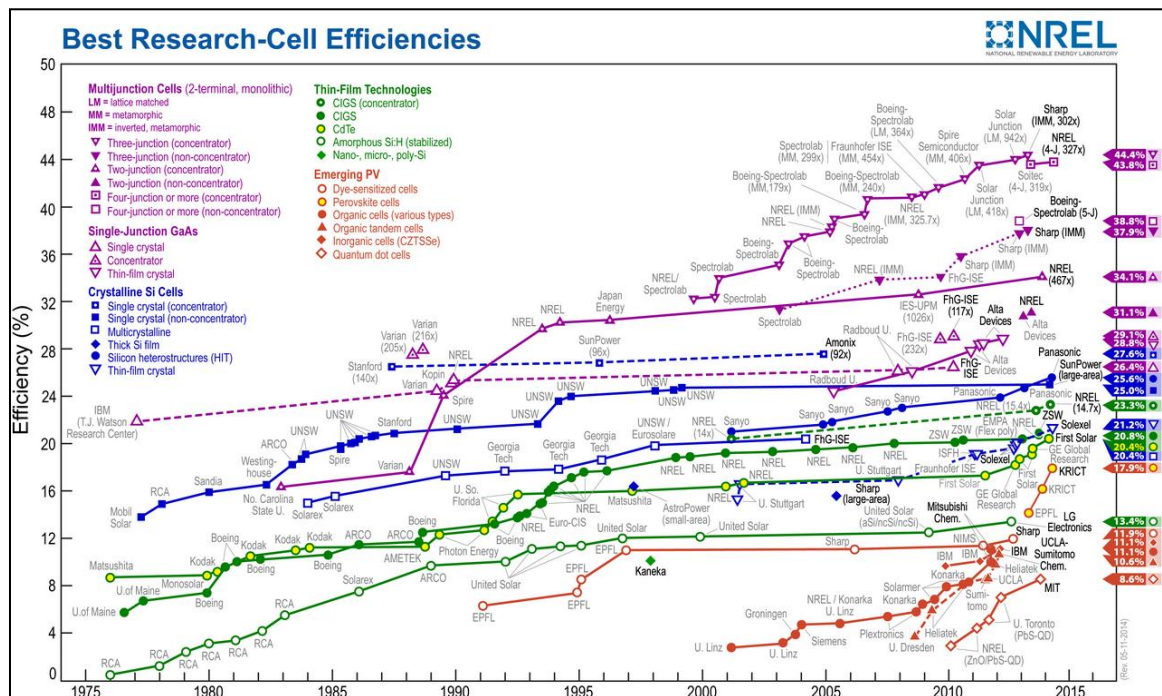
1.0 Background on Solar Energy

Dependency upon energy resources (primarily non-renewable energy sources) has created challenges related to climate change, wars over energy supplies, famine, poverty, and cycles of deforestation concerns (Bradford 2006). As populations increase and economic development progresses, energy demand grows, and ultimately the scalability of the problems associated with non-renewable energy resources. In response to the viable potential of renewable energy, the U.S. government has invested millions of dollars into the research and development of renewable energy technologies.

In 2011, nine percent of the total U.S. energy consumption was sourced by renewable energy, and within the category of renewable energy, only about 1% was contributed by solar energy (U.S. Energy Information Administration 2012). However, as an emerging technology, from 2005 to 2011, solar energy consumption has increased over 80%. Furthermore, solar energy consumption is projected to increase an additional 14% between 2012 and 2013. Solar energy is the fastest growing renewable energy technology estimated as a \$6 billion industry in the 2010 U.S. market, an increase from \$3.6 billion in 2009 (U.S. Energy Information Administration 2011). In 2010, the U.S. Department of Energy announced the SunShot Initiative, which aims to reduce the total installed cost of solar technologies by 75% between 2010 and 2020. This implies that solar energy is a top priority in the U.S. and many other countries, and in particular, the race to maximize efficiency of solar energy systems.

The photovoltaic effect was discovered by Edmond Becquerel in 1839. Since then, research has come a long way. Figure 1 provides the best research cell efficiencies of the past 40 years, with solar cell materials categorized as multi-junction concentrators, crystalline silicon cells, thin-film and emerging PV. This chart was last updated 5-11-2014 and is updated regularly by the National Renewable Energy Laboratory.

Figure 1: History of Best Research Cell Efficiencies



The proposed research aims to further develop solar energy initiatives through improved understanding of performance and reliability of solar modules. Since the lifetime of most solar modules is above 20 years, solar module degradation is used as a surrogate for modeling solar module reliability, with performance measurements focused on degradation due to the attendant failure mechanisms. Moreover, there remains a surprising dearth of relative performance data for different photovoltaic technologies

under real-world conditions, making technology selection decisions—and therefore actual market penetration—a serious challenge.

1.1 Research Motivation

The dissertation research is focused on creating a model to better understand the performance of photovoltaic (PV) energy systems over time. The model will be used to predict the performance of PV systems, taking into consideration common performance loss issues such as PV module specific characteristics, temperature coefficient, shading, inverter performance, and general degradation effects. The overall research goal is to build a “Solar Energy Blue Book,” conceptually similar to the Kelley Blue Book, which allows consumers to estimate the value of new and used cars. The Solar Energy Blue Book, a solar energy system evaluation tool, will allow consumers to estimate the value of a solar energy system, taking into consideration many factors. For example, amongst many other factors, location will be used to estimate the expected quantity of incoming solar irradiation; zip code will be used to estimate the approximate cost of electricity; and age and performance warranties will be used to estimate the degradation over time. The Solar Blue Book will allow potential solar energy system consumers the opportunity to understand the return on investment for new and, in particular, used solar energy systems.

This research is important to advancing knowledge and understanding within the academic field of solar energy system performance. Practically speaking, this research is important for providing manufacturers predictive capabilities for determining warranty offers, and is just as important for consumers to make educated choices about which types of solar modules are best for a specific application and geographical location. The

core of the research explores the potentially transformative concept of utilizing a solar energy research facility to investigate the climatic differences attributable specifically to the Midwest area. Working in collaboration with Argonne National Laboratory, the state-of-the-art solar energy research facility is already installed and the first known facility located within the Midwest area of the United States.

There are numerous solar energy testing facilities throughout the United States, such as National Renewable Energy Laboratory (Colorado), Solar Technology Acceleration Center (Colorado), Sandia National Laboratories (New Mexico), Solar Test and Research Center (Arizona), and Florida Solar Energy Center (Florida). Unfortunately, facilities representing the Midwest region of the United States are limited. Moreover, few if any of these facilities are outfitted with multiple module technologies for side-by-side comparison. Thus, a comparative study of different solar modules would be beneficial both to establish novel relative analyses and to explore the climatic and geographical effects and differences throughout the United States.

1.2 Research Plan

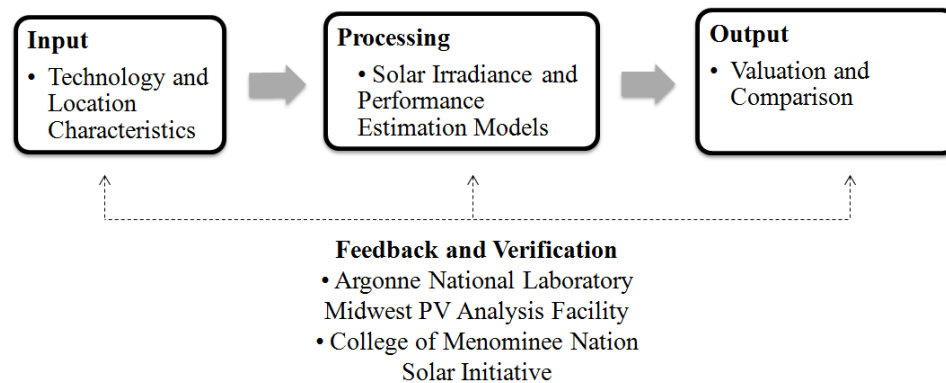
The research objectives are as follows:

1. Investigate the real-world performance of six types of commercial solar modules in order to establish a complete performance comparative analysis using live current-voltage data coupled with local meteorological data.
2. Develop a framework to model the production and efficiency of solar energy systems, to estimate the system performance at any given point in time, for new and in particular, used solar energy systems.

3. Develop a method to denoise and convert actual raw continuous PV system and weather data (e.g. incoming solar irradiation, temperature, generated DC electricity, inverter converted AC electricity) into useful performance metrics.
4. Verify the accuracy of the solar energy system performance model through comparison to real-time solar energy system performance data.

The development and verification of the solar energy system performance model will require several different sets of data. Figure 2 incorporates the systems perspective of the I-P-O model to show the high level data input, processing, output, as well as the continuously occurring feedback verification.

Figure 2: High Level Solar Energy System Performance I-P-O Model



Chapter 2 provides a background on current PV performance and evaluation models, clearly identifying the gaps in the current models, stating the contributions of this dissertation research, providing continued motivation for the research. Chapter 3 offers a literature review of factors affecting PV performance and return on investment, relaying the anticipated inputs and outputs into the I-P-O model. Chapter 4 describes the data collection process, applied through Argonne National Laboratory, used to provide feedback and verification to the I-P-O model. Chapter 5 details the models, formulas, and

analysis used for the processing part of the I-P-O model, and provides a visual representation of the model, developed using Visual Basic for Applications. Finally, Chapter 6 concludes with limitations and recommendations for future research.

Chapter 2

2.0 Introduction to Performance and Evaluation Models

This chapter provides a background on current PV performance and evaluation models, clearly identifying the gaps in the current models, stating the contributions of this dissertation research, providing continued motivation for the research.

2.1 Literature Review

There are several easily accessible tools available online to predict the PV energy production performance and associated value, however, many can be costly, focus on hybrid renewable energy systems, or are simply outdated. Table 1 provides a list of PV performance and evaluation tools that are free (either through a website or download), focus on PV systems, and are current and up-to-date.

2.1.1 5-Parameter Array Performance Model

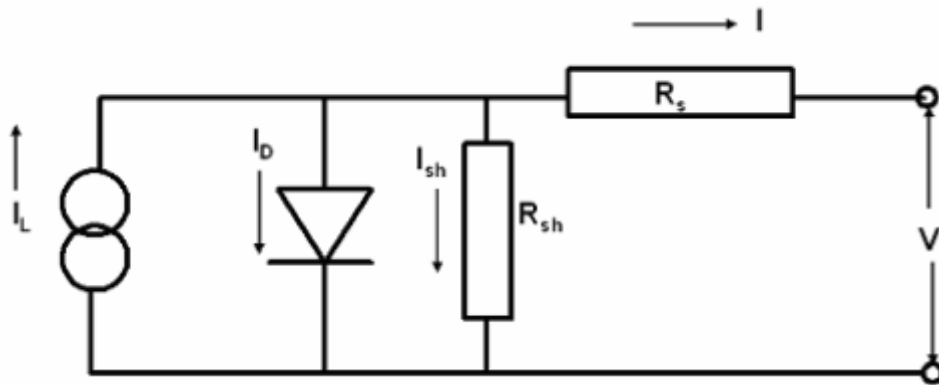
The 5-Parameter Array Performance Model was developed in 1989 by the Wisconsin Solar Energy Laboratory. It is a semi-empirical model, utilizing data from manufacturers in addition to theoretical equations, to predict the power outcome of solar modules based off 5 parameters: light current (I_L), diode reverse saturation current (I_o), series resistance (R_s), shunt resistance (R_{sh}), and a modified ideality factor ($a \equiv N_s n_1 k T / q$) (DeSoto, Klein et al. 2006). The main advantage of this model is module manufacture datasheets can be used to calculate the required parameters. The model can be downloaded for free online (<http://sel.me.wisc.edu/software.shtml>).

Table 1: Literature Review for PV Performance and Evaluation Tools

Tool	Developer(s)	Performance Model Description	Evaluation Model Description
5-Parameter Array Performance Model	Wisconsin Solar Energy Laboratory	Semi-empirical model, based off theoretical relationships and empirical equations, to predict PV array power output.	n/a
Sandia Array Performance Model	Sandia National Laboratory	Empirical model developed for PV array analysis based on non-standard STC parameters.	n/a
Sandia Inverter Performance Model	Sandia National Laboratory	Empirical model developed for PV inverter analysis based on non-standard STC parameters.	n/a
PVWatts	National Renewable Energy Laboratory	Developed for PV systems to estimate annual energy generation and associated cost savings.	Provides basic monthly energy savings based off energy generation and cost of electricity.
Solar Estimate	Energy Matters LLC	PVWatts	Provides financial incentives based off location and utility company, energy savings, and system lifetime cash flows.
PV Value	Sandia National Laboratory and Energy Sense Finance	PVWatts	Evaluates a new or existing system, for the purpose of appraisal, underwriting, credit analysis, and insurance claims.
Solar Advisor Model	National Renewable Energy Laboratory, Sandia National Laboratories, Wisconsin Solar Energy Laboratory	PVWatts, Sandia Array Performance Model, Sandia Inverter Performance Model	Provides economic analysis based off energy costs, ability to finance, depreciation, tax incentives, lifecycle cash flows, and levelize cost of electricity.
RETScreen Photovoltaic Project Model	Natural Resources Canada	Predicts energy production, worldwide, for multiple configurations.	Evaluates financial output, including energy savings, project costs, economic feasibility, and lifecycle cash flows.

The equivalent circuit for the 5-Parameter Array Performance Model is shown in Figure 3. This model is currently being used as an input to the System Advisor Model, which will be further discussed in section 2.1.6.

Figure 3: Equivalent circuit for 5-Parameter model (DeSoto, Klein et al. 2006)



2.1.2 Sandia Array Performance Model

The Sandia Array Performance Model was developed in 1991 by Sandia National Laboratories. It is an empirical model developed for PV array analysis based on non-standard STC parameters. The model is used to analyze and model the electrical PV module performance (King, Boyson et al. 2004), assuming manufacturing data sheet information and weather information is available. The database of manufacturers' data sheets and empirical module performance parameters, developed through this model, can be downloaded from the Sandia website (<http://www.sandia.gov/pv>). The benefit of using both types of data is to better understand performance under non-standard test conditions.

2.1.3 Sandia Inverter Performance Model

Sandia Inverter Performance Model was developed in 2007 by Sandia National Laboratory (King, Gonzalez et al. 2007). Similar to the Sandia Array Performance

Model, this is an empirical model developed for further analysis based on non-standard STC parameters. The purpose of the model is to simply simulate the inverter power deliver parameters of the DC-AC conversion process. The database of manufacturers' data sheets and empirical inverter performance parameters, developed through this model, can be downloaded from the Sandia website (<http://www.sandia.gov>) under the PV Systems Reliability Program.

2.1.4 PV Watts

PVWatts was developed in 1999 by National Renewable Energy Laboratory, and is the standard industry tool used to estimate PV system energy production and resulting cost of energy. Upon identifying a location to get started, the user must enter System Info, including DC System Size, Rating, Array Type, DC-to-AC Derate Factor, Tilt, Azimuth, System Type (optional), Cost of Electricity (optional), and Initial Cost (optional), as shown in Figure 4. The results include average daily solar radiation per month, monthly AC energy production, and the associated AC energy value.

Figure 4: PV Watts System Info

RESOURCE DATA SYSTEM INFO RESULTS

SYSTEM INFO RESTORE DEFAULTS

Modify the inputs below to run the simulation.

Go to resource data

DC System Size (kW): 4 i

Array Type: Fixed (open rack) i

DC-to-AC Derate Factor: 0.77 i Derate Calc.

Tilt (deg): 41.9 i

Azimuth (deg): 180 i

Draw Your System

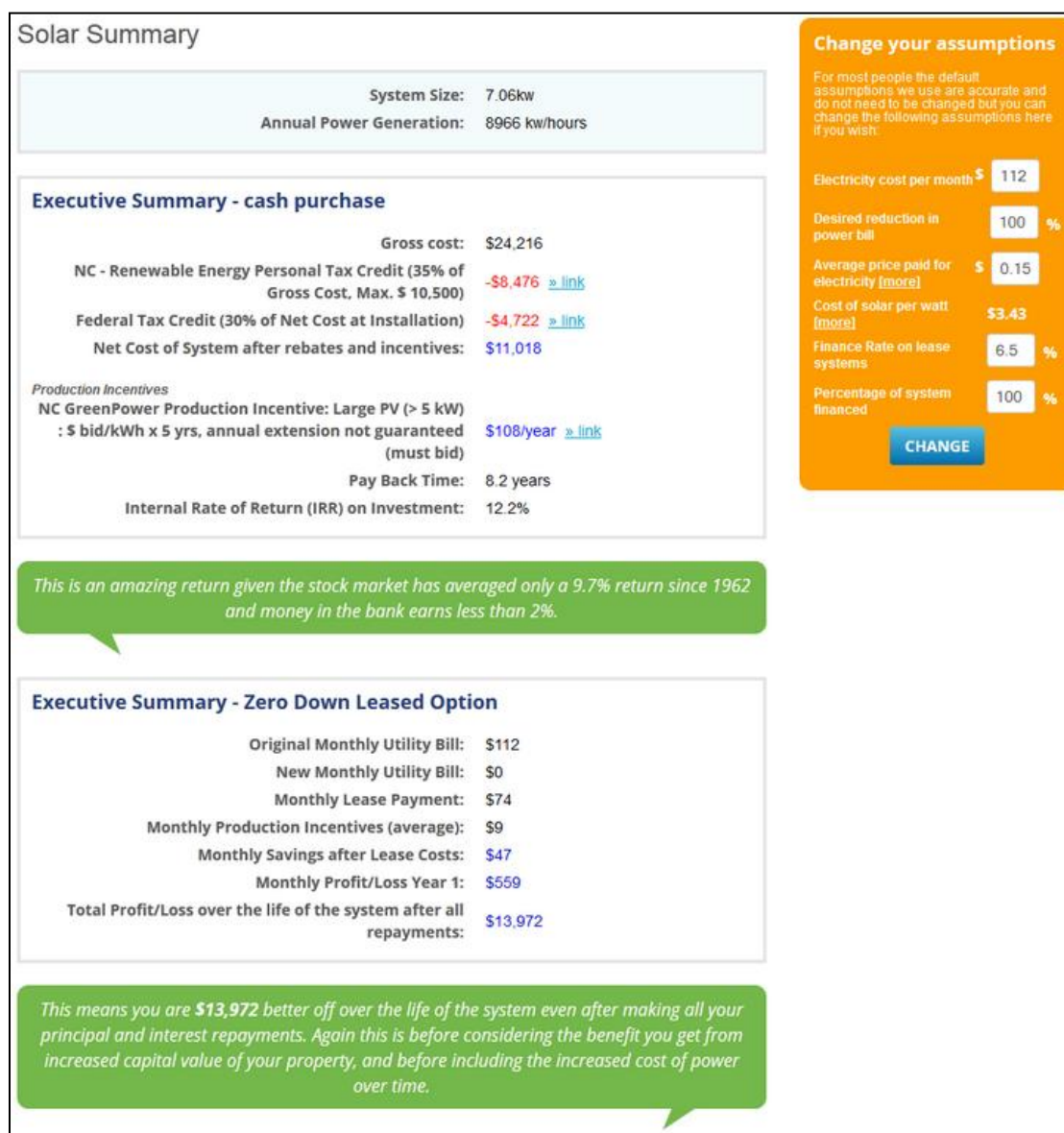
Click below to customize your system on a map. (optional)

Go to PVWatts® results

2.1.5 Solar Estimate

Solar Estimate was developed in 2000 by Energy Matters LLC (Energy Matters LLC 2009). The performance analysis uses PVWatts, and the evaluation model provides financial incentives based off location and utility company, energy savings, and system lifetime cash flows. Actual system inputs include location, average cost of electricity per month and per kWh, desired reduction in utility bill, cost of solar energy system, finance rate, and percentage of system being financed. The resulting summary, as shown in Figure 5, provides an estimate of the size of system and roof space required, available incentives and tax credits, an estimated cost based on industry averages, and quotes from local PV electrical installers.

Figure 5: Solar Estimate sample output



2.1.6 PV Value

PV Value was developed in 2011 by Sandia National Laboratory and Energy Sense Finance (Klise, Johnson et al. 2013). This tool is in the form of an Excel spreadsheet and is freely available online through www.pvvalue.com, as shown in Figure 6.

Figure 6: PV Value example of input

PV Value[®] Photovoltaic Energy Valuation Model v. 1.1

Choose Property Type: Residential Dual-Family Townhouse Condo Commercial

Solar Resource Calculation		Discount Rate Calculation		Electricity Rate Inputs		Operation & Maintenance Inputs	
Zip Code	54128	Basis Points (low)	50	Click to Update Utility Specific Electricity Rate	<i>Tucson Electric Power Co</i>	15-Year O&M Expenses as a function of the system size	
System Size in Watts	1,000	Basis Points (high)	200	Residential Rate c/kWh	9.87	O&M Expenses c/W	75
Derate Factor	0.960	Basis Points (average)	125	<input type="checkbox"/> User Defined (check box) c/kWh		Est. Inverter Replacement Cost \$	396.34
<small>Commissioning report # is required to override default derate factor</small>		Choose Net Yield Rate		Utility Escalation Rates for	AZ	System Age and Remaining Lifetime	
Commissioning Report #		<input type="checkbox"/> 12/17/2013 Rate is Out of Date		Residential Escalation Rate - EIA	0.40	Module Warranty/Years	25
Module Degradation Rate	1			<input checked="" type="checkbox"/> User Defined (check box)	1.25	Age of System/Years	0
Array Type	Fixed					Remaining Energy/Years	25
Array Tilt (unchecked = latitude)	0.0	Discount Rate (low)	3.59				
Array Azimuth (default = South)	180	Discount Rate (average)	4.34				
Click to Calculate PV Production	kWh Produced/Year	Discount Rate (high)	5.09				
	10,284						

User Input
User Input Override
Calculated Value

Appraisal Range of Value Estimate		
Low	\$	14,557.10
Average	\$	15,633.28
High	\$	16,839.42

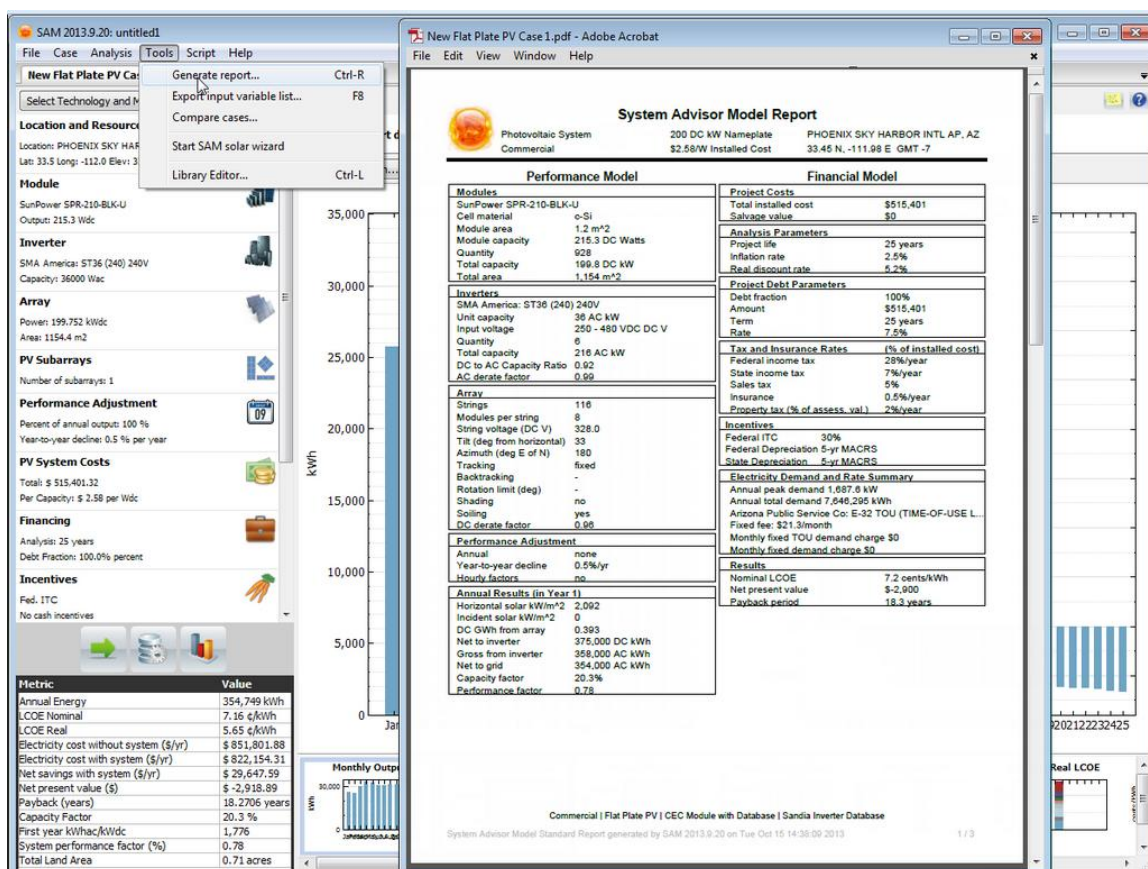
Is this a Lease to Purchase option? Check for Buyout Valuation

PV Value uses PVWatts for the performance model to estimate energy program. The evaluation model is targeted towards realtors, insurance companies, and appraisers, and it evaluates a new or existing system, for the purpose of appraisal, underwriting, credit analysis, and insurance claims. Additional system inputs include operation and maintenance costs, and system age. The analysis uses an income-based approach and discounted cash flow. The output includes low, average, and high appraisal value estimations.

2.1.7 Solar Advisor Model

Solar Advisor Model (SAM) was developed in 2006 by National Renewable Energy Laboratory, Sandia National Laboratories, and Wisconsin Solar Energy Laboratory (National Renewable Energy Laboratory 2014). SAM uses three different models to calculate PV performance: Sandia Array Performance Model (2.1.2), PVWatts (2.1.4), and Sandia Inverter Performance Model (2.1.7) (Mehos and Mooney 2005). SAM's evaluation model provides economic analysis based off of energy costs, ability to finance, depreciation, tax incentives, lifecycle cash flows, and levelized cost of electricity. SAM has a report generator, Figure 7, providing a summary of the system output, and offers additional analysis options including parametric analysis, sensitivity analysis, further statistical and graphing options, and P50/P90 analysis (for locations with available weather data).

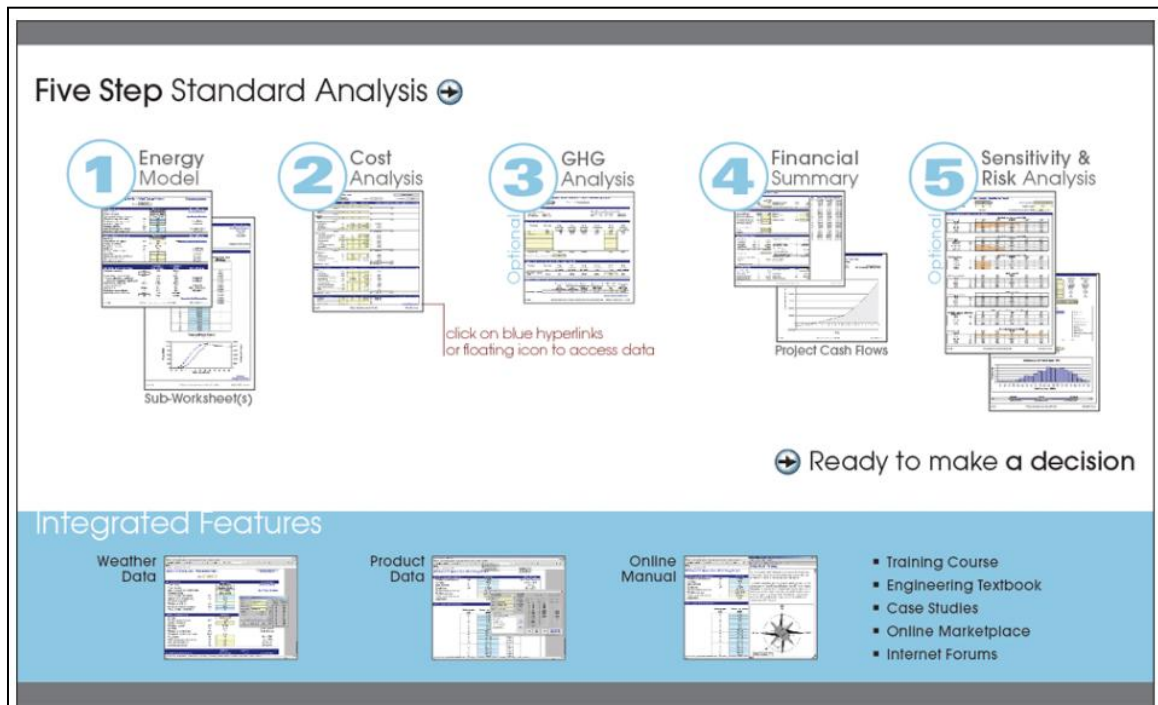
Figure 7: System Advisor Model report generator



2.1.8 RETScreen Photovoltaic Project Model

The RETScreen Photovoltaic Project Model was developed in 1989 by Natural Resources Canada. This model is all-inclusive in that it provides its own energy production prediction model for worldwide locations and multiple configurations, and it provides an evaluation model assessing financial output, including energy savings, project costs, economic feasibility, and lifecycle cash flows (Clean Energy Decision Support Centre 2004; Clean Energy Decision Support Centre 2005).

Figure 8: RETScreen Five Step Standard Analysis



The software model flow has 5 steps as show in Figure 8. Step 1 is the Energy Model, which calculates the estimated annual PV production according to location and system characteristics. Step 2, the Cost Analysis step, estimates the initial investment costs based upon an online product database. Step 3 is the Greenhouse Gas (GHG) Emission Reduction Analysis, which approximates the potential GHG emission reduction of the PV installation. Step 4, the Financial Summary, assesses common financial parameters including project costs, savings, cash flow, and feasibility. Finally, Step 5 offers an optional Sensitivity and Risk Analysis, used to estimate the general sensitivity and statistical risk associated with the project.

2.2 Proposed Contributions

Table 2: Limitations of current PV performance and evaluation tools

Limitation	Performance and Evaluation Tool							
	[1]	[2]	[3]	[4]	[5]	[6]	[7]	[8]
System Configuration								Gray
Monthly Derate Factor	Gray	Gray	Gray	Gray	Gray	Gray	Gray	Gray
Annual Degradation by Component	Gray	Gray	White	Gray	Gray	Gray	Gray	Gray
PV Module Selection	Gray	Gray	White	White	White	White	Black	Black
Cylindrical Panel Performance							White	White
Albedo Coefficient							Gray	Gray
Inverter Selection			Gray	White	White	White	Gray	Gray
Project Comparison							Gray	White
Various Valuation Techniques						Gray	Gray	Gray
Note (1): [1] 5-Parameter Array Performance Model, [2] Sandia Array Performance Model, [3] Sandia Inverter Performance Model, [4] PVWatts, [5] Solar Estimate, [6] PV Value, [7] Solar Advisor Model, and [8] RETScreen Photovoltaic Project Model Note (2): Black = Full coverage, Gray = Partial coverage, White = No coverage								

A PV performance estimator tool is only as good as its weakest link. As explained in the first section, accelerated environmental stress tests provide a wealth of knowledge about module expectations at standard test conditions. However, estimating factors and interactions of real-world performance can be complex and difficult. The PV system performance and evaluation tools, from Table 1, make an attempt to better understand, or at least better account for these uncertainties and real-world variables, and provide a great starting point for quantifying anticipated energy production and value. However, the tools

have several limitations, as identified in Table 2, which are further discussed in this section.

2.2.1 System Configuration

In general, there are two main types of PV systems, grid-tied systems and off-grid systems. Off-grid systems can function regardless of whether the utility grid is up and running. However, grid-tied systems can only function when the grid is up and running, due to anti-islanding policies (Ye, Walling et al. 2004).

Off-grid PV systems are used as an alternative to utility grid-tied electricity. Figure 9 is an example of an off-grid DC direct system used as a water pump, in this case, for cattle. For an off-grid direct system, the electricity is consumed as it is generated. Thus, the availability of electricity is limited on cloudy days and at night when no sun is available. Furthermore, the DC rating limits the loads to lights, fans, water pumps, or other loads that typically run full-time and have low power needs.

Figure 9: Example of Off-Grid DC Direct PV Systems (U.S. Department of Energy: Energy Efficiency & Renewable Energy Last Updated 06/18/2013)

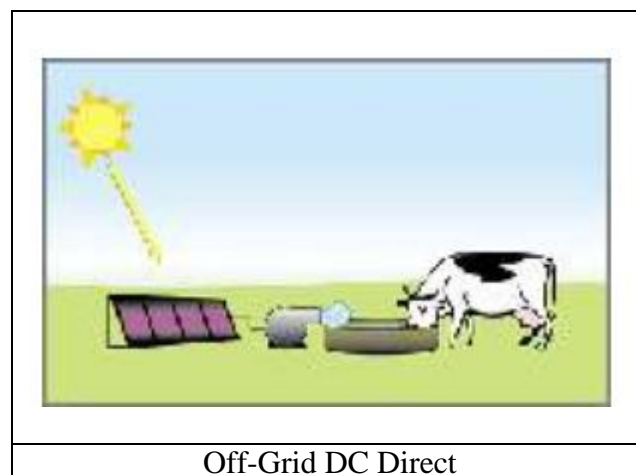


Figure 10 is an off-grid DC direct system with batteries, which allows the electricity to be stored and used in non-sunlight hours, for example as a flashing light on a highway sign. The inclusion of batteries allows electricity to be used on cloudy days and at night when no sun is available, however, the electricity is limited to DC loads.

Figure 10: Example of Off-Grid DC Direct with Battery PV Systems (U.S. Department of Energy: Energy Efficiency & Renewable Energy Last Updated 06/18/2013)

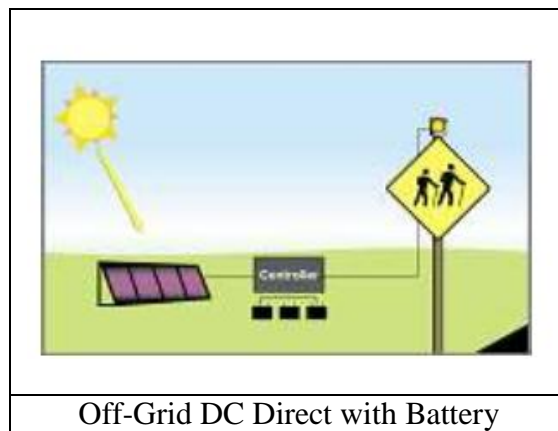
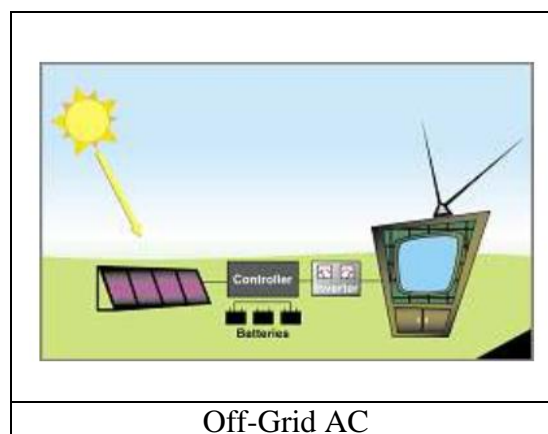


Figure 11 is an off-grid AC system, which uses a controller to determine if electricity is needed, and uses an inverter to convert the DC to AC, or if electricity is not needed, the DC electricity is directed to the battery storage for later use. The inclusion of batteries allows electricity to be used on cloudy days and at night when no sun is available. Furthermore, the AC electricity can be used for common household appliances including TVs, refrigerators, and microwaves.

Figure 11: Example of Off-Grid AC PV Systems (U.S. Department of Energy: Energy Efficiency & Renewable Energy Last Updated 06/18/2013)



Grid-direct systems are tied directly into the utility lines, as shown in Figure 12. All grid-direct systems include a DC-AC inverter and at least one meter. If the utility company offers net-metering, one meter will be used that spins backwards when PV electricity is generated and spins forward when the utility generated electricity is used. If the utility company requires feed-in tariffs, where the PV electricity generated is sold directly to the utility company, two meters will be used, one to measure the utility generated electricity consumed by the homeowner and one to measure the PV electricity generated by the homeowner. Net-metering and feed-in tariffs are further explained in the costs section. Additionally, some homeowners prefer a grid-direct system with battery back-up to ensure electricity is available if, and when, the grid goes down.

Figure 12: Grid-Direct System (U.S. Department of Energy: Energy Efficiency & Renewable Energy Last Updated 06/18/2013)

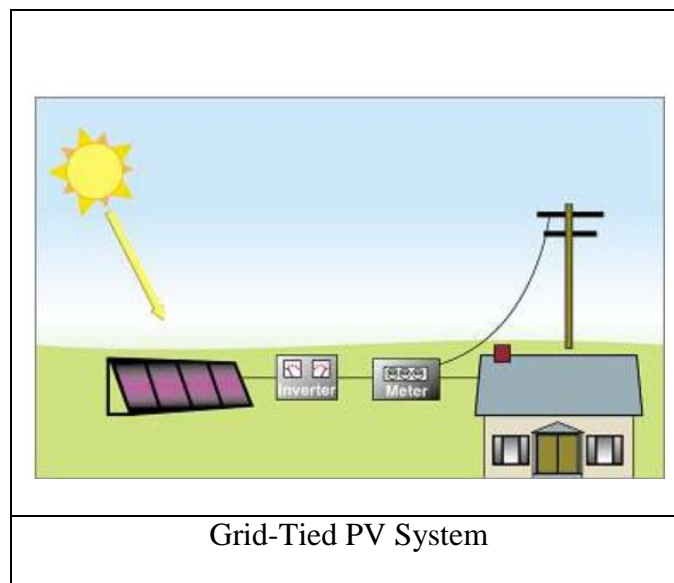


Table 3 provides a summary of PV system configurations and their associated components. For example, an off-grid DC direct system only has 3 major components: PV array, racking, and DC wiring. The efficiency should be calculated differently in comparison to a grid-tied AC with battery system which has all 7 major components. The laws of system efficiency tell us that an increase in individual system components is likely to lower overall system performance. Similarly, a decrease in individual system components is likely to improve overall system performance. As such, it is important to consider the type of PV system configuration because the quantity of components will increase the probability of system degradation or likelihood of a system failure. PVWatts is limited to one system configuration, a grid-tied PV system. However, it is important to understand the possibility of grid-tied PV with batteries or off-grid stand alone PV systems.

Table 3: Components vs Configurations

Component	Configuration					
	Off-Grid				Grid-Tied	
	DC Direct	DC Direct with Battery	AC	AC with Battery	AC	AC with Battery
PV Array						
Racking						
DC Wiring						
Battery and Charge Controller						
Inverter and Transformer						
AC Wiring						
Utility Grid						

The majority of performance and evaluation tools only consider DC-AC Grid Direct PV Systems, and fail to analyze multiple configurations as shown in Table 3.

2.2.2 Monthly Derate Factor

Many performance and evaluation tools make effort in considering system inefficiencies by providing the derate factor parameter. However, there is limited information about the range values or recommendations on how the value should be assigned. Furthermore, the derate factor lacks an overall systems perspective. Finally, the derate factor considers the potential of shading, soil, and snow, yet, it does not allow for monthly changes. For example, shading varies depending on time of year, due to the position of the sun. Additionally, snow and other potential soiling causes also vary depending on time of year.

The NREL PVWatts derate factor of Diodes and Connections has a default efficiency of 0.995, with a range of 0.990 to 0.997. Unfortunately, PVWatts gives the user limited explanation as to the selected range and recommended default value. This

example highlights the need to provide further explanation and recommendations when estimating efficiencies associated with overall system performance.

2.2.3 Annual Degradation by Component

The PV systems overall efficiency refers to the reliability of the solar technology over time, taking into consideration the degradation associated with the module and system components over their service time. Stability, or degradation, of solar energy technologies is extremely complex due to the large quantity of components and variety of system configurations. Failures can occur at different levels of analysis, including system, array, panel, module, or cell levels, and, furthermore, the degree (or probability) of a failure depends on the type of solar material used and the environmental conditions.

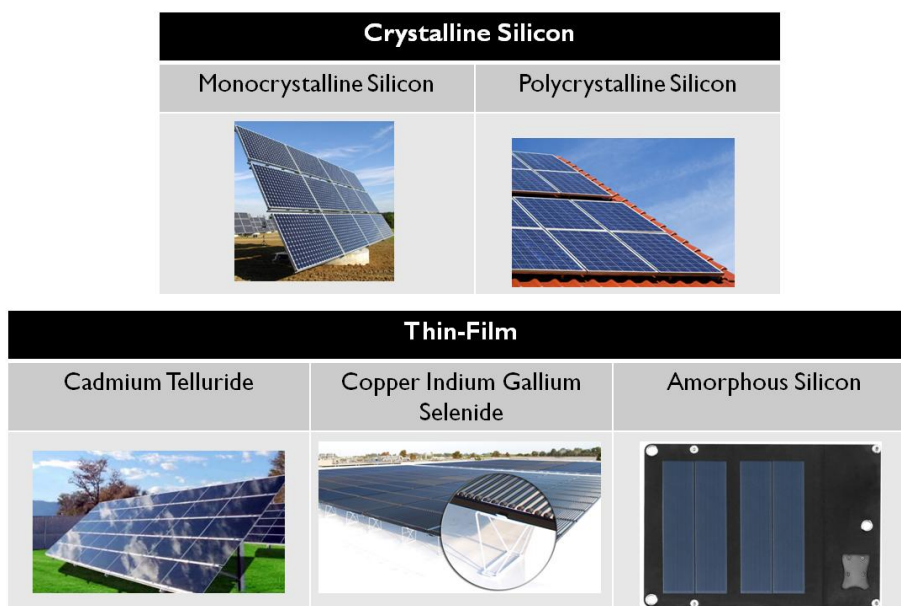
Many performance and evaluation tools make reference to the derate factor of Age as it relates to the weathering of PV modules. Unfortunately, tools do not consider the age of inverter or possibly the battery age, either of which can potentially affect the overall system performance differently. This example highlights the need to consider degradation from a systems perspective, understanding the potential degradation factors associated with all system components.

2.2.4 PV Module Specific Characteristics

There are many different types of PV modules available on the residential, commercial, and utility market. There are crystalline silicon based modules and there are thin-film modules, two different generations and categories of solar technology. As shown in Figure 13, crystalline silicon modules include mono-crystalline silicon and

poly-crystalline silicon; thin-film modules include amorphous silicon, cadmium telluride, and copper indium gallium selenide.

Figure 13: Major PV Technologies



In general, advantages of crystalline silicon technologies (in comparison to thin-film) include higher conversion efficiency, established longevity, robustness, and maturity. On the other hand, thin-film technologies have a superior temperature coefficient, meaning that they hold up better under warmer temperatures. Also, the different thin-film materials allow them to be lightweight, versatile, and flexible. For example, a-Si is what is used for solar powered calculators. Lastly, thin-film have a better shade tolerance, meaning that they are less sensitive to shade received from buildings, trees, or cloud coverage. Unfortunately, some thin-film PV include hazardous materials include cadmium, tellurium, and hydrogen selenide.

Setting aside the type of materials, specific module performance attributes vary depending upon model and manufacturer (even when using the same type of material).

These module specific characteristics include conversion efficiency, temperature coefficient, power tolerance, and panel type.

First, conversion efficiency is the modules ability to convert incoming sunlight into DC energy. A module with a conversion efficiency of 10% in comparison to a module with a conversion efficiency of 20% will take up twice the quantity of space, and racking, to achieve the same DC power rating. It is important to consider efficiency, with respect to space and racking, because the quantity of components will increase the probability of system degradation or likelihood of a system failure.

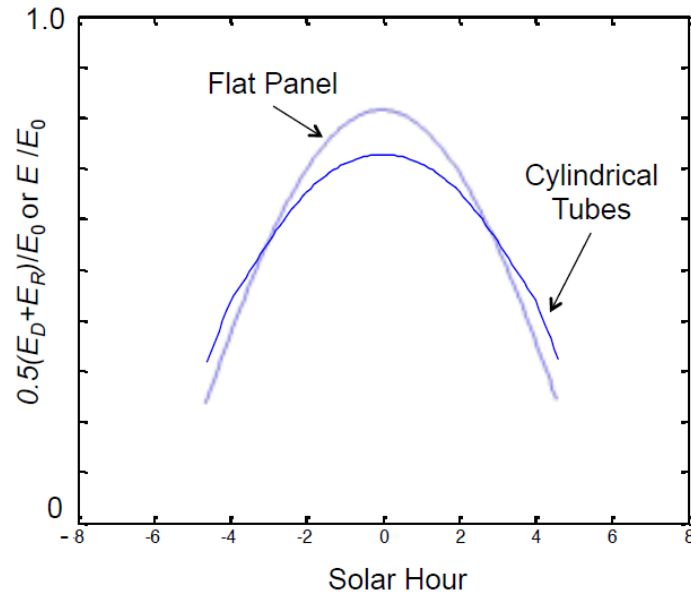
Second, the PV module temperature coefficient describes the power percentage change for each Celsius degree change from the STC value of 25°C. A module with a higher temperature coefficient will perform worse in hotter temperatures, yet, it will perform better in lower temperatures. Thus, it is important to consider the rated temperature coefficient with respect to system efficiencies.

Third, the power tolerance describes the upper and lower bound of variation, if any, for the DC power rating. Even though a module may have a DC power rating of 250W, a power tolerance of +/- 10% has the ability to change the potential DC power rating to an upper bound of 275W and a lower bound of 225W. Also, amorphous silicon modules are known to have an initial period of high voltage, as commonly stated on the module specification sheets, which is followed by a significant decline in power. Thus, it is important to consider the effects of potential DC power rating on the overall system performance.

Fourth, the panel type can include the common flat panel or the new cylindrical panel used for thin-film CIGS technology. The collector geometry of the cylindrical

panel allows it to increase in performance during the early and late hours, as shown in Figure 14.

Figure 14: Comparison of Flat Panel to Cylindrical Tubes (Koshel, Smestad et al. 2012)



Many performance and evaluation tools only consider crystalline silicon PV modules. Furthermore, they lack consideration for important module specific performance attributes. As discussed in this section, it is important for a PV performance tool to go beyond one type of PV technology, to increase inclusiveness to market available thin-film modules. More importantly, a PV performance tool should allow the user to modify performance parameters such as efficiency, temperature coefficient, power tolerance, and panel type to gain an understanding of how the PV module affects the overall system performance.

2.2.5 Albedo Coefficient

The albedo coefficient is the portion of Global Horizontal Radiation reflected by the ground, or surface, in front of a tilted PV array. Depending on the reflecting surface,

the albedo coefficient can range from 0.15 – 0.25 for grass all the way up to 0.85 for aluminum, as shown in Table 4. However, PV Watts assumes a default of 0.2 for the albedo coefficient, with the exception of 0.6 during snow fall.

Table 4: Albedo Coefficient Values (Mermoud and Wittmer 2014)

Urban environment	0.14 - 0.22
Grass	0.15 - 0.25
Fresh grass	0.26
Fresh snow	0.82
Wet snow	0.55-0.75
Dry asphalt	0.09-0.15
Wet Asphalt	0.18
Concrete	0.25-0.35
Red tiles	0.33
Aluminium	0.85
Copper	0.74
New galvanized steel	0.35
Very dirty galvanized	0.08

2.2.6 Inverter Selection

The purpose of the inverter is to convert DC electricity, generated by the PV array, into AC electricity required by the utility grid and most household appliances. Inverters can be used in both off-grid and utility grid-tied configurations, however, the requirements for grid-tied inverters are more stringent due to safety concerns if and when the grid shuts down. Grid-tied inverters must be equipped with anti-islanding protection, an automatic shut-off when the grid goes down, and ultimately preventing utility lineman from being electrocuted by a distributed generation source.

There are two general types of inverters used in AC-based PV systems, which include string or central inverters, and microinverters. A central inverter (Figure 15A) connects PV arrays in series to one central inverter. In contrast, the microinverter (Figure

15B) connects PV arrays in parallel, allowing each PV panel its own inverter. Central inverters perform best when all modules are the same size, orientation, and tilt. Microinverters optimize an individual panel output regardless of size, orientation, and tilt of neighboring panels.

Taking into consideration overall PV system efficiency, the central inverter is likely to produce differing operating efficiencies in comparison to its more expensive counterpart, the microinverter. First, with respect to shading, a string inverter allows shading on one module to impact the output for all modules. However, a microinverter limits the affects of shading to the specific module. Second, if a central inverter fails, the entire system goes down, however, if a microinverter fails, only that particular portion of the system goes down. Third, microinverters are sensitive to temperature and as such, the operating temperature increases when the microinverter is mounted underneath the PV array leading to lower efficiency and life span. Most performance and evaluation tools were researched and developed during a time when microinverters were non-existent. As such, the tool would benefit from an upgrade beyond the basic central inverter to include the newly developed and adopted microinverters.

Figure 15: String Inverter vs Microinverter (Enecsys Micro Inverters Retrieved 06/28/2013)

Figure 15A. Central Inverter

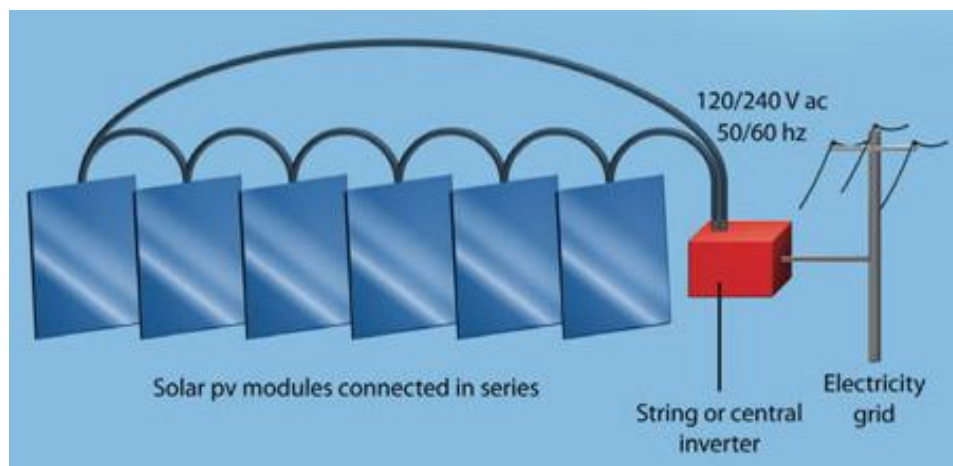
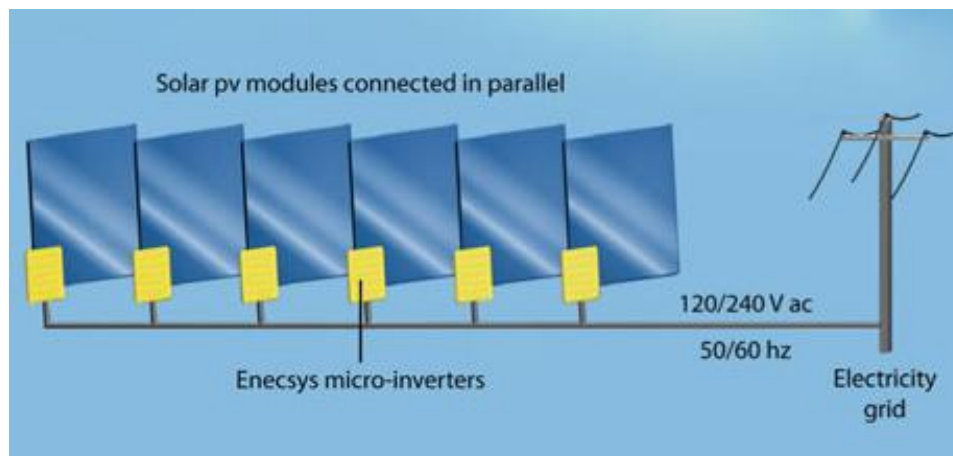


Figure 15B. Microinverter



2.2.7 Multiple PV Comparison

Research and comparison is an important requirement of any purchasing decision, especially for long-term investing in solar energy. The current performance and evaluation tools do not have the capability to view multiple PV system options all at one time and on one screen, promoting understanding of the potential impact of any input factors related to the performance of the PV system installation.

2.2.8 Differing Valuation Techniques

Accurate insurance and appraisal evaluation is important to homebuyers to correctly assess the value of the PV system in the event of an unexpected natural disaster. Two important valuation techniques include replacement value (current cost to replace the original PV system) and actual cash value (which takes into considering depreciation and degradation). The current PV system performance and evaluation tools consider only AC energy value when valuing the system as a whole.

Chapter 3

3.0 Introduction to Factors Affecting Return on Investment

This chapter offers a literature review composed of factors affecting PV performance and return on investment, relaying the anticipated inputs and outputs into the I-P-O model.

3.1 PV Array

The PV array is the central component of all PV system configurations. The performance and reliability of a PV array is highly dependent upon two major factors: sun tracking capability and module specific information.

3.1.1 Sun Tracking

The overall performance of solar energy technologies is highly attributable to the quantity of incoming solar irradiation. As such, the ability of a PV array to obtain sun light is the largest factor affecting the efficiency of any PV array. Without sunlight, solar energy technologies will not perform. If no sun is available, for example at night, no electricity can be generated. There are six main variables that influence a PV array's ability to collect sun light. These are PV array location, orientation, tilt, tracking capability, shading, and soiling.

3.1.1.1 Location

Most locations on earth receive sunlight at least part of the day; however, the quantity of solar irradiation received can be affected by time of day, climate, location, and season changes. During the spring and fall equinox, both hemispheres receive the

same 12 hours of daylight, as shown in Figure 16. During the winter months, the midday sun achieves its peak in the southern hemisphere, resulting in a longer day for the southern hemisphere and a shorter day for the northern hemisphere. During the summer months, the midday sun achieves its peak in the northern hemisphere, resulting in a longer day for the northern hemisphere and shorter day for the southern hemisphere.

Figure 17 portrays the implications solar irradiation on latitude throughout the world.

Figure 16: Quantity of Daylight as Function of Month and Earth's Rotation (solarenergyfallacies.com Retrieved 06/28/2013)

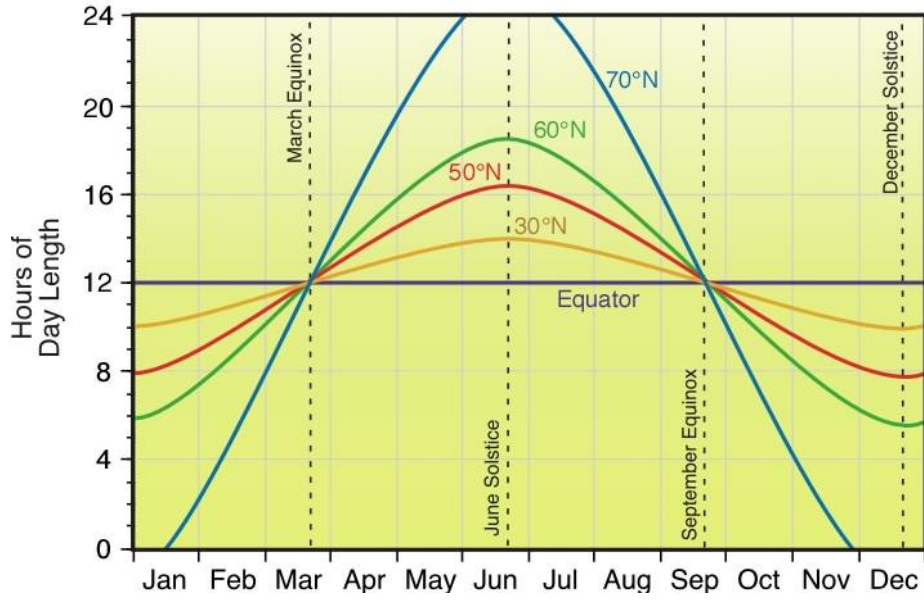
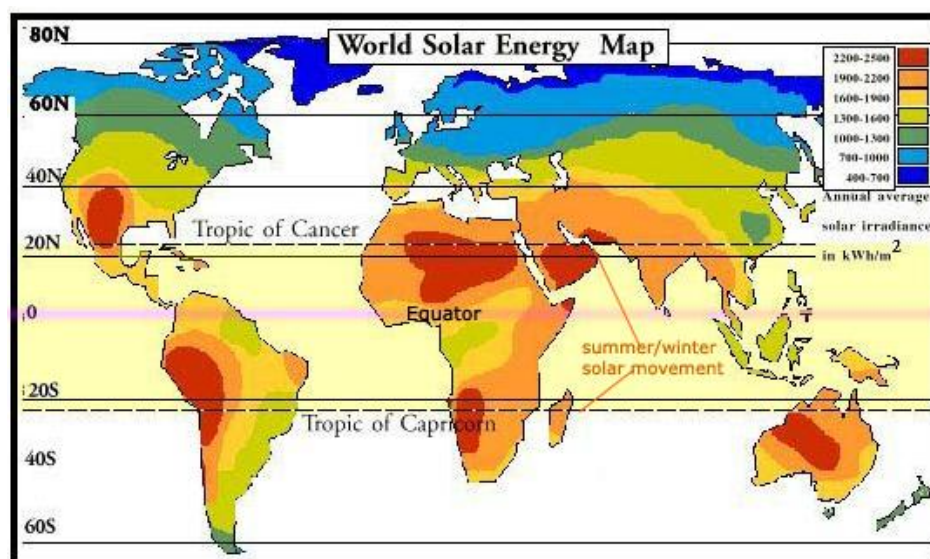


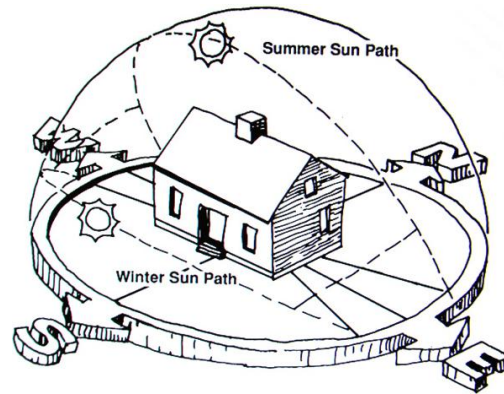
Figure 17: Solar Irradiation through the World (solarenergyfallacies.com Retrieved 06/28/2013)



3.1.1.2 Orientation

Since solar irradiation changes from location to location, module orientation and tilt are of particular important to optimize the quantity of sun light received and collected by PV solar arrays. First, the optimal orientation for the PV arrays located in the northern hemisphere is due south towards the equator. For PV arrays located in the southern hemisphere, the optimal orientation is due north toward the equator. Figure 18 shows a PV array located in the northern hemisphere will receive the sun at a lower altitude in the winter and a higher altitude in the summer, but in either case, the origination of the sun is still coming from the south. The southern hemisphere will follow the same sun path but the origination of the sun is from the north. As such, a flat panel vertically mounted (90°) in the northern hemisphere will perform better during the winter months (lower altitude) than during the summer months (higher altitude), and a flat panel horizontally mounted (0°) will perform better in the summer months (higher altitude) than during the winter months (lower altitude).

Figure 18: Example of PV Array in Northern Hemisphere



3.1.1.3 Tilt

PV module tilt can be fixed, manually adjusted throughout the seasons, or optimized for incoming solar irradiation using a variety of tracking mechanisms.

First, in the case that the PV array will be mounted to a pre-existing roof surface, if possible, tilt should be adjusted according to Figure 19 to maximize incoming solar irradiation. In the case the PV array will be ground or pole mounted, a year-round fixed tilt will be beneficial. Figure 20 shows the necessary tilt angle to optimize the incoming sunlight throughout the year.

Figure 19: Recommended PV Array Tilt for Roof Pitch

Roof Pitch	Tilt Angle (°)
4/12	18.4
5/12	22.6
6/12	26.6
7/12	30.3
8/12	33.7
9/12	36.9
10/12	39.8
11/12	42.5
12/12	45.0

Figure 20: Optimal PV Array Tilt Angle (RS Components 2005)

Latitude of site	Tilt angle
0-4°	10°
5-20°	Add 5° to local latitude
21-45°	Add 10° to local latitude
45-65°	Add 15° to local latitude
65-75°	80°

Second, in the case it is possible to manually adjust the PV array tilt through the year; the optimal tilt change depends on the latitude. For example, Green Alchemy Solar Power Farm is located in Pennsylvania at 40° latitude. Figure 21 shows the recommended seasonal PV array tilt to maximize incoming solar irradiation.

Figure 21: Recommended PV Array Tilt for Green Alchemy Solar Power Farm (Green Alchemy Retrieved 07/06/2013)

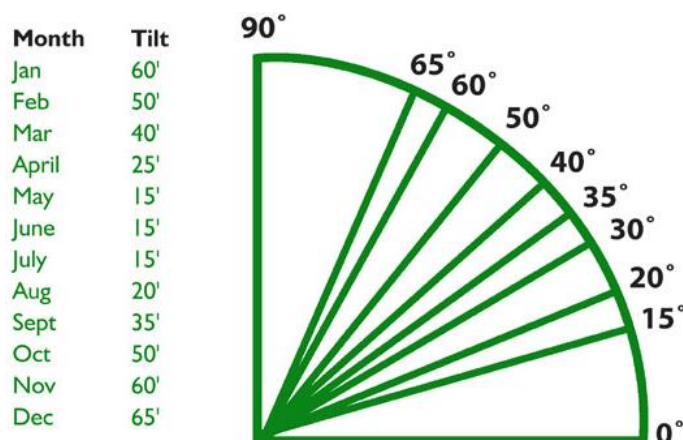
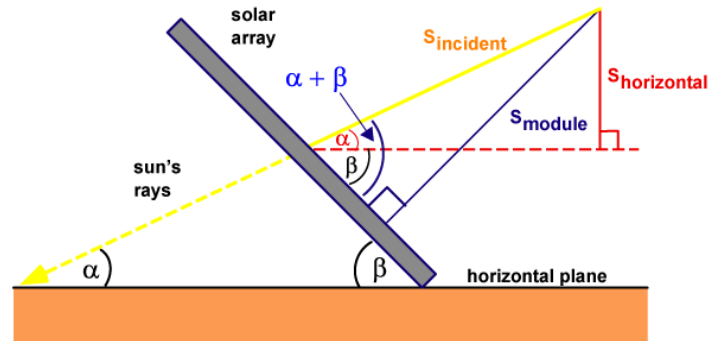


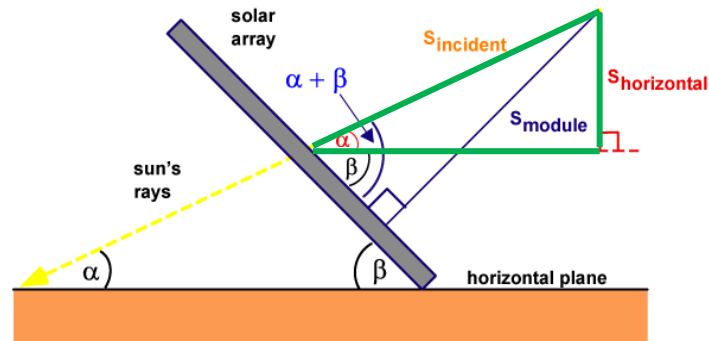
Figure 22 provides a visual display of the different types of solar irradiation on a tilted solar array. The sun's rays are indicated by S_{incident} . The solar irradiation, as measured by an upright pyranometer, is given by $S_{\text{horizontal}}$. The solar irradiation actually entering the PV module is given by S_{module} . Two angles are given; beta (β) describes the PV module tilt angle from the horizontal plane and alpha (α) describes the sun's angle of elevation above the horizon.

Figure 22: Solar Radiation on Tilted Surface (Honsberg and Bowden Obtained 01/21/2014)



To calculate PV module solar irradiation (S_{module}), the solar irradiation is trigonometrically decomposed as shown in Figure 23 and Figure 24.

Figure 23: Green Outline of First Triangle Calculation



According to the Law of Sines:

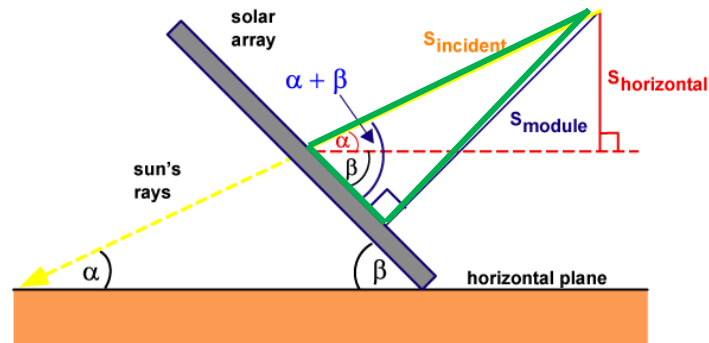
$$\frac{\sin(\alpha)}{S_{horizontal}} = \frac{\sin(90)}{S_{incident}}$$

When solving for $S_{incident}$ and since $\sin(90) = 1$, the equation changes as follows:

$$S_{incident} = \frac{S_{horizontal}}{\sin(\alpha)}$$

The second triangle is shown in Figure 24.

Figure 24: Green Outline of Second Triangle Calculation



According to the Law of Sines:

$$\frac{\sin(\alpha + \beta)}{S_{module}} = \frac{\sin(90)}{S_{incident}}$$

When solving for S_{module} , which is the ultimate goal to understand the incoming solar irradiation, the equation changes as follows:

$$S_{module} = \frac{S_{incident} * \sin(\alpha + \beta)}{\sin(90)}$$

Since $\sin(90) = 1$, the equation can be further simplified as follows:

$$S_{module} = S_{incident} * \sin(\alpha + \beta)$$

This equation changes slightly when considering the sun azimuth angle (θ) and orientation angle (φ), in addition to tilt angle (β) and sun's angle of elevation (α) above the horizon. The final equation required for calculating PV module solar irradiation (S_{module}) is as follows:

$$S_{module} = S_{incident} * [\cos \alpha \sin \beta \cos(\varphi - \theta) + \sin \alpha \cos \beta]$$

Note that it may be necessary to convert radians to degrees or degrees to radians as follows:

$$\text{degrees} = \text{radians} \times \frac{180}{\pi}$$

$$\text{radians} = \text{degrees} \times \frac{\pi}{180}$$

3.1.1.4 Tracking Capability

Solar PV trackers are an optimal route for maximizing incoming solar irradiation; however, this option can be quite expensive. There are two different types of trackers, single-axis and dual-axis (Figure 25). Single-axis trackers can be tilted at a fixed position off the horizon and follow the location of the sun from east to west (Figure 25A), they can be oriented at a fixed position vertically and track the altitude of the sun on the horizontal axis (Figure 25B), or they can have a rotating base (Figure 25C).

Dual-axis trackers account for the change in sun's altitude and adjust for the location of the sun from east to west. Figure 25D is an example of a dual-axis with rotating base to follow the sun's course from east to west and vertical tracker to follow the sun's altitude, Figure 25E provides dual-axis within the frame itself, and Figure 25F allows a group of trackers to rotate at the base with individual trackers to follow the sun's altitude.

Figure 25: Examples of Single-Axis and Dual-Axis PV Array Tracking Designs (Juda 2013)

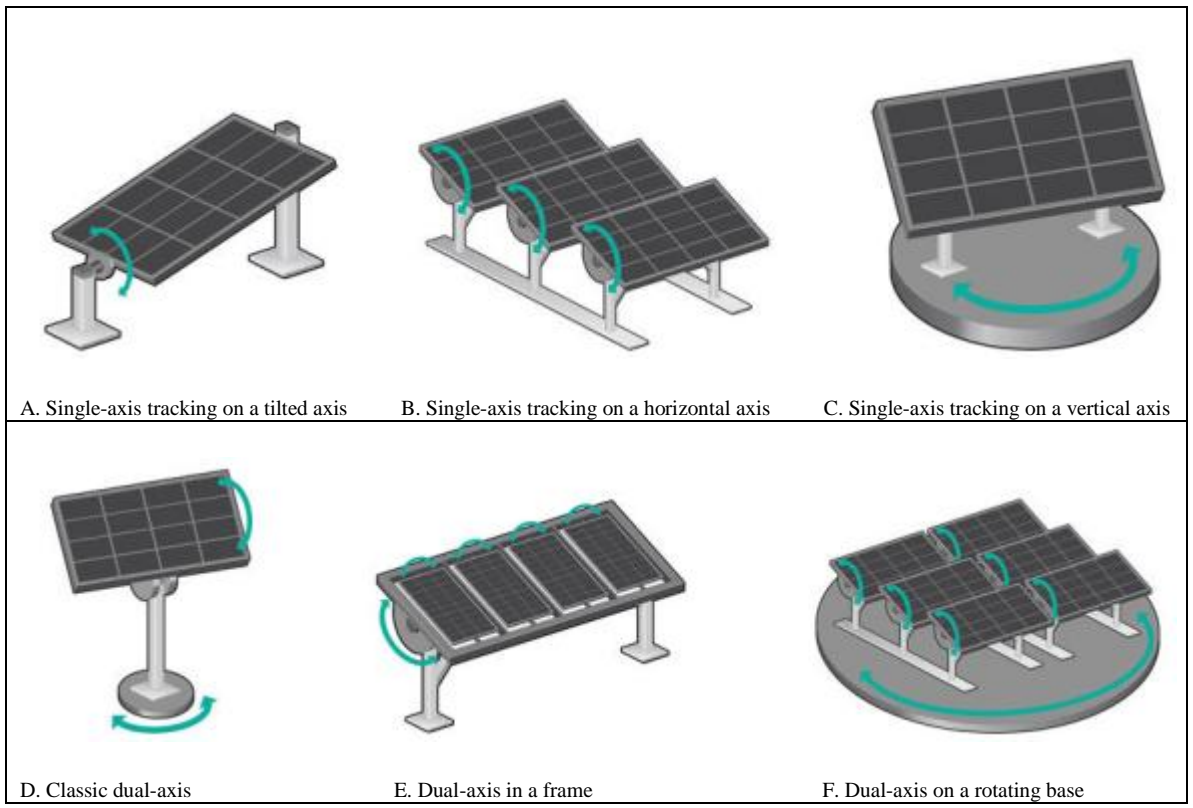
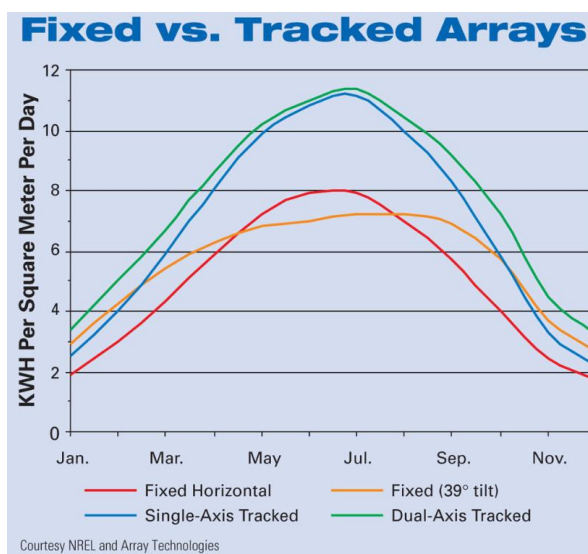


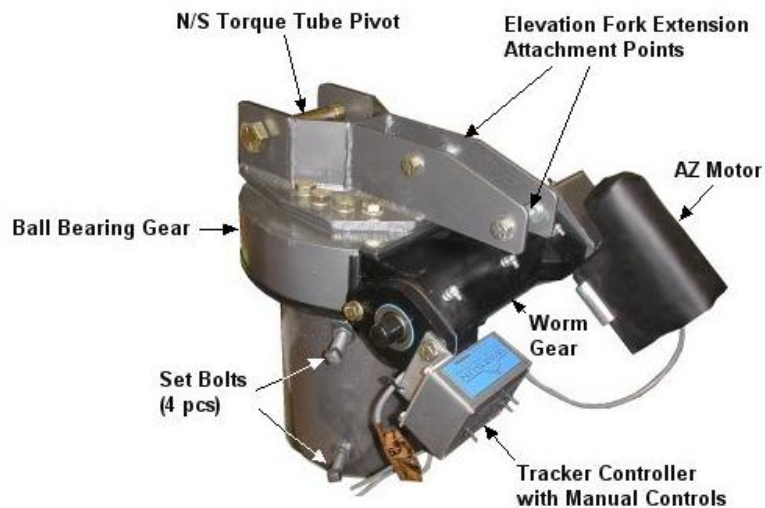
Figure 26 provides insight into the expected energy gain of a fixed position versus the use of a tracker. The chart indicates that both single-axis tracking and dual-axis tracking provide a great benefit over fixed position for the majority of the year.

Figure 26: Comparison of Fixed and Tracked PV Arrays (Home Power 2013)



There are two different mechanisms for controlling trackers, active and passive. Active trackers use motors, gears, and controls to adjust the east-west path of the sun and/or account for altitude changes in the position of the sun. Figure 27 shows an example of a dual-axis Wattsun AZ-225 Gear Drive tracker, which tracks the sun's course east to west by rotating around the pipe mast, and tilts for elevation and altitude changes. Passive trackers are single-axis non-motorized trackers that track the sun's course from east to west using a refrigerant-like gas within a sealed frame and reflective mirrors. In general, passive trackers, although lower in cost, are less accurate than active motorized trackers.

Figure 27: Wattsun AZ-225 Solar Tracker for 12 Kyocera 200 Modules (Infinigi Infinite Energy Solutions 2013)



4.1.1.5 Shading



PV owners should make every attempt to ensure shadowing by nearby trees, houses, buildings, PV modules or other permanent fixtures will not be an issue. Shading should be avoided at all costs. However, if shading is an issue and requires assessment, a solar site evaluation tool should be used. Table 5 provides a comparison of several solar evaluation tools.

The two most popular tools are the Solar Pathfinder and Solmetric SunEye, shown in Figure 28. The Solar Pathfinder is mechanical and costs about \$250. The Solmetric SunEye is electrical and costs about \$2000. Either tool will identify the monthly expected percentage losses due to shading, based on the position of the sun. Since the Solar Pathfinder is the less expensive option, its capabilities will be further discussed in this section.

Table 5: Comparison of Solar Evaluation Tools (Duluk, Nelson et al. 2013)

Tool	Solar Transit	Solar Pathfinder	Solometric Suneve	HORlcatcher	Sun Seeker	Solmetric iPV
Cost	\$10.00	\$259.00	\$1,995.00	\$1526.00 (1400CHF)	\$8.99	\$39.99
Ease of Use	Hard	Easy	Medium	Easy	Easy	Easy
Output	Manually drawn horizon shading mask diagram	Manually drawn horizon shading mask diagram	Digital fisheye image and horizon shading mask diagram	Fisheye image- as a horizon image for Meteonorm software	Digital read of azimuth and altitude manually drawn on horizon shading mask diagram	Digital image of unwrapped horizon shading mask diagram
Software	N/A	Thermal Assistant \$199.00	PV Designer Software \$400	Meteonorm \$710(650 CHF)	N/A	N/A
Operating System	Manual	PC	PC	PC	iPhone Application	iPhone Application
GPS	basic compass	basic compass	full GPS	basic compass	basic compass	basic compass
Types of Radiation Measured						
Global		✓	✓	✓		✓
Direct-Beam				✓		
Diffuse				✓		
Reflected				✓		
Recognized Types of Obstructions						
Permanent	✓	✓	✓	✓	✓	✓
Deciduous		✓				
Overhead	✓	✓	✓		✓	

Figure 28: Shading Site Assessment Tools

Solar Pathfinder (www.solarpathfinder.com)	Solmetric SunEye 210 Shade Tool (www.solmetric.com)
 <p>The Solar Pathfinder is a circular, blue-rimmed device with a polished, convex, transparent dome. The dome provides a panoramic view of the intended PV array site. The device features a grid of lines representing months and hours of the day. The months are labeled around the perimeter, starting with December at the top and ending with June at the bottom. The hours of the day are labeled along the bottom edge, with the center indicating noon or 12pm. The numbers in between each of the column lines specify the percentage of sun of the day's incoming solar irradiation received during that time of day. For example, from 12:00 – 12:30pm, during the months of October through February, there is an 8. This implies that 8% of the day's incoming solar irradiation is received during this time. This also means that if this area is shaded, 8% of the day's solar irradiation will be lost.</p>	 <p>The Solmetric SunEye 210 Shade Tool is a blue handheld device with a camera lens at the top and a screen in the middle. The screen displays a map of the sun's path over a grid, with a small table of data below it. The device has several buttons, including a central orange button and a directional pad.</p>

The Solar Pathfinder, as shown up close in Figure 29, uses a polished, convex, transparent dome to provide the panoramic view of the intended PV array site. The rows indicate the month, starting with December (provides the least amount of sunshine) and ending with June (provides the greatest amount of sunshine). The columns indicate the hour of the day, with the center indicating noon or 12pm. The numbers in between each of the column lines specify the percentage of sun of the day's incoming solar irradiation received during that time of day. For example, from 12:00 – 12:30pm, during the months of October through February, there is an 8. This implies that 8% of the day's incoming solar irradiation is received during this time. This also means that if this area is shaded, 8% of the day's solar irradiation will be lost.

Figure 29: Solar Pathfinder Example









This specific example uses a red line to highlight the shading limitations. For example, during the month of December, a house will be shading the PV array up until about 9:30am. Also, in December, a tree will start to shade the PV array around 2:15pm. This leaves an open solar window from 9:30am – 2:15pm, resulting losses of about 31%, or more importantly, a gain of about 69% of that day's incoming solar irradiation. The

shading percentage loss can be averaged out across the months to gain the annual derate factor.

3.1.1.6 Soiling

Soiling is an all-inclusive term to classify PV array cleanliness attributable to the environment. To understand the potential impacts of soiling, it is first important to consider the PV array mounting application.

Figure 30: Examples of Different Types of Mounting Options

Figure 30A. Roof Mount (Curthoys 2012)	Figure 30B. Ballasted Flat Roof Mount (SolarWorld Obtained 06/27/2013)	Figure 30C. Rail Ground Mount (www.powertripenergy.com 2006)
 A photograph showing a residential house with a dark green roof. A large array of solar panels is mounted on the roof, following the slope of the gable.	 A photograph of a flat roof on a large building. Solar panels are mounted on the roof using ballasts, and the panels are tilted at an angle.	 A photograph of a ground-mounted solar array. The panels are supported by a metal rail structure and are tilted. The array is situated in a grassy area with a fence and trees in the background.
Figure 30D. Cement Ground Mount (www.powertripenergy.com)	Figure 30E. Pole Mount (Curthoys 2012)	Figure 30F. Building- Integrated PV
 A photograph of a ground-mounted solar array. The panels are supported by concrete blocks. A person is standing next to the array for scale. The background shows trees and a building.	 A photograph of a solar panel mounted on a tall metal pole. The panel is tilted and is situated in a grassy area with trees in the background.	 A close-up photograph of a roof with blue and red tiles. A solar panel is integrated into the roof structure, appearing as a dark rectangular section among the tiles.

There are many different types of mounting options available including roof mounts, ballasted mounts, ground mounts, pole mounts, and building-integrated PV (Figure 30). Roof mounts (Figure 30A) use racking materials to mount the PV array

directly on the roof's surface, however, the tilt is limited to the pitch of the roof's surface. Ballasted mounts (Figure 30B) are used for flat roofs and allow the PV array to be mounted to ballasted cement blocks to prevent the array from movement or swaying in the wind. This option allows a stable position for the PV array without penetrating into the structure of the roof and allows for the optimization of tilt. Ground mounts (Figure 30C and D) use rail sections or cement blocks to hold the PV arrays, without penetrating the surface of the ground. Pole mounts (Figure 30E) use a ground hole and cement to stabilize the pole in the ground with a rack and PV array mounted at the top of the pole. Building-integrated PV (Figure 30F) is a new technology that incorporates the PV cells directly into the building materials, as such, the BIPV becomes the roof.

Next it is important to consider potential environmental factors, including the negative influence of material build-up due to snow, pollen, pollution, and animal droppings.

For PV arrays located in a dryer climate, where it seldom rains, the owner should consider the potential of pollen, sand, or other pollution build-up. Similarly, for PV arrays located in colder, snowy climates, the owner should consider the potential for snow to build-up on the PV array. A ground mount, or even pole mount, makes cleaning the PV array much more manageable than the roof mount or ballasted flat roof mount. In the event of a dry spell, is someone available to clean the pollen or other pollution build-up from the PV array or will this be viewed as a loss until the next rainfall? Is someone available to brush off the snow build-up from the PV array or will this be viewed as a loss until it melts away?

Once the PV solar arrays are installed, PV owners should routinely check the solar panels to ensure environmental factors do not create a barrier for incoming sunlight. If the PV solar arrays are installed in a location with easy access to outsiders, for example a ground mounted solar array, PV owners might find a benefit in installing a fence or another barrier to protect the investment from animals, vandalism or theft.

3.1.2 Module Specific Information

The ability for a PV array to generate DC electricity is greatly dependent upon module- and manufacturer-specific information, such as nameplate DC power rating, temperature coefficient, power tolerance, and power warranty. This information is obtained as a result of accelerated environmental stress tests and through the use of standard test conditions (STC), and reported on either the Module Nameplate or the Manufacturer's Technical Datasheet.

3.1.2.1 Standard Test Conditions

Accelerated environmental stress tests, including temperature, light soaking, thermal cycling, moisture, and real-time tests, have been used in a laboratory setting to accelerate the degradation of solar modules to invoke failures in an attempt to better understand the factors leading to degradation of solar modules. Real-time tests provide additional insight into solar cell and solar module performance outside of the Standard Test Conditions (STC) used within the physical laboratory environment. STC is a term commonly used within the solar industry, with the purpose of using standard or consistent environmental conditions to compare and contrast different solar materials. These conditions are as follows: (1) 1,000 W/m² of sunlight, (2) 25°C cell temperature, and (3) Spectrum at air mass of 1.5.

Figure 31: Typical Testing Sequence for Crystalline Silicon Modules (Osterwald and McMahon 2009).

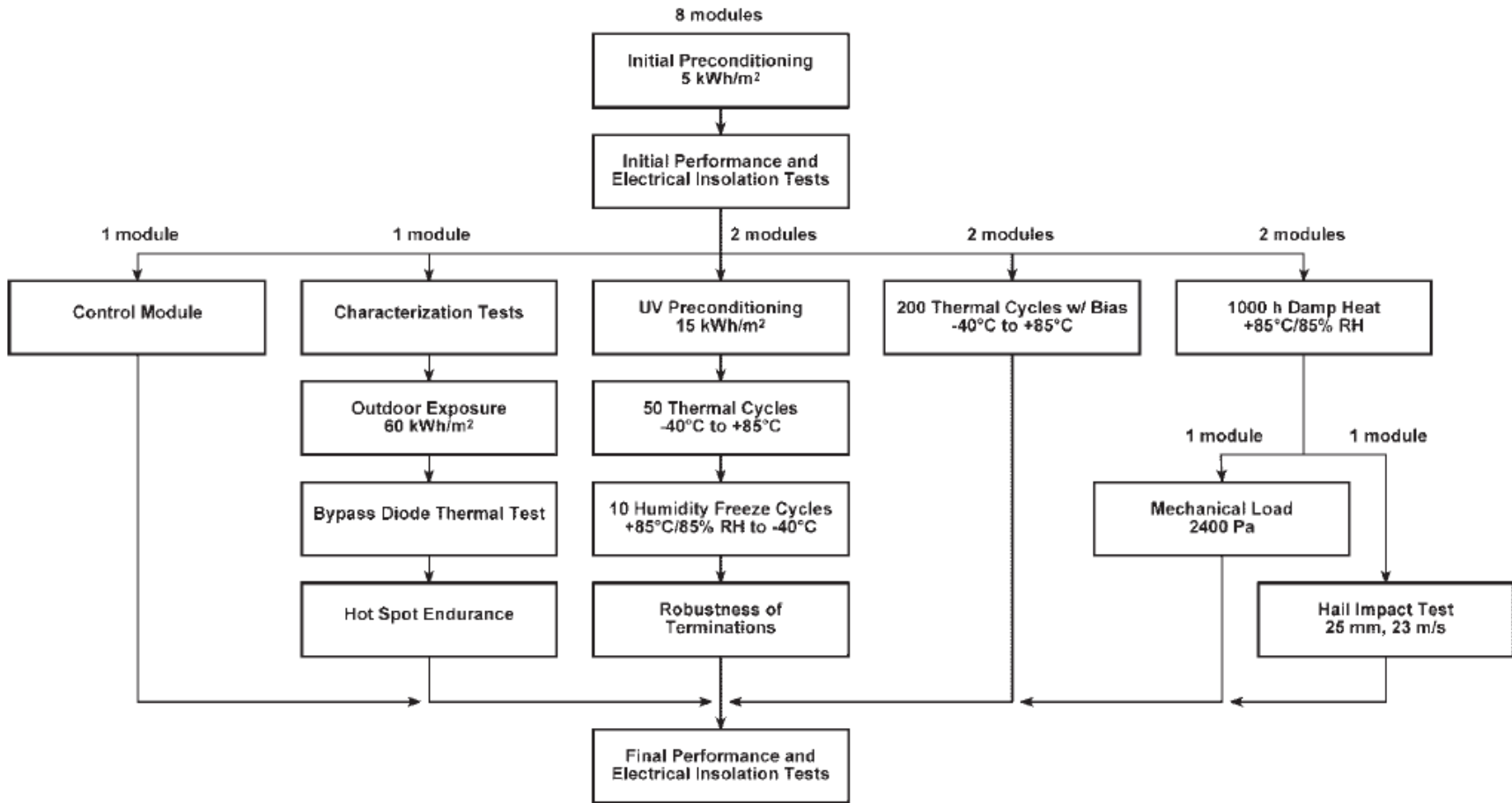


Figure 31 shows a typical qualification testing sequence for crystalline silicon modules, using principal accelerated tests including thermal cycling (TC), ultra-violet (UV) exposure, damp-heat (HT) exposure, humidity-freeze (HF) cycling, and outdoor exposure (OE). At a minimum, modules must preserve a required amount of initial output power to move on to the next test. Typical reliability issues across all technologies include loss of grounding resulting from corrosion and/or improper insulation, reliability of the quick connectors, delamination, glass fracture, failure of bypass diode, reliability of inverter, and moisture ingress (Bosco 2010).

Accelerated life and environmental testing provide a great deal of information for predicting solar module performance expectations. However, there are still many challenges and a lot of work to be completed with respect to solar module reliability. Areas include the standard 25-year warranty, ill-defined field conditions, varied outdoor conditions, materials used near limits, limited acceleration factors, and cumulative effects (Zielnik 2009). The standard 25-year warranty proposes a challenge because it is difficult to prove the modules will still be performing at a specified level at the end of the 25-year life. In addition, the warranty period differs from one PV technology to another. Field conditions are not well defined because it is difficult for a warranty to apply for all conditions on the same module. Outdoor conditions can be extremely harsh and greatly vary beyond the STC solar irradiation, temperature, and air mass, resulting in other than expected STC performance outcomes. Lab testing is commonly completed on new materials, as such, little is known about the impact of lab-induced factors on used materials over time. Lab testing considers only a limited array of acceleration factors, commonly related to temperature, humidity, and light, however, there are many other

factors, difficult to study, which may influence the performance of solar modules. Lastly, an installed PV system is very complex and consists of many components with the capacity to degrade or fail. The variety of components, factors, and failure modes creates a multitude of interactions, which make the reality of cumulative effects difficult to quantify.

3.1.2.2 STC Technical Data Sheet Information

A typical PV module nameplate label is shown in Figure 32, and includes IV curve related information. A typical manufacturer's PV module technical datasheet is shown in Figure 33, and includes electrical parameters, such as power tolerance and temperature coefficients, in addition to power warranty information. For the purpose of discussion in the upcoming sections, Table 6 provides examples of 3 different manufacturers of 5 major materials used in the production of PV modules. The purpose of this table is to highlight the diversity in manufacturer specifications, even for modules with similar DC power ratings. This is why it is important to understand the individual parameters and not generalize PV performance according to material type (e.g. crystalline silicon versus thin-film).

Figure 32: Typical information required for a PV module nameplate label.

Manufacturer 123		
Made in Country ABC		
Model	XYZ	Serial Number 123456789
Performance at Standard Test Conditions: (1) 1,000 W/m ² of sunlight, (2) 25°C cell temperature, and (3) spectrum at air mass of 1.5.		
Max Power (P_{mp})	Voltage at P_{max} (V_{mp})	Current at P_{max} (I_{mp})
170 W	35.4 V	4.8 A
Open-circuit Voltage (V_{oc})	Short-circuit Current (I_{sc})	
44.2 V	5.0 A	
Max System Voltage	Max Series Fusing	
600 V	15 A	

Figure 33: Typical Manufacturer's Technical Datasheet (Hren 2011)

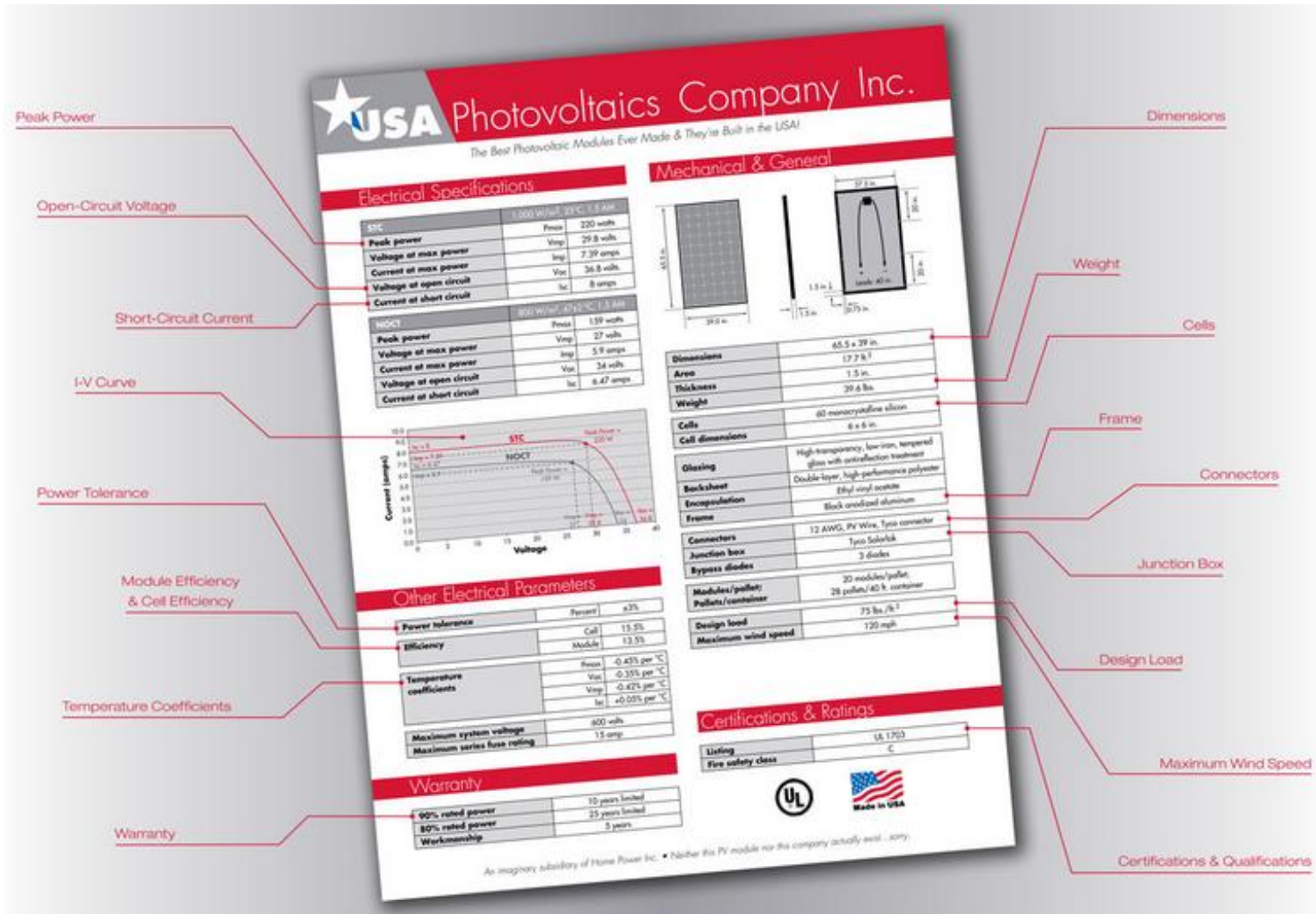


Table 6: Sample list of modules and attributes.

Technology	Manufacturer	Model	Module Efficiency	DC Rating (Wp)	Temperature Coefficient (%/°C)	Power Tolerance	Power Output Warranty
Monocrystalline Silicon	Sharp Electronics Corporation	NU-U235F1	14.40%	235	-0.485	+10% / -5%	25
	Canadian Solar	CS6P-235M	14.61%	235	-0.45	+5% / -0%	10 (at 90%), 25 (at 80%)
	Isofoton	ISF-250	15.10%	250	-0.44	+3% / -0%	10 (at 90%), 25 (at 80%),
Polycrystalline Silicon	Sharp Electronics Corporation	ND-224UC1	13.74%	224	-0.485	+10% / -5%	25
	Kyocera	KD220GX-LFBS Blk	Not available	220	-0.46	+5% / -3%	10 (at 90%), 20 (at 80%)
	REC	230PE BLK	13.90%	230	-0.4	+5% / -0%	10 (at 90%), 25 (at 80%)
Amorphous Silicon	United Solar Ovanic	PVL-68	Not available	68	-0.21	+/-5%	20 (at 80%)
	Xunlight	XRU-10	Not available	71	-0.23	+/-5%	25 (at 80%)
	Schott Solar	SCHOTT ASI 95	6.60%	95	-0.2	+/-5%	25
Cadmium Telluride	First Solar	FS-272	10.07%	72.5	-0.25	+/-5%	10 (at 90%), 25 (at 80%)
	General Electric	GE-CdTe78	10.80%	78	-0.25	+/-5%	Not available
	Calyxo	CX75	Not available	75	-0.25	+/-5%	10 (at 90%), 25 (at 80%)
Copper Indium Gallium Selenide	Solyndra	SL-200-182	Not available	182	-0.38	+/-4%	25
	Manz	m-ges101	14.6	104.8	-0.36	+2.5% / -0%	Not available
	Solar Frontier	SF160-S	13%	160	-0.31	+10% / -5%	Not available

3.1.2.3 DC Power Rating

The DC power rating is the standard “industry talk” for stating the expected PV module DC electricity generation at standard test conditions (STC), including 1,000 W/m² solar irradiance, 25°C PV module temperature, and 1.5 air mass. However, scientists and researchers, in general, tend to prefer the focus on cell efficiency and module efficiency with the hope to increase the efficiencies while decreasing cost. This section will explain the relationship between efficiency and DC power rating.

Conversion efficiency is often considered at both the cell and module level, as shown in Table 7. Understandably so, module efficiency will always be lower than cell efficiency – the more components, the lower the efficiency and overall reliability. Conversion efficiency is a ratio of incoming sunlight to outgoing electricity produced, given an irradiance of 1000 watts per square meter (STC). For example, if there is a one square meter crystalline silicon panel with an efficiency of 13%, this implies the panel will generate 130 watts, which would be the listed DC power rating. Typically module efficiencies are shown in Table 7. Conversion efficiency, although interesting to note, is typically not provided on module technical datasheets. Instead, the DC power rating is given.

Table 7: Typical Module Efficiencies

Technology	Module Efficiency	Best Cell Efficiency (NREL)
Monocrystalline Silicon	12 – 15%	25%
Polycrystalline Silicon	11 – 14%	20.4%
Copper Indium Gallium Selenide (CIGS)	10 – 13%	20.4%
Cadmium Telluride (CdTe)	9 – 12%	19.0%
Amorphous Silicon (a-Si)	5 – 7%	13.4%

The relationship between DC power rating and module conversion efficiency can be calculated through the following equation:

$$\text{Conversion Efficiency} = \left(\frac{\text{DC Power Rating (W)}}{\text{Module Size (m}^2\text{)}} \right) \div \text{STC Solar Irradiance} \left(\frac{\text{W}}{\text{m}^2} \right)$$

The equation can be shown using the Canadian Solar polycrystalline silicon example from Table 6. The calculated conversion efficiency is consistent with the information obtained from the table.

$$\text{DC Power Rating} = 235 \text{ W}$$

$$\text{Module Size (obtained from technical datasheet)} = 1.638\text{m} \times 0.982\text{m} = 1.609\text{m}^2$$

$$\text{STC Solar Irradiance (standard)} = 1000\text{W/m}^2$$

$$\text{Conversion Efficiency} = \left(\frac{235\text{W}}{1.609\text{m}^2} \right) \div 1000 \frac{\text{W}}{\text{m}^2} = 0.1461 = 14.61\%$$

There is a clear and concise relationship between conversion efficiency and DC power rating. Scientists and researchers alike, tend to focus efforts on cell and module efficiency. Ultimately, these are the people charged with innovating and improving cell efficiency. However, from a practical standpoint, industry people are more concerned with DC power rating because this is what is most important to the consumer, who wants to know how much it will cost per W of power and the expected electricity savings in kWh. The remainder of this section will use the DC power rating to show the impacts of temperature coefficient, power tolerance, and power warranty.

3.1.2.4 Power Tolerance

The power tolerance is the upper and lower (+/-) value with relationship to DC power rating. For example, given the DC power rating of 235 W and the power tolerance of +10%/-5%, the upper and lower DC power rating would be calculated as follows.

$$\text{Lower DC power rating} = 235 + (235 \times 10\%) = 258.5 \text{ W}$$

$$\text{Upper DC power rating} = 235 - (235 \times 5\%) = 223.25 \text{ W}$$

It is important to note that the lower DC power rating, in this case 223.25 W, is the quantity DC power actually warranted through the module's power warranty (the power warranty is further discussed in the next section). Power tolerance has less to do with the specific technology and is highly dictated by the manufacturer and production process. The manufacturing technical datasheet should list the power tolerance values in an effort to provide the consumer with a well-rounded expectation of system performance. Since the lower DC power rating is the value actually warranted by the manufacturer, it is recommended to use this value when considering the DC power rating of the system.

3.1.2.5 Temperature Coefficient

A change in temperature, from the STC 25° C, impacts the PV array voltage production for the majority of PV technologies, including crystalline silicon and thin-film technologies. This section will first explain how voltage and current work together to create power. Next, it will explain how the temperature coefficient influences the production of DC power.

Figure 34 shows a sample module technical datasheet for the Aleo 225 W, a polycrystalline silicon PV module. The numbers of importance include the Rated Power ($P_{MPP} = 225\text{W}$), Rated Voltage ($U_{MPP} = 28.9\text{V}$), Rated Current ($I_{MPP} = 7.78\text{A}$), Open-Circuit Voltage ($U_{OC} = 36.4\text{V}$), and Short-Circuit Current ($I_{SC} = 8.34\text{A}$).

Figure 34: Module Technical Datasheet Aleo 225W (Aleo Solar AG 2011)

aleo s_18 sol

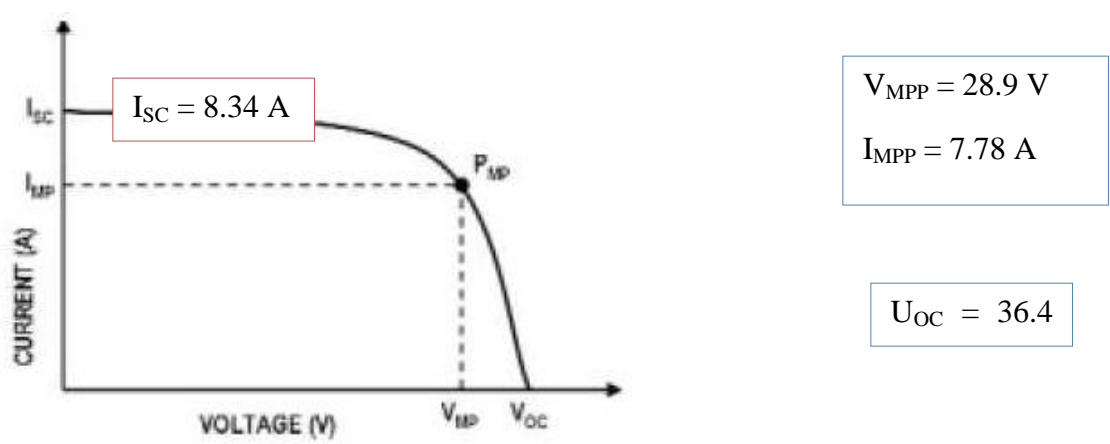
Electrical data (STC)			S 18.220T	S 18.225T	S 18.230T
Rated power	P_{MPP}	[W]	220	225	230
Rated voltage	U_{MPP}	[V]	28.7	28.9	29.1
Rated current	I_{MPP}	[A]	7.65	7.78	7.90
Open-circuit voltage	U_{OC}	[V]	36.3	36.4	36.6
Short-circuit current	I_{SC}	[A]	8.24	8.34	8.44
Efficiency	η	[%]	12.7	13.0	13.3
Area-to-power ratio	A_p	[m ² /kW _p]	7.86	7.69	7.52

Electrical values measured under standard test conditions (STC): 1000 W/m²; 25°C; AM 1.5

Temperature coefficients			
1 st temperature coefficient	$\alpha (I_{SC})$	[%/K]	+0.04
2 nd temperature coefficient	$\beta (U_{OC})$	[%/K]	-0.34
3 rd temperature coefficient	$\gamma (P_{MPP})$	[%/K]	-0.46

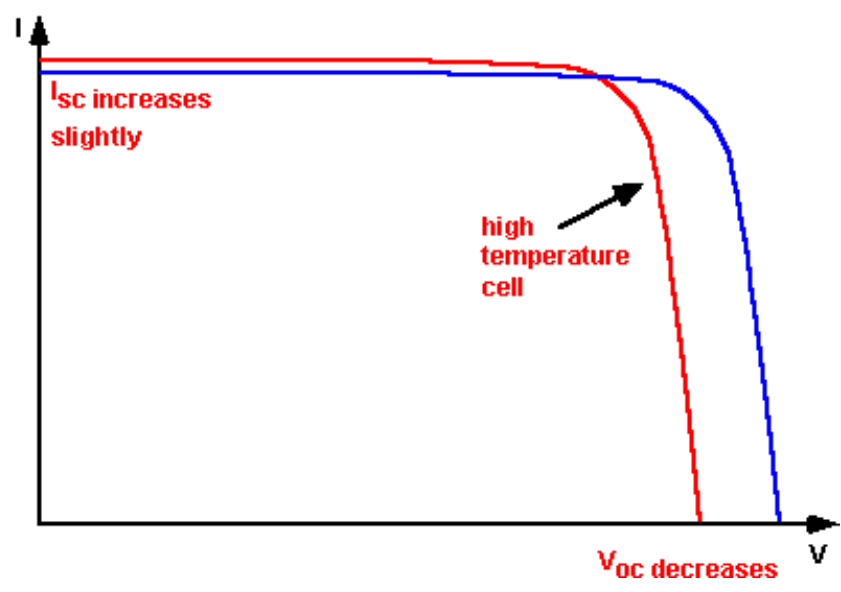
These indices can be best understood through the PV module I-V curve, as shown in Figure 35. The short circuit current (I_{SC}) is the maximum current at zero volts. Similarly, the open-circuit voltage (U_{OC}) is the maximum voltage at zero amps. The “knee” of the curve represents the rated power, also known as the maximum power point (P_{MPP}), which is the product of the rated voltage (U_{MPP}) and rated current (I_{MPP}), generating the maximum electrical DC power.

Figure 35: Aleo 225W PV Module I-V Curve



The figure above displays the maximum power point at constant temperature, STC 25° C. However, as temperatures increase, the voltage decreases and the current only slightly increases, thus decreasing power. Conversely, when temperatures decrease the voltage increases and the current only slightly decreases, thus increasing power. Figure 36 visually portrays the influence of temperature on the I-V curve.

Figure 36: Example portraying the influence of temperature on the I-V curve



The expected change in maximum power point (P_{MPP}) can now be calculated.

$$P_{MPPnew} = P_{MPP} + (P_{MPP} * (T_m - NOCT) * P_{MPP}TempCoef)$$

P_{MPPnew} = new maximum power point

P_{MPP} = maximum power point (see manufacturer technical datasheet)

T_m = module temperature

NOCT = Nominal operation cell temperature = 25° C

$P_{MPP}TempCoef$ = temperature coefficient at P_{MPP} (see manufacturer technical datasheet)

As an example for an *increase* in temperature, we will assume the module temperature (T_m) is 51.25° C and the solar irradiation (E) is 1000 W/m². Using information based on the Aleo technical datasheet, the maximum power point (P_{MPP}) is 225 W and the temperature coefficient at P_{MPP} is -0.46%/°C. The expected power can now be calculated.

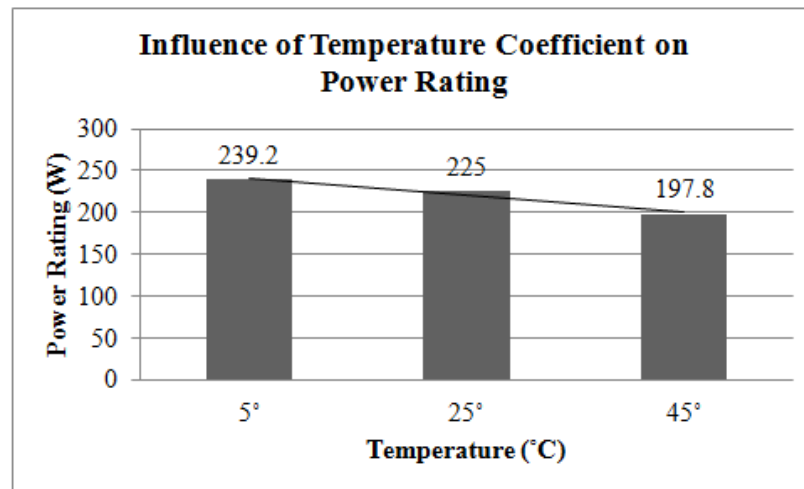
$$P_{MPPnew} = 225W + (225W * (51.25°C - 25°C) * -0.0046) = 197.8W$$

As an example for a *decrease* in temperature, assuming the module temperature (T_m) is 11.25° C and the solar irradiation (E) is 1000 W/m². Using information based on the Aleo technical datasheet, the maximum power point (P_{MPP}) is 225 W and the temperature coefficient at P_{MPP} is -0.46%/°C. The expected power can now be calculated.

$$P_{MPPnew} = 225W + (225W * (11.25°C - 25°C) * -0.0046) = 239.2W$$

In summary, keeping the solar irradiation constant and simply comparing a change in temperature, the following results can be observed in Figure 37. As the temperature increases, the power rating decreases.

Figure 37: Example results for change in temperature

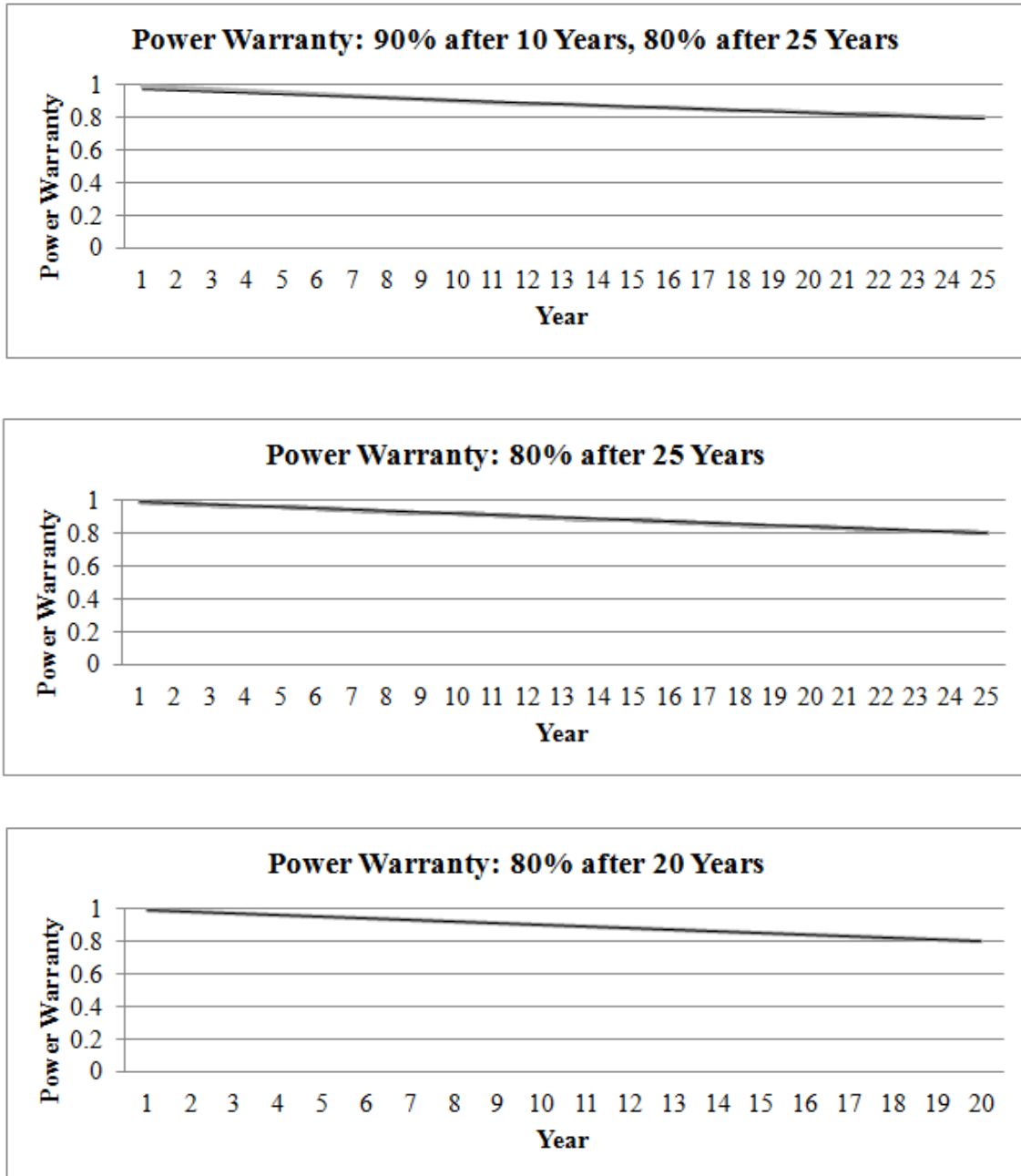


3.1.2.6 Power Warranty

The power warranty, located on the technical datasheet, is an indication of the expected life or stability of the solar module itself. Aging and degradation are part of the natural life cycle for any electronic, and in general, it is estimated that modules typically degrade less than 1% per year (Jordan, Smith et al. 2010). However, if a power warranty is provided, the actual degradation can be estimated through a linear regression.

For example, common power warranties include (1) 90% after 10 years, 80% after 25 years, (2) 80% after 25 years, and (3) 80% at 20 years. As such, the power warranty derate factor associated with these options are shown in Figure 38.

Figure 38: Example Warranty Degradation Derate Factors



3.2 DC and AC Wiring Losses

First of all, when it comes to wiring, all PV system configurations will have to consider DC wiring losses. However, AC wiring losses only apply to those system

configurations with an inverter, which converts the DC electricity to household usable AC electricity.

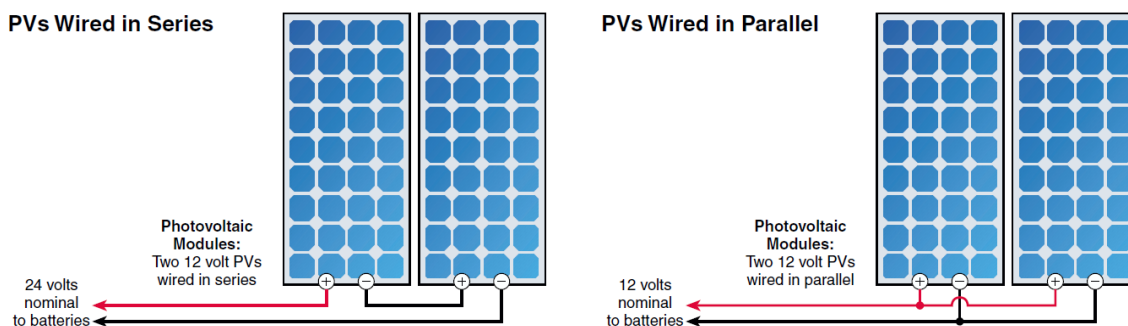
There are two main considerations when wiring a PV system. First, the installer must decide to wire in series or parallel. This decision is highly dependent upon the voltage size of other system components, including battery, charge controller, and inverter. Second, the installer must figure out the correct wire size to ensure proper resistance capabilities. Once the PV system is installed and ready for commissioning, the PV wire insulation resistance should be tested to assess the quantity of losses, if any, due to the DC and AC wiring.

3.2.1 Wiring Considerations

3.2.1.1 Series vs. Parallel

PV modules can be wired in series or in parallel, as shown in Figure 39. The option of applying series or parallel wiring, or a combination thereof, results in the same quantity of power output. However, PVs wired in series produce more volts and fewer amps; PVs wired in parallel produce fewer volts and more amps. Using Figure 39 as an example, each module panel is measured at 12 volts DC and 2 amps. When PV modules are wired in series, the volts are additive, resulting in 24 volts DC and 2 amps for a total of 48 watts ($P = V \times A$). When PV modules are wired in parallel, the amps are additive, resulting in 12 volts DC and 4 amps for a total of 48 watts. In either case, the watts (or power) stays the same. However, the voltage quantity is often dictated by inverter requirements. The larger the inverter, the larger the voltage required to ensure inverter efficiency. A mismatch in system components (module, inverter, wiring, etc...) can lead to a change in performance outcomes.

Figure 39: Series vs Parallel (Schwartz 2002)



3.2.1.2 Wire Size

Wire size selection takes into consideration ampacity and voltage drop. Ampacity is the maximum allowable amount of electrical current a conductor can carry before deteriorating. Voltage drop is the voltage loss due to wire resistance, which is influenced by temperature, wire size, length, and current. As a rule of thumb, voltage drop should be 3% or less (California Energy Commission 2001), which equates to about 2% on the DC wiring and about 1% on the AC wiring, so that the total voltage drop from the PV array to the utility meter should be 3% or less. There are many cable size calculators freely available online.

3.2.2 Insulation Resistance Testing

Insulation resistance testing is assessed using a megohmmeter, such as a Megger (Figure 40). The megohmmeter tests the overall insulation resistance in PV systems, measuring the quantity of DC or AC current, if any, lost to ground. The megohmmeter works by applying an extremely large DC voltage to test the high resistance of the conductor. This device will verify power losses due to DC and AC wiring.

Figure 40: Megger Megohmmeter



3.3 DC-AC Inverter

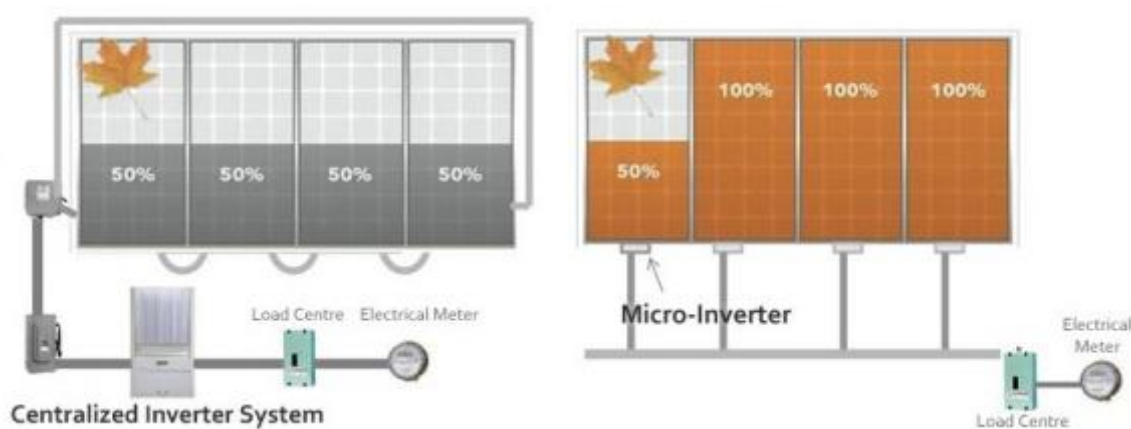
The purpose of the inverter is to convert DC electricity, generated by the PV array, into AC electricity required by the utility grid and most household appliances. Inverters can be used in both off-grid and utility grid-tied configurations. However, the requirements for grid-tied inverters are more stringent due to safety concerns if and when the grid shuts down. Grid-tied inverters must be equipped with anti-islanding protection, an automatic shut-off for when the grid goes down, ultimately preventing utility linemen from being electrocuted by a distributed generation source. There are two main categories influencing the overall inverter performance and efficiency. These are inverter specific information (inverter efficiency and warranty) and PV module related issues (module mismatch, shading, soiling, and diodes and connections) applicable to central string inverters only.

3.4.1 Inverter Specific Information

There are two general types of inverters used in AC-based PV systems, which include string or central inverters, and micro inverters. A string inverter connects PV arrays in series, like a string, to one central inverter. In contrast, the micro inverter

connects PV arrays in parallel, allowing each PV array its own inverter. Central inverters require all modules to be the same size, orientation, and tilt. Micro inverters allow modules to be different size, orientation, tilt. As shown in Figure 41, in a central inverter system, a small leaf shading a portion of the one solar panel will influence the performance outcome of all panels. However, in the micro inverter system, each panel has its own individual inverter, promoting maximum array performance.

Figure 41: Centralized Inverter vs Micro inverter (CPS Solar Retrieved 07/01/14)



Taking into consideration overall PV system efficiency, the central inverter is less efficient in comparison to its more expensive counterpart, the microinverter. Central inverters allow the impacts of one module to impact the output for all modules. Regardless of the issue (module mismatch, shading, soiling, or diodes and connections), if one module's performance decreases, the performance of all modules decrease.

3.4.2 Inverter Efficiency

The choice of inverter depends on the PV array size, in terms of watts, the output voltage required for the residential applications, commonly 240 volts AC, and the range of DC input voltage expected from the PV array.

Figure 42: Example String Inverter Specification Data Sheet (PV Powered 2009)

ELECTRICAL SPECIFICATIONS

MODEL	PVP1100	PVP2000	PVP2500	PVP2800	PVP3000	PVP3500	PVP4600	PVP4800	PVP5200
Continuous Output Power (watts)	1100	2000	2500	2800	3000	3500	4600	4800	5200
Weighted CEC Efficiency (%)	90.5	92	94.5	92	93.5	95.5	95.5	96	96
Maximum DC Input Voltage (VOC)	500	500	500	500	500	500	500	500	500
DC Voltage Operating Range (V)	115-450	115-450	140-450	180-450	170-450	200-450	205-450	200-450	240-450
DC Minimum Start Voltage	130	130	155	195	185	215	220	215	255
DC Isc Maximum Current (A)	26	26	26	26	26	26	48	48	48
DC Imp Nominal Current (A)	10	18	20	18	18	18	25	26	25
AC Maximum Continuous Current (Amps)	10	9	11	13	13	15	23	21	23
AC Nominal Voltage (V)	120	240	240	208	240	240	208	240	240
AC Output Voltage Range (V)	105.6-132.5	211-264	211-264	183-229	211-264	211-264	183-229	211-264	211-264
AC Frequency Range (Hz)	59.3-60.5	59.3-60.5	59.3-60.5	59.3-60.5	59.3-60.5	59.3-60.5	59.3-60.5	59.3-60.5	59.3-60.5

MECHANICAL SPECIFICATIONS

MODEL	PVP1100	PVP2000	PVP2500	PVP2800	PVP3000	PVP3500	PVP4600	PVP4800	PVP5200	
Inverter with Factory-Integrated AC and DC PV System Disconnect										
NEMA 3R Steel Enclosure, Wall Mount Bracket Included										
Temperature	-25°C to 40°C									
Weight (lbs)	55	65	70	80	80	85	135	135	135	
Inverter with Disconnect Dimensions	30 3/8" H x 15 5/8" W x 8 1/4" D	30 3/8" H x 15 5/8" W x 8 1/4" D	30 3/8" H x 15 5/8" W x 8 1/4" D	30 3/8" H x 15 5/8" W x 8 1/4" D	30 3/8" H x 15 5/8" W x 8 1/4" D	30 3/8" H x 15 5/8" W x 8 1/4" D	30 3/8" H x 15 5/8" W x 8 1/4" D	35" H x 18 1/8" W x 8 5/8" D	35" H x 18 1/8" W x 8 5/8" D	35" H x 18 1/8" W x 8 5/8" D

AGENCY APPROVALS

MODEL	PVP1100	PVP2000	PVP2500	PVP2800	PVP3000	PVP3500	PVP4600	PVP4800	PVP5200
-------	---------	---------	---------	---------	---------	---------	---------	---------	---------

UL 98 13th Edition, Enclosed and Dead-Front Switches, UL 1741 Nov 2005 Revision, CSA C22.2 107.1 2006 Revision, IEEE 1547 Compliant, FCC Class A & B

The inverter manufacturer's specification data sheets list the electrical specifications, which include the inverter efficiency. Specifically, the data sheet should call out the Weighted CEC Efficiency. Using the example, as shown in Figure 42, the weighted CEC efficiency for a string inverter model PVP1100 is 90.5%.

Due to reasons mentioned in the previous section, theoretically, a group of microinverters that optimize the strength of each individual panel, should be more efficient than a string inverter that optimizes to the weakest solar panel.

3.4.3 Inverter Warranty

There are many ways inverters can fail, however, the most vulnerable inverter component is the dc-bus capacitor (Ton and Bower 2005). Inverter failure can occur due to various reasons, including but not limited to lightning strike, plumbing failure, ground fault and PCU fan (Ristow, Begovic et al. 2008).

Table 8: Example Inverter Warranties

Manufacturer	Website	Warranty Years	Inverter Type	Country
SMA Solar Technology of America	www.sma-america.com	5 or 10	Central	Germany
Power One (Aurora)	www.power-one.com	5 or 10	Central	U.S.
Schneider Electric	www2.schneider-electric.com/sites/corporate/en/products-services/solar	5	Central	U.S.
Fronius	www.fronius.com	10	Central	U.S.
Enphase	www.enphase.com	25	Micro	U.S.
Enecsys	www.enecsys.com	25	Micro	United Kingdom
SolarBridge Technologies	www.solarbridgetech.com	25	Micro	U.S.
Siemens	w3.usa.siemens.com/powerdistribution/us/en/product-portfolio/microsolar	25	Micro	U.S.

Central inverters tend to come with 5-10 year warranties, while microinverters typically have a 20-25 year warranty. As such, string inverters will typically need to be replaced throughout the life of the system. Table 8, obtained 03/09/2014, provides example inverter warranties for both string inverters and microinverters.

3.4 Utility Grid Availability

The availability of the utility grid is only of concern for grid-tied PV systems. Grid-tied PV systems are legally required to feature an anti-islanding function that shuts down the inverter, and thus entire PV system, whenever the utility grid is down. This feature prevents utility workers from being electrocuted when attempting to bring the utility grid back up.

Within the United States, the Federal Energy Regulatory Commission (FERC) has sanctioned individual states to oversee the regulation of utility distribution systems (Hesmondhalgh, Zarakas et al. 2012). The FERC requires states to provide a high quality of service to its customers. However, the FERC does not specify how the quality is assessed and furthermore, the FERC does not require individual states to report on the quality of service. That being said, most states do require energy distributors to track and report several reliability distribution metrics, commonly keeping distributors motivated with targeted utility availability goals.

The North American Electric Reliability Corporation (NERC) is a non-profit organization focused on assuring reliability of the power systems throughout North America, through development and enforcement of reliability standards.

The most common standard utility reliability, or distribution reliability, indices include SAIDI (System Average Interruption Duration Index), SAIFI (System Average

Interruption Frequency Index), CAIDI (Customer Average Interruption Duration Index), MAIFI (Momentary Average Interruption Frequency Index), and ASAI (Average System Availability Index) (Pham 2003). However, for the purpose of understanding grid availability, ASAI is the most appropriate metric, as it is a representation of grid uptime or grid availability.

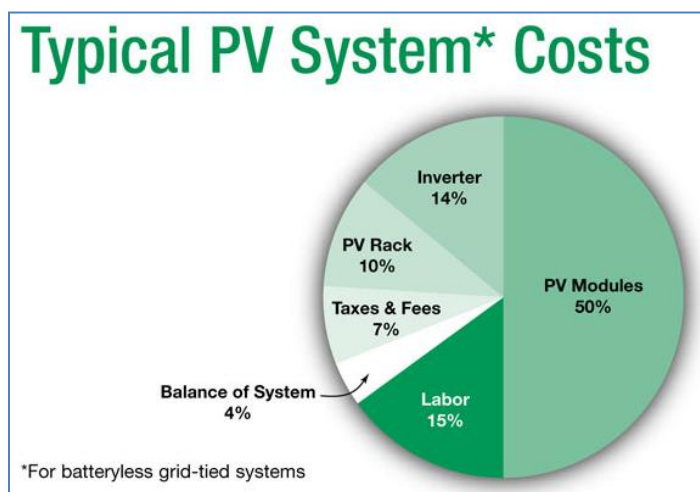
3.5 System Costs

Cost varies depending on application, customer, industry segment, type of PV material used (technology), state and federal incentives, and utility rates. Applications of solar energy technology can include lighting, battery charging, supplying electricity to the power grid, and water pumping. Customers typically include commercial, residential, and utility. Industry segments can include manufacturing, service, and transportation. The types of PV material can include crystalline silicon and thin film technologies. State and federal incentives can be in the form of tax write-offs, rebates, discounts, and reimbursements. Utility rates can be offered through net-metering and/or feed-in tariffs. All of these factors and more influence the decision to invest in photovoltaic technology and its anticipated return on investment.

This section will provide an overview of the costs of investing in a PV system. In general, typical grid-tied PV system costs can be categorized according to Figure 43, with the PV modules accounting for about 50% of the overall PV system costs. Together, the inverter, PV racking, and labor account for about 40% of the overall PV system costs, with taxes & fees and balance of system entailing the final 10%. For the purpose of this

section, the PV System Costs will be split between PV Modules and Balance of System (including labor and installation, inverter, racking, and taxes and fees).

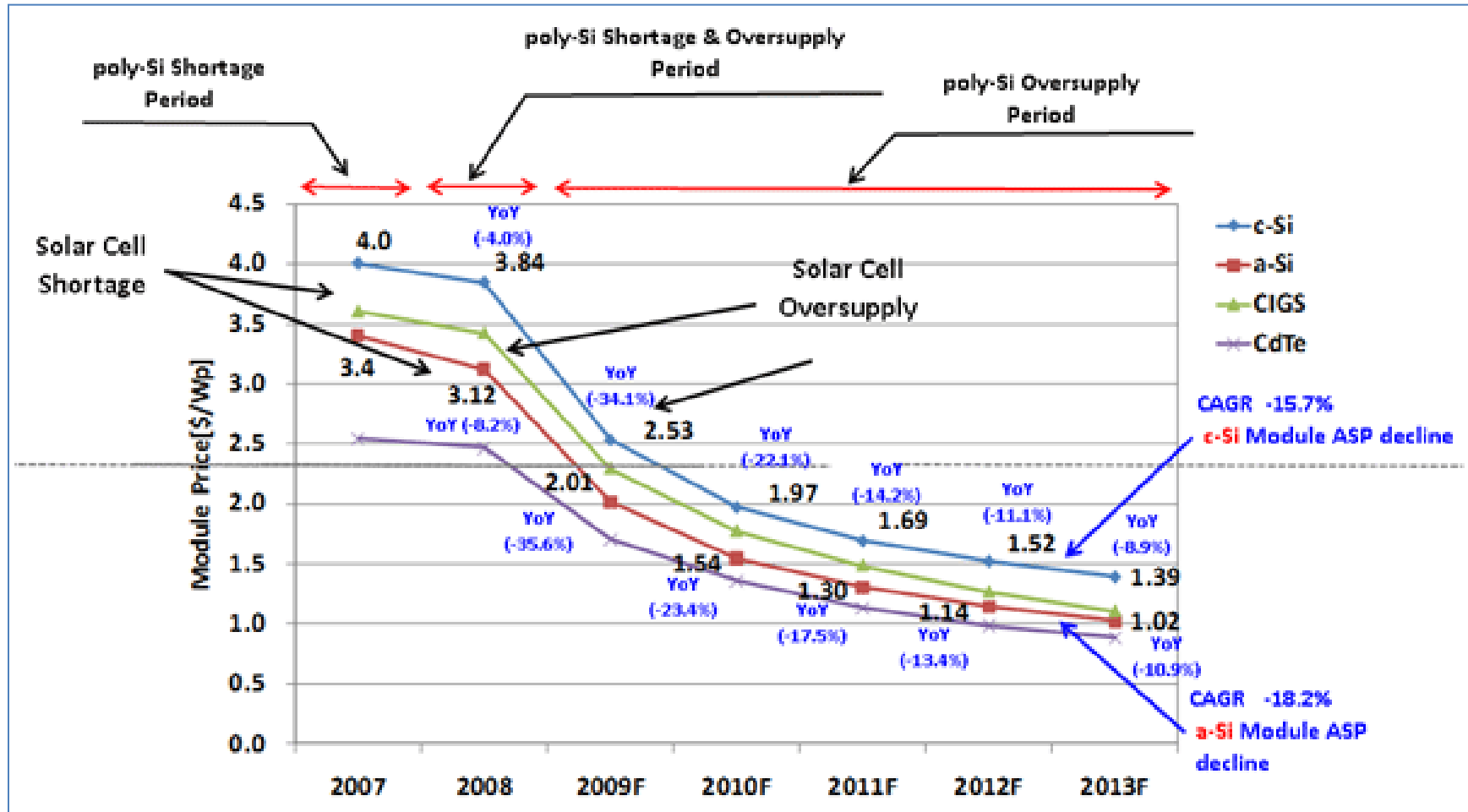
Figure 43: Typical PV System Costs (Schwartz, Woofenden et al. 2013)



3.5.1 PV Modules

From 2008 to 2012, PV module prices have fallen about 80% (Shahan 2013). As of 2013, Figure 44 shows that crystalline silicon modules are about \$1.39/W and thin-film amorphous silicon is about \$1.02/W. According to one Chinese producer, Best-in-Class, the key drivers in PV cost reduction are (1) avoid cost increases due to labor rates, savings estimated at about \$0.02/W, (2) drive down consumables pricing, savings estimated at about \$0.036/W, (3) incorporation of innovative technology, savings estimated at about \$0.069/W, (4) focus on economies of scale, savings estimated at about \$0.028/W, and (5) investing in automation, savings estimated at about \$0.028/W (Carus 2013). That being said, the levelized cost of energy (LCOE) is considered a better metric. It assesses the overall competitiveness of generating technologies over the expected life of the technology, taking into consideration utilization rates and costs related to initial capital, fuel, maintenance and operation, and financing.

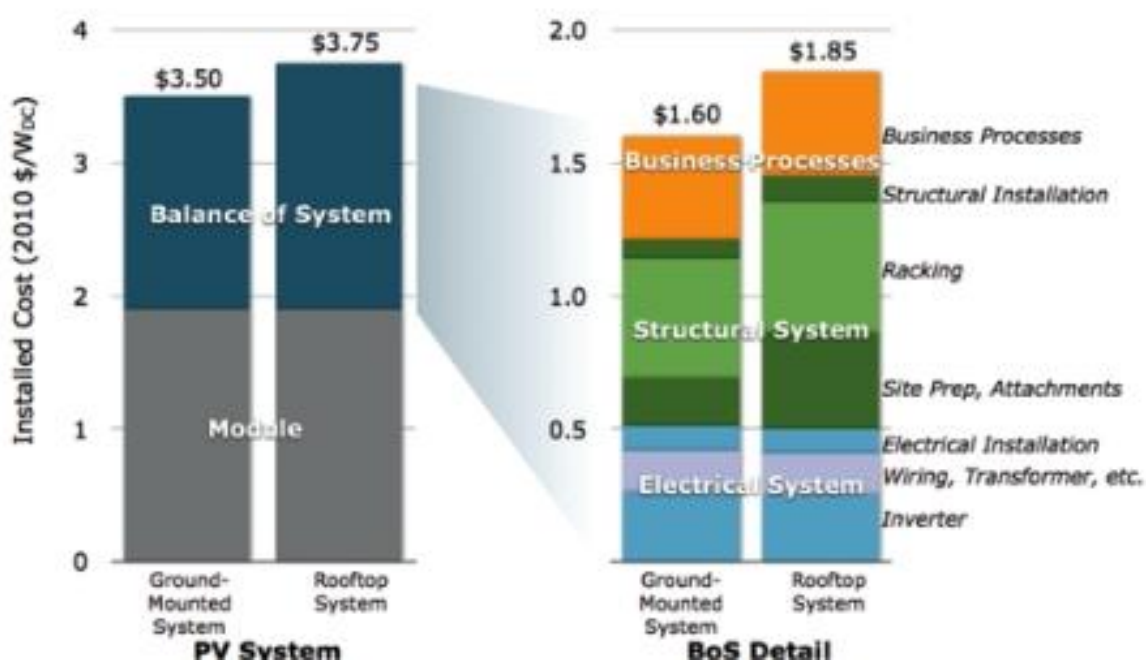
Figure 44: Solar Module Price Trends 2007-2013 (SNE Research 2009)



3.5.2 Balance of System

The Balance of System, as shown in Figure 45, can be broken down into three groupings including Electrical System (inverter, electrical installation, wiring, and transformer), Structural System (racking, structural installation, site prep and attachments), and Business Processes (taxes, fees, and other paperwork). The major difference in pricing between a ground mounted system and rooftop system, is the structural component (e.g. site prep and attachments).

Figure 45: Cost breakdown of conventional U.S. PV system (Browning 2011)

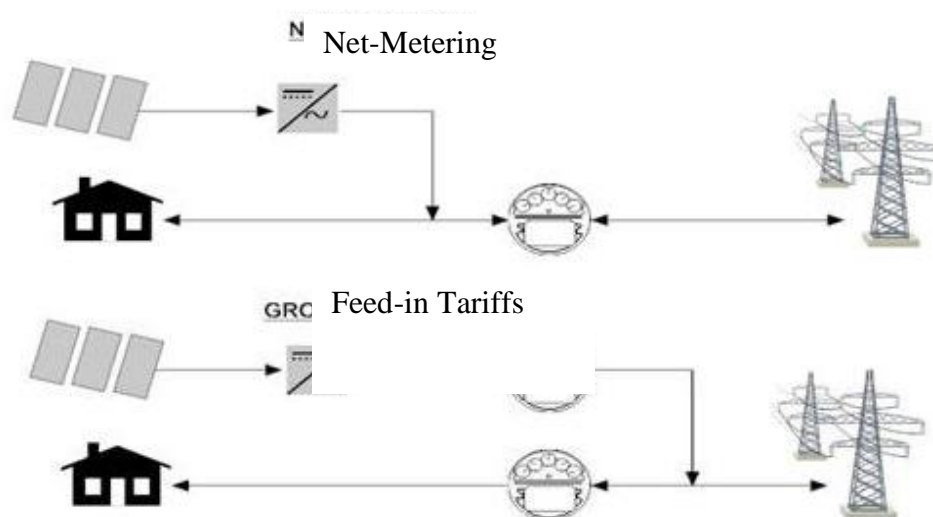


3.6 Grid-Tied Electricity Rates

Within the United States, utility companies commonly offer one of two electricity rate policies for use with PV applications, net-metering and feed-in-tariffs, as shown in Figure 46. Net-metering uses one meter that keeps track of electricity pulled from the utility grid. However, net-metering uses PV generated electricity when available, prior to

using utility-generated electricity. If a customer produces more PV-generated electricity than is used, sometimes utility companies allow the excess to be credited to the customer's account on a periodic basis. Thus, essentially, the customer is credited at the same rate for consumption and production. Feed-in-tariffs (FIT) are a second, more complex option for utilities to implement. Here, customers have two separate meters; one meter measures electricity consumed from the utility grid and a second meter measures electricity generated by the PV system. This option allows utility companies to offer different rate schemes for both electricity generation and electricity consumption. Then, on a periodic basis, a check is sent to the customer for any electricity generated.

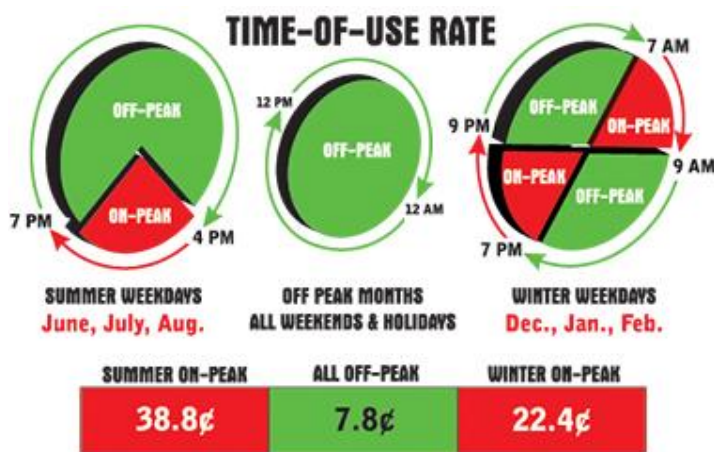
Figure 46: Net-metering vs. Feed-in tariffs (Austech Forums Jan 2008)



Utility companies often supplement the rate policies with additional time-of-use and tiered-use incentives, or a combination thereof. Time-of-use incentives change the rate depending upon the time of day and season the electricity is consumed (or in the case of FIT, when the electricity is generated). Figure 47 shows that electricity consumed during the summer on-peak 4pm-7pm is about five times as expensive, \$0.388, than

electricity consumed during the off-peak 7pm-4pm, \$0.078. This is likely because 4pm-7pm are prime hours for customers coming home from work, turning on air conditioners, using kitchen appliances to make dinner, relaxing and watching television, running a load of laundry, and doing other miscellaneous household chores eating up electricity. Furthermore, the chart shows that during the winter weekdays, the on-peak rates run from 7am-9am and 7pm-9pm. This is likely because customers are turning up the heat first thing in the morning as they get ready for work and last thing at night while they settle in to sleep. In conclusion, the time-of-use rate encourages customers to use less electricity during on-peak hours to save money on the utility bill. This also helps the utility companies better manage electricity needs throughout the designated area. From a PV perspective, customers can use PV-generated electricity during the on-peak times to offset the greater cost of electricity during on-peak times.

Figure 47: Example Time-of-Use Rate Strategy (Bartholomew County REMC Obtained 07/01/2013)

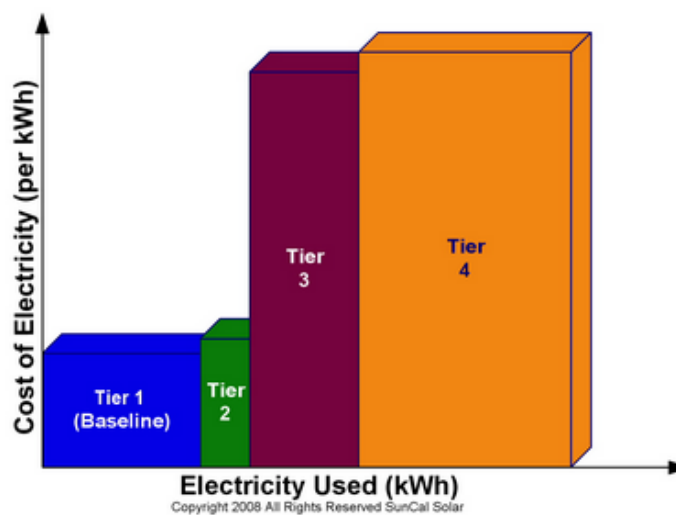


Tiered electricity rates increase as the consumption increases, as shown in Figure 48. For example, let's consider a billing scheme as \$0.0955 per kWh for Tier 1 (first 500 kWh), \$0.1112 per kWh for Tier 2 (501 kWh to 600 kWh), \$0.2974 per kWh for Tier 3

(601 kWh to 900 kWh), and \$0.3452 for Tier 4 (anything over 901 kWh). The more electricity is consumed by the customer, the more expensive the cost per kWh. Thus, utility electricity consumed at the end of the month costs more than at the beginning of the month. Likewise, PV generated at the end of the month creates more value than PV generated at the beginning of the month.

Utility companies can also run a combination of incentives to lower electricity consumption and/or increase PV electricity generation during certain times. Some combination examples include (1) Tiered + Time-of-Use, (2) Tiered + Seasonal, (3) Time-of-Use + Seasonal, and (4) Tiered + Time-of-Use + Seasonal. Additionally, utility companies may offer monthly credit rollovers to account for PV electricity generated throughout the year.

Figure 48: Visual Illustration Depicting Tiered Electricity Rate Plans



3.7 U.S. Federal and State Incentives for Investing in PV System

The Database of State Incentives for Renewables and Efficiency (DSIRE) is the go-to website (dsireusa.org) to learn about federal and state incentives for the United States market. Incentives can be found at www.dsireusa.org, and are available for both residential and commercial and typically include net-metering and feed-in tariffs (Figure 49), grant programs (Figure 50), property tax credits (Figure 51), sales tax incentives (Figure 52), rebate programs (Figure 53), tax credits and accelerated depreciation (Figure 54), loan programs (Figure 55), and other renewable energy credits.

Figure 49: U.S. Net Metering Policies

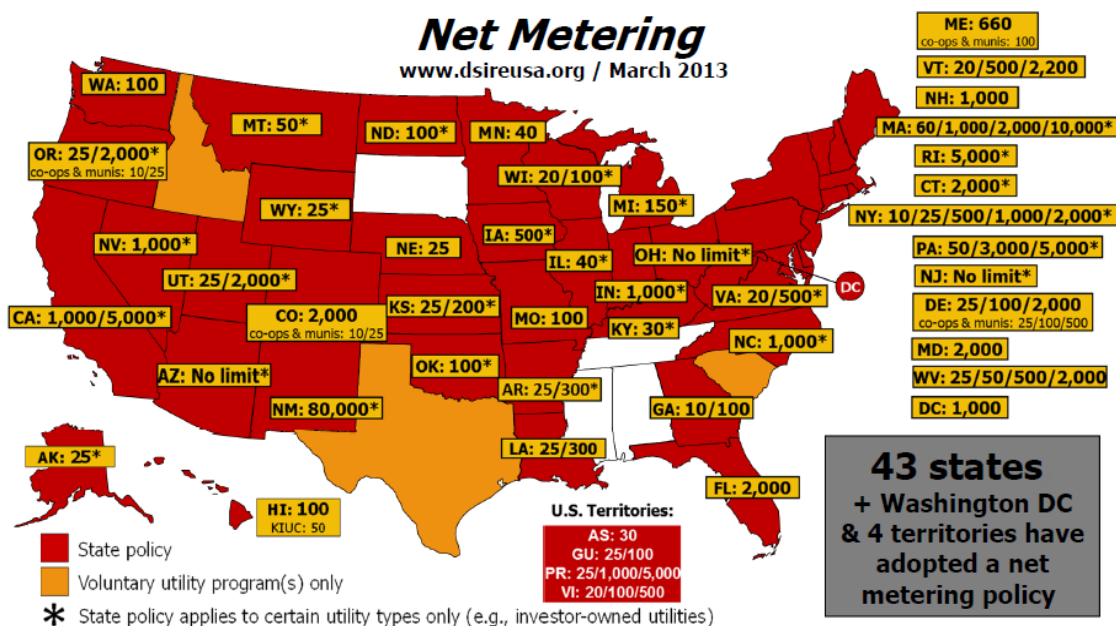


Figure 50: U.S. Grant Programs for Renewable Energy

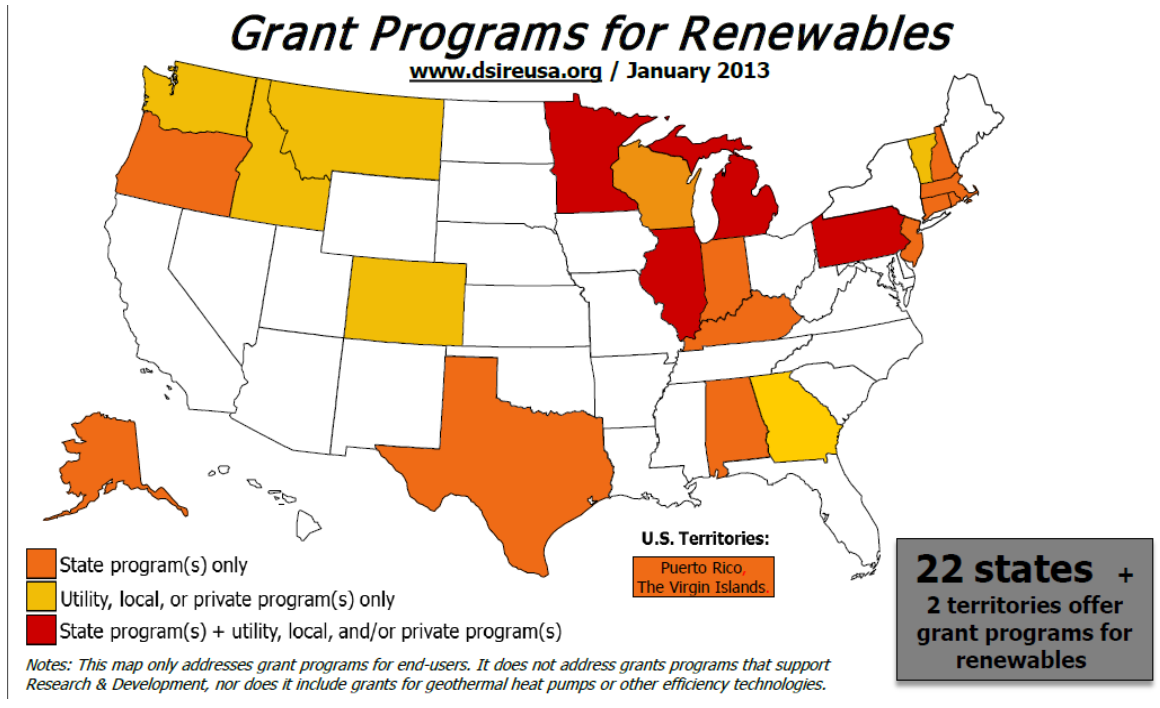


Figure 51: U.S. Property Tax Credits for Renewable Energy

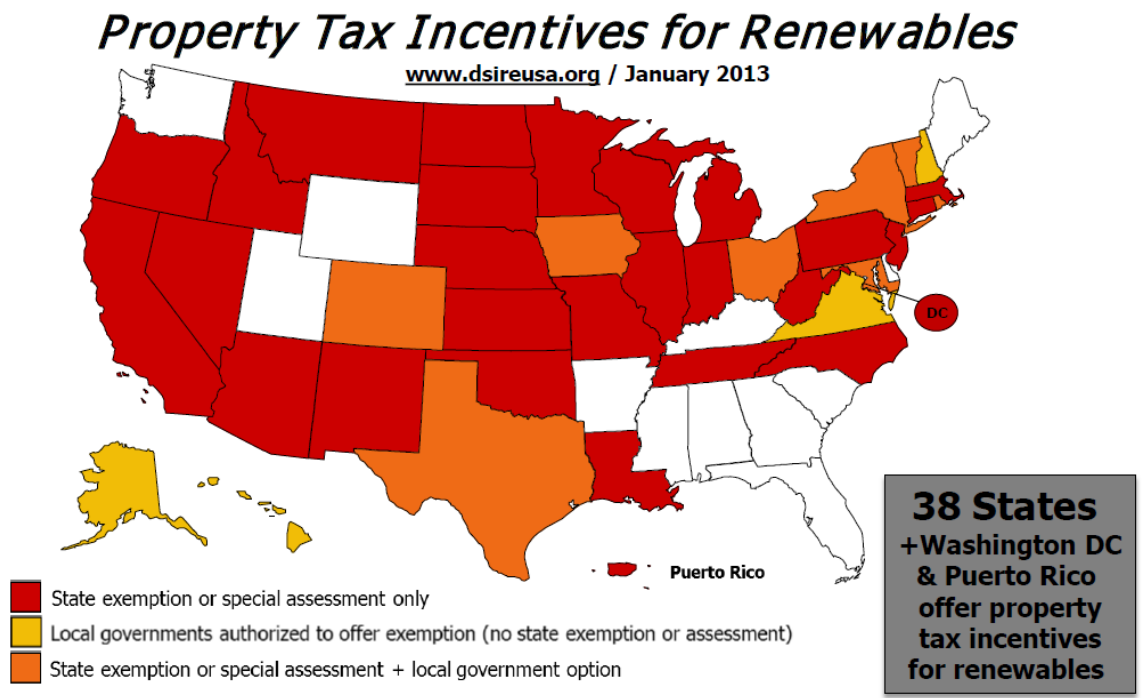


Figure 52: U.S. Sales Tax Incentives for Renewable Energy

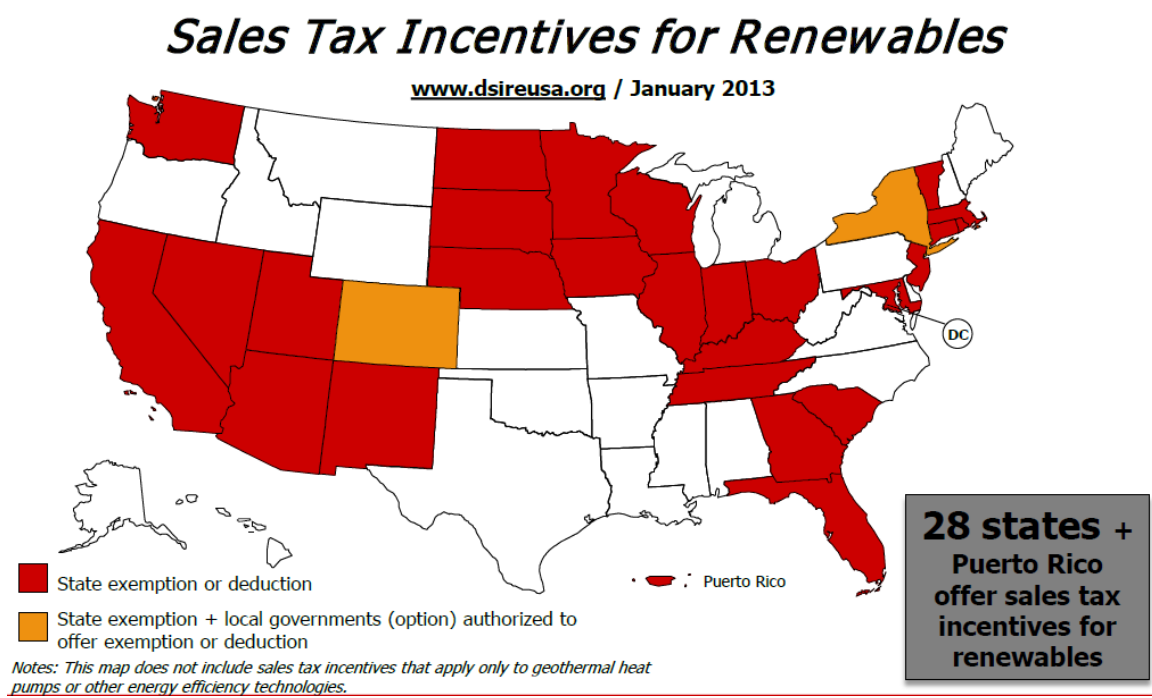


Figure 53: U.S. Rebate Programs for Renewable Energy

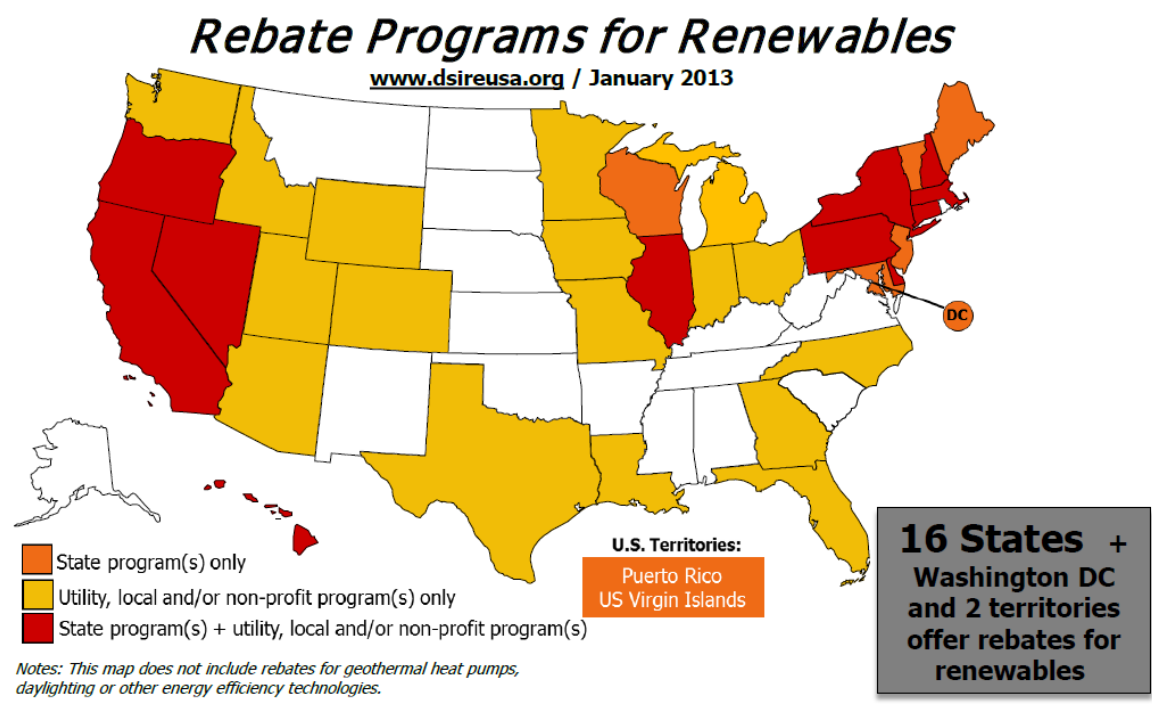


Figure 54: U.S. Tax Credits for Renewable Energy

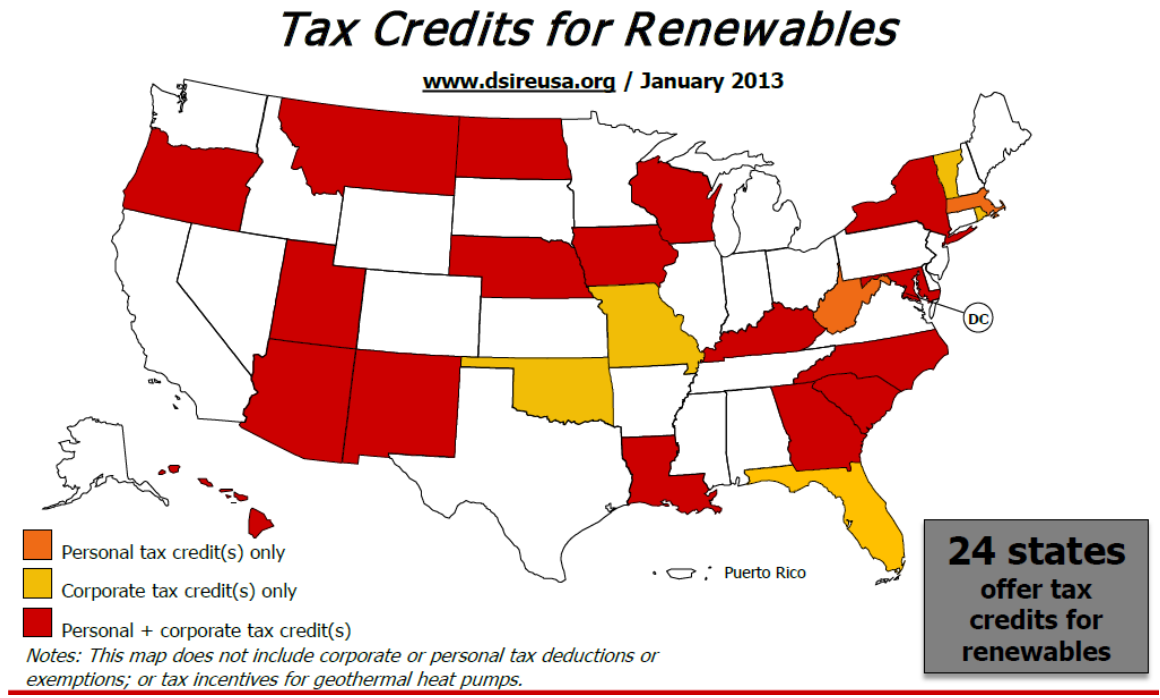
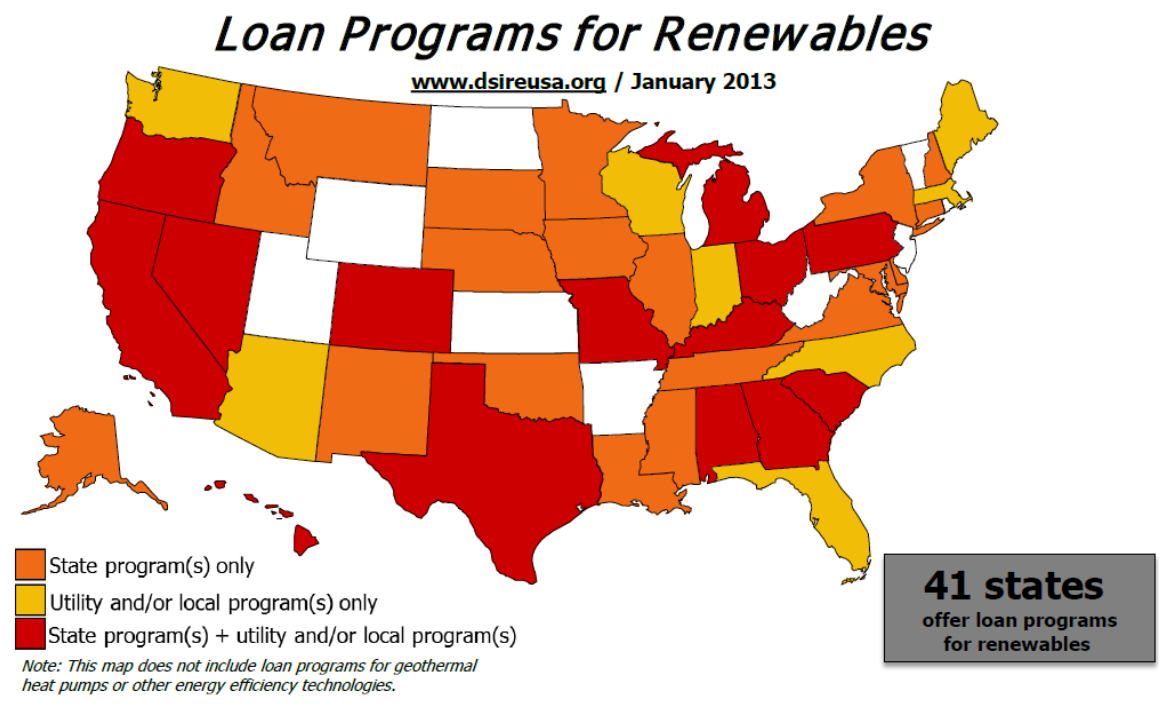


Figure 55: U.S. Loan Programs for Renewable Energy <http://www.dsireusa.org/>



Chapter 4

4.0 Introduction to Data Collection

This chapter describes the data collection process used to provide feedback and verification to the I-P-O model, through data obtained from Argonne National Laboratory's Midwest Photovoltaics Analysis Facility and the College of Menominee Nation's Solar Initiative facility.

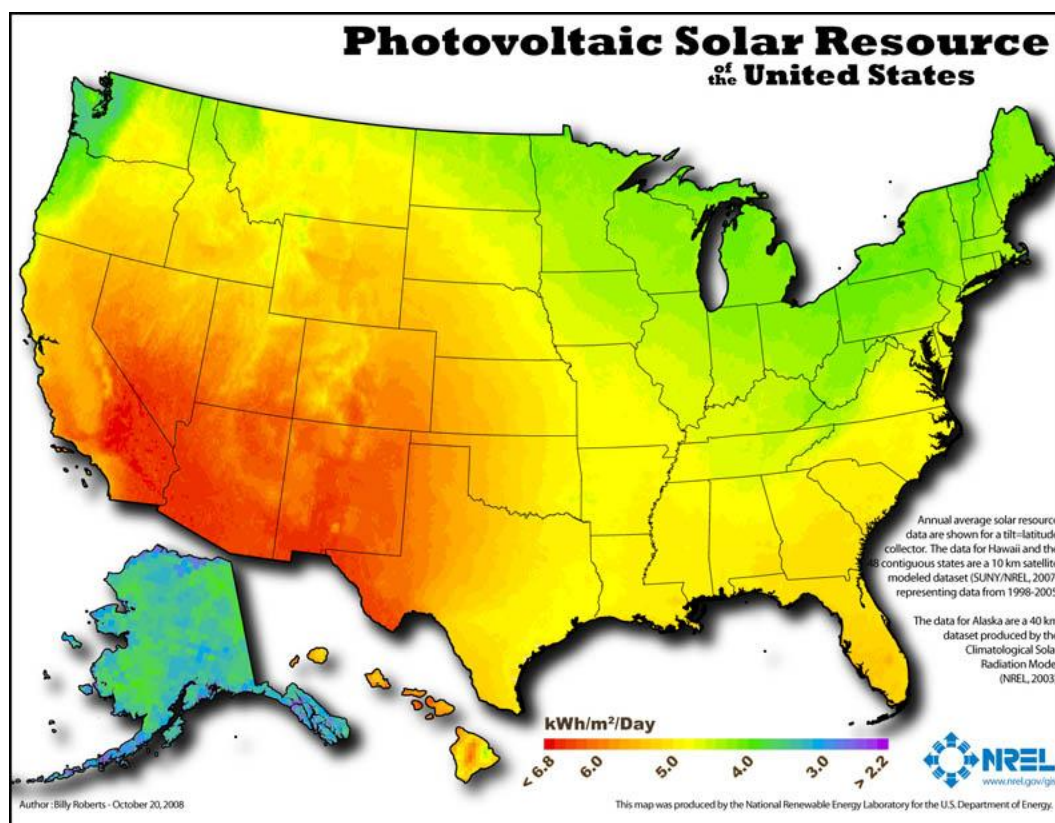
4.1 Motivation for U.S. Midwest

Solar energy is a renewable energy resource capable of supplying 100% of the global energy needs. According to the U.S. Energy Information Administration, global energy consumption for the year 2030 is predicted to be 23 TW (tera watts). On the supply side, first, there is about 174,000 TW of incoming sunlight striking the Earth, of which 96,000 TW of sunlight is absorbed and reflected by the earth's surface. Second, the Earth consists of both ocean and land, which limits the quantity of absorbed and reflected sunlight on land down to 28,000 TW. Third, realistically speaking, not all land is available, but a focus on 2% of the land area would still leave 560 TW remaining. Fourth, solar cell conversion efficiency is about 12% on average, resulting in 67 TW. Bringing this around full circle, 67 TW is more than twice the predicted global energy consumption of 23 TW in 2030. Thus, solar energy is capable of supplying 100% of the global energy needs.

However, this relatively young technology is still in the research phase. As such, there are limited quantities of real-world performance facilities, particularly in the U.S.

Midwest. Figure 56 shows the average quantity of solar irradiation received through the U.S. Solar energy testing facilities throughout the United States, such as National Renewable Energy Laboratory (Colorado), Solar Technology Acceleration Center (Colorado), Sandia National Laboratories (New Mexico), Solar Test and Research Center (Arizona), and Florida Solar Energy Center (Florida) are, understandably so, in ideal locations to conduct solar research due to the large quantity of incoming solar irradiation. However, the unique climate differences, varying solar irradiation, and latitude of the U.S. Midwest provides a complex mixture of factors and a distinctive avenue for solar technology research. The current industry standard for best cost per area efficiencies is crystalline silicon. However, depending upon a user's needs, including seasonal demands, and the common degradation issues associated with the Midwest (extreme weather conditions including snow, ice and freezing temperatures), there is still much to learn for decision makers in the Midwest area. Thus, a comparative study of different solar modules would be beneficial both to establish novel relative analyses and to explore the climatic and geographical effects and differences throughout the United States.

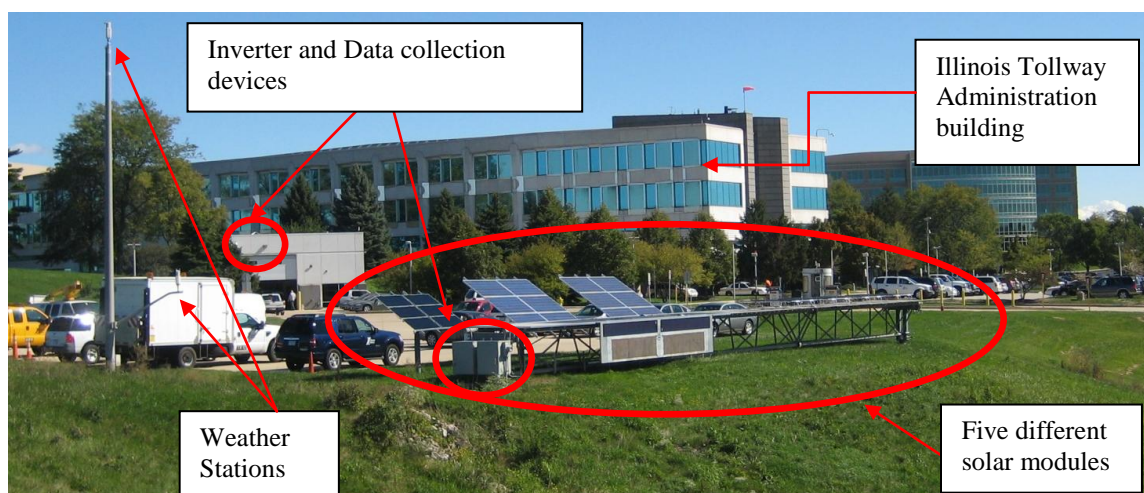
Figure 56: Photovoltaic Solar Resources of the United States



4.2 Argonne National Laboratory's Midwest PV Analysis Facility

The Midwest PV Analysis Facility (MPAF) was established as a result of a collaborative effort between Dr. Seth Darling, Strategy Leader for Solar Energy Systems at Argonne National Laboratory, and the Illinois Tollway Administration. The MPAF was built in 2011 and is located at the Illinois Tollway Administration Headquarters in Downers Grove, IL (about 30 miles west of Chicago, IL).

Figure 57: Midwest PV Analysis Facility



The purpose of the MPAF is to better understand the reliability and efficiency of the different PV technologies, tilts, and suppliers in various weather conditions; and to determine the most suitable modules and module orientation in the U.S. Midwest region. The data collected at this facility includes weather and power conversion efficiency-related information. As such, the MPAF consists of five different PV module configurations (different technologies, tilt and suppliers), a central inverter, two weather stations, and several monitoring devices (see Figure 57). Official real-time data collection started August 2012; the performance data continues to be collected presently with limited disruptions, while the weather data collection has been periodically problematic.

4.2.1 Solar Modules

The performance data includes the outgoing current and voltage from each individual solar module, for five different types of solar module technology as shown in Figure 58. Key information about the solar modules, including data obtained from the manufacturing data sheets, is shown in Table 9.

Figure 58: Five different Solar Modules at the Midwest PV Analysis Facility

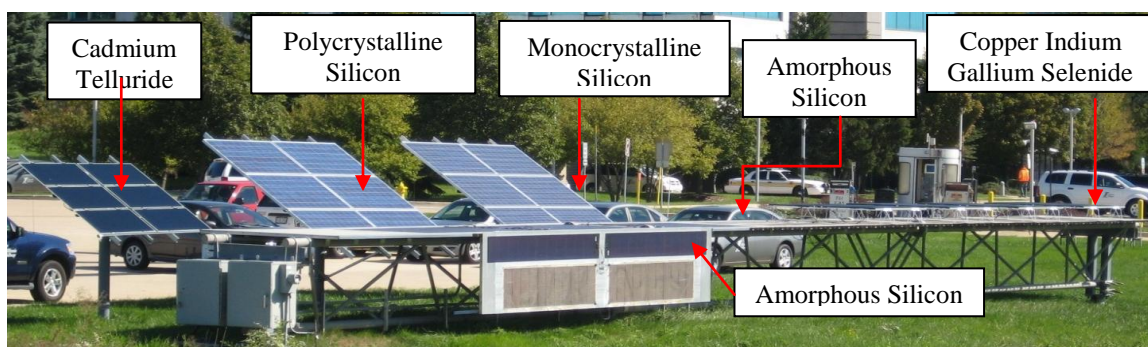


Table 9: Comparative Data Sheet Information for Five Different Solar Modules

Information	CdTe	p-Si	m-Si	CIGS	a-Si	a-Si
Number of Panels	6	6	6	8	12*	2*
Manufacturer	First Solar	Sharp Electronics Corporation	Sharp Electronics Corporation	Solyndra	United Solar Ovanic	United Solar Ovanic
Model	FS-272	ND-224UC1	NU-U235F1	SL-001-182	PVL-68	PVL-68
Efficiency	Medium	High	High	Medium	Low	Low
Rated Max Power	72.5 W	224 W	235 W	182 W	136 W	136 W
Length (m)	1.2	1.64	1.64	1.82	2.845	2.845
Width (m)	0.6	0.994	0.994	1.08	0.394	0.394
Tilt (degrees)	35	35	35	0	0	90
*Note: Due to lower power outputs, a single vBoost device records data for two panels connected in series.						

Cadmium Telluride (CdTe), Polycrystalline Silicon (p-Si), and Monocrystalline Silicon (m-Si) each have 6 panels and are installed at a fixed 30° angle, per manufacturing specifications. Copper Indium Gallium Selenide (CIGS) has 8 panels is installed at a fixed 0° horizontal tilt, per manufacturing specifications. Amorphous Silicon (a-Si) is mounted use 2 different tilts; 12 panels are installed at a fixed 0° horizontal tilt and 2 panels are installed at a fixed 90° vertical tilt. For the purpose of data

collection, these panels are paired up due to the lower power outputs. Additionally, the reason behind the horizontal and vertical installation is to determine the influence of mounting orientation on seasonal PV performance. Furthermore, the a-Si technologies have potential application in so-called curtain wall installations, where sides of building are utilized for power generation, yet little data exist on their performance in such an environment.

4.2.2 Inverter

The performance data also consist of central inverter data, including the outgoing voltage and current for the group of modules as a whole. The inverter converts the DC electricity generated by the solar panels into usable AC electricity that goes straight into the utility grid. See Chapter 3 to understand the difference between a central inverter and a microinverter. The specific inverter used is SMA's Sunny Boy 5000-US DC-to-AC Inverter (Figure 59), which has a max input DC power of 5300 W, max output AC power of 5000 W, max DC to AC conversion efficiency of about 97%, full power operating temperature range of $-25\text{ }^{\circ}\text{C}$ to $45\text{ }^{\circ}\text{C}$ ($-13\text{ }^{\circ}\text{F}$ to $113\text{ }^{\circ}\text{F}$), and 10 year warranty.

Figure 59: SMA's Sunny Boy 5000-US DC-to-AC Inverter



4.2.3 Weather Stations

The weather data are obtained from two different weather stations, one located at the standard meteorological measurement height of 10 meters and the other located at the height of the solar modules at about 2 meters. The specific devices installed are WeatherHawk 520 weather stations (Figure 60). These devices record several different weather parameters including ambient air temperature, wind speed, wind direction, air pressure, and relative humidity. Additionally, the weather stations incorporate an Apogee SP-110 pyranometer (Figure 61), which measures global horizontal solar irradiance.

Figure 60: WeatherHawk 520 Weather Station



Figure 61: Apogee Instruments SP-110 Pyranometer Sensor



4.2.4 Monitoring, Data Collection, and Data Processing

Table 10 highlights the data collection device(s), time interval, and parameters for each of the three main solar energy system components (solar modules, weather stations, and inverter). The solar modules each had an eiQ vBoost DC-to-DC converter to measure the generated DC electricity and maintain max power point operation, using approximately 60 second intervals. Due to lower power output of the amorphous silicon modules, a single vBoost device was used for two panels connected in series. The eiQ vComm communication module was used to wirelessly send the collected power data to the onsite MPAF computer.

The weather stations used the Campbell Scientific CR200 data logger for data collection purposes using approximately 30 second intervals. Additionally, the WeatherHawk-IP Server Module was used to wirelessly send the collected weather and solar radiation data to the onsite MPAF computer. Lastly, the inverter used the all-in-one

SMA Sunny Webbox for data collection and communication to the onsite MPAF computer using approximately 15 minute intervals.

Table 10: MPAF Data Collection Devices

Component	Device	Interval	Parameters
Solar Modules	eiQ's vBoost DC-to-DC converter; eiQ's vComm communication module	~ 60 sec	Individual module power output, including input and output voltage and current
Weather Stations	Campbell Scientific CR200 data logger; WeatherHawk-IP Server Module	~ 30 sec	Ambient air temperature, wind speed, wind direction, air pressure, and relative humidity
Inverter	SMA's Sunny Webbox communication module	~ 15 min	Input current and voltage, output power

Raw data is transmitted wirelessly from the MPAF facility to a computer located at the facility for temporary storage, then transmitted over the internet to an MPAF server located on the Argonne campus for long-term storage and further processing. The data processing was completed using the open source Python programming language Version 2.7.3. Python offers many advantages including relative simplicity, built-in text and XML capabilities, and broad set of libraries for analytical computing (Beazley 2009). For the purpose of the MPAF data processing, two different libraries were used. First, SciPy Version 0.11.0 was used to deliver sophisticated routines to semi-automate the data processing. Second, PyEphem Version 3.7.5.1 was used to calculate the position of the sun (elevation and azimuth) for a given date and time.

4.3 College of Menominee Nation's Solar Initiative

The College of Menominee Nation (CMN) Solar Initiative was established as a result of a collaborative funding effort between CMN, the Environmental Protection Agency (EPA), and the State of Wisconsin Focus on Energy program. The dissertation

author, Lisa Bosman, was the EPA grant principle investigator (PI) and solar installation project manager for this collaborative funding effort. CMN's Solar Initiative was established in April 2014 and is located on the Trade's Building on CMN's campus located in Keshena, WI (about 45 minutes west of Green Bay, WI).

The purpose of CMN's Solar Initiative is to better understand the reliability and efficiency of the different PV technologies incorporating microinverters. The data collected at this location includes solar irradiance, weather, and power production information. Official real-time data collection started April 2014 and continues to be collected presently with limited disruptions.

4.3.1 Solar Modules

The PV module data includes both weather and electricity generation performance for each individual solar panel. There are two different types of solar module technology installed (see Figure 62). Key information about the solar modules, including data obtained from the manufacturing data sheets, is shown in Table 11. Polycrystalline Silicon (p-Si) and Monocrystalline Silicon (m-Si) each have 6 panels and are installed at the roof pitch of 26°.

Figure 62: Two different PV technologies within CMN's Solar Initiative

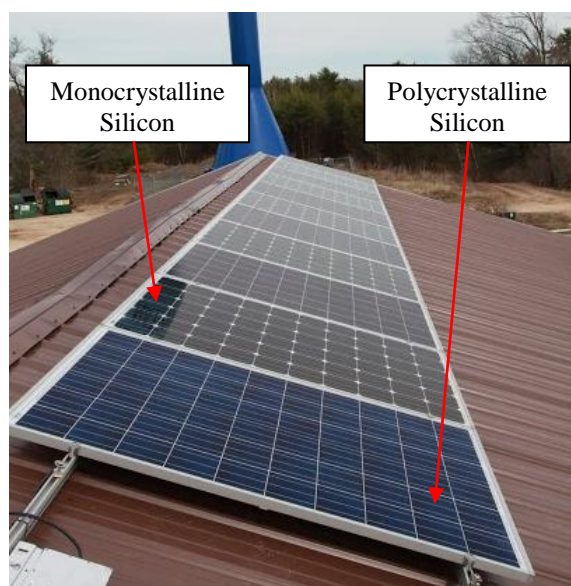


Table 11: Comparative Data Sheet Information for CMN's Solar Initiative

Information	p-Si	m-Si
Number of Panels	6	6
Manufacturer	Solar World	Solar World
Model	SW-01-6050US	SW-02-5001US
Efficiency	High	High
Rated Max Power	250W	250W
Length (m)	1.675	1.675
Width (m)	1.001	1.001
Tilt (degrees)	26	26

4.3.2 Inverter

The performance data also consists of microinverter data, including the outgoing voltage and current for the 12 individual panels. The microinverter is connected to the back of the panel and converts the DC electricity generated by the solar panels into usable AC electricity provided to CMN's campus. See Chapter 3 to understand the difference between a central or string inverter and a microinverter. The specific inverter used is the Enphase M215 (Figure 63), which has a recommended input power range of

190 to 270 W, a max conversion efficiency of 99.4%, a CEC weighted of 96.5 %, a full power operating temperature range of $-40\text{ }^{\circ}\text{C}$ to $65\text{ }^{\circ}\text{C}$, and a 25 year warranty.

Figure 63: Enphase M215 Microinverter



4.3.3 Weather Stations

The weather data are obtained from an SMA weather station located on the roof at the height of the solar panels. The specific device installed directly onto the solar panel, is the SMA Sunny Sensorbox (Figure 64), which measures plane-of-array solar irradiance (global horizontal solar irradiance) and module temperature. Also, two additional sensors were installed to measure wind speed and ambient temperature.

Figure 64: SMA Sunny SensorBox



4.3.4 Monitoring, Data Collection, and Data Processing

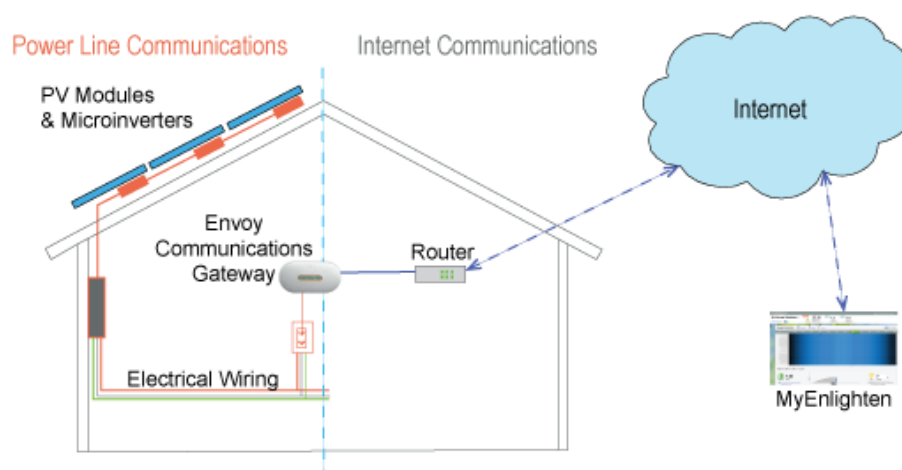
Table 12 highlights the data communication and monitoring device, time interval, and parameters for each of the two main solar energy system components (inverter and weather stations).

Table 12: CMN's Solar Initiative Communication and Monitoring Devices

Component	Communication	Monitoring	Interval	Parameters
Inverter Performance	Enphase Envoy	Enphase Enlighten	~ 5 min	Individual panel power output
Weather Stations	SMA's Sunny Webbox Data Logger	SMA Sunny Portal	~ 5 min	Solar irradiance, Ambient temperature, Module temperature, Wind speed

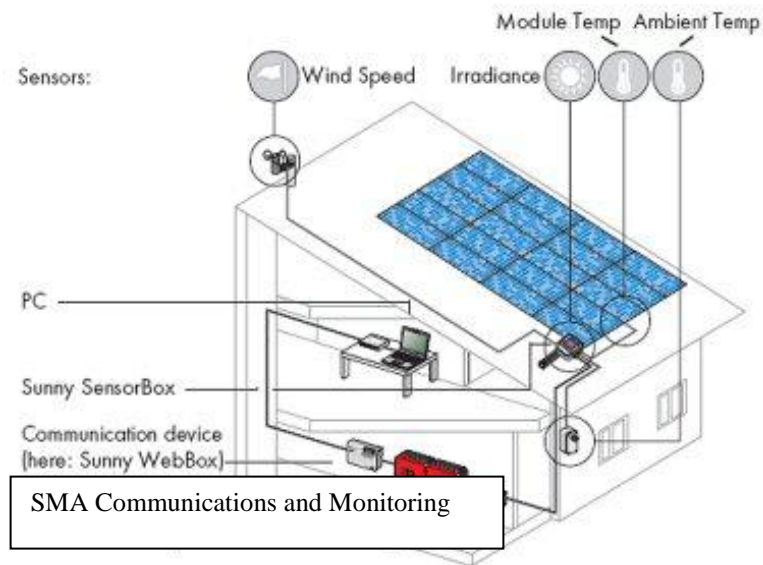
The communication and monitoring associated with the Enphase microinverters is visually depicted in Figure 65, using approximately 5 minute intervals. The PV panel and associated microinverter communicate directly with the Envoy communications gateway, which uploads data to the internet for monitoring and further reporting using the Enphase Enlighten online portal.

Figure 65: Enphase communication and monitoring



The communication and monitoring associated with the SMA weather sensors is visually depicted in Figure 66, using approximately 5 minute intervals. The 4 sensors (solar irradiance, wind speed, ambient temperature, and module temperature) communicate directly with the Sunny Webbox data logger, which uploads data to the internet for monitoring and further reporting using the online SMA Sunny Portal.

Figure 66: SMA weather communication and monitoring

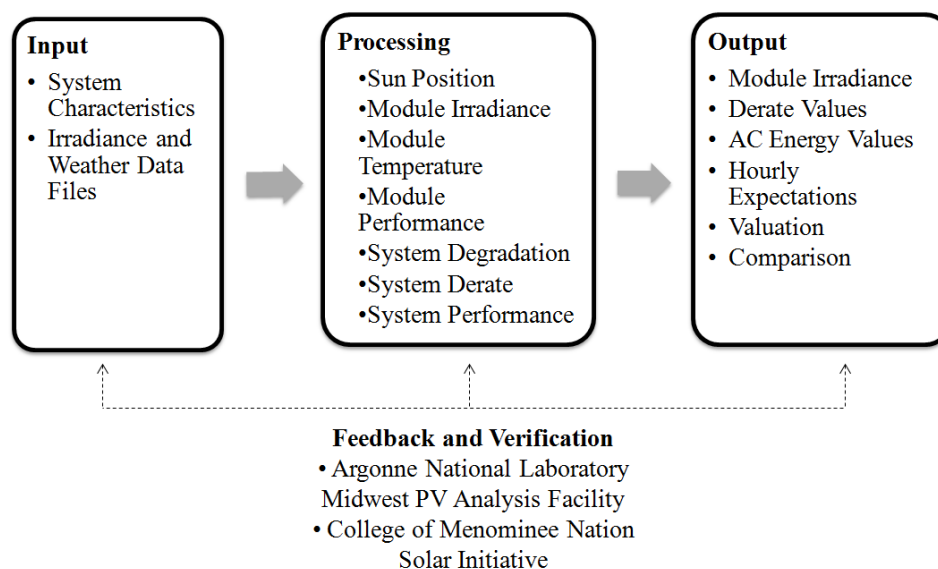


Chapter 5

5.0 Introduction to PVSysCo

This chapter details the models, formulas, and analysis used for the processing part of the I-P-O model, and provides a visual representation of the model, developed using Visual Basic for Applications. An outline of the PV System Performance and Evaluation Model is provided in Figure 67. The inputs include system characteristics and location specific data files including solar irradiance and weather parameters. The processing and analysis is broken into five basic sub-models: sun position, module irradiance, module temperature, module performance, system derate and degradation, and system performance. The output of the performance model includes estimations of array solar irradiance supplied, AC energy production, valuation, and comparison. Feedback, for the purpose of verification is provided through Argonne National Laboratory and the College of Menominee Nation. PV Watts is used for comparative analysis.

Figure 67: Solar Energy System Performance I-P-O Model



5.1 Input

5.1.1 System Characteristics

System characteristics, entered by the user, included information associated with location, array, electricity costs, battery, inverter and PV warranty, and potential derate factors. The location information includes selection of weather station by state and city, for the purpose of importing the correct Typical Meteorological Year 2 (TMY2) data sets, and calculating sun position. The array information includes azimuth, axis type (fixed, 1-axis, or 2-axis), tilt, technology, DC rating, temperature coefficient, and panel type. The array information is used to calculate the array performance based on the weather and solar irradiance data sets. The electricity cost and battery information is used for the valuation component of the model. The warranty length, percentage, and current age of the PV array and inverter is required for the valuation component of the model. The potential derate factors consider the monthly influence of efficiency losses potentially due to inverter, wiring, shading, soiling, snow, and utility outages.

5.1.2 Irradiance and Weather Data Files

The plane-of-array irradiance (W/m^2) and PV cell temperature ($^{\circ}\text{C}$) is calculated based off location specific Typical Meteorological Year 2 (TMY2) data sets. TMY2 data covers 1961-1990 and includes 239 stations, and TMY3 data is updated to include 1991-2005 and includes 1020 locations. However, for the purpose of creating a manageable PC-generated simulation, the smaller TMY2 data sets were used and will be further discussed in this section. A list of TMY2 data parameters is provided in Table 13.

Table 13: List of TMY2 Data Parameters

TMY2 Parameters
Extraterrestrial Horizontal Radiation
Extraterrestrial Direct Normal Radiation
Global Horizontal Radiation
Direct Normal Radiation
Diffuse Horizontal Radiation
Global Horizontal Illuminance
Direct Normal Illuminance
Diffuse Horizontal Illuminance
Zenith Luminance
Total Sky Cover
Opaque Sky Cover
Dry Bulb Temperature
Dew Point Temperature
Relative Humidity
Atmospheric Pressure
Wind Direction
Wind Speed
Horizontal Visibility
Ceiling Height
Present Weather
Precipitable Water
Broadband Aerosol Optical Depth
Snow Depth
Days Since Last Snowfall

The TMY2 data sets offer hourly values of solar irradiance and meteorological parameters for 1 year periods, with the intended use for simulating PV performance for locations in the United States. Because of the “typical” nature of the data sets, they are not designed for worst case conditions. The methodology applied to determine the individual months for each location is the Sandia method (Hall, Prairie et al. 1978), which selects 12 typical months from different years based on five parameters: global

horizontal radiation, direct normal radiation, dry bulb temperature, dew point temperature, and wind speed (Marion and Urban 1995; Wilcox and Marion 2008). “For example, in the case of the NSRDB that contains 30 years of data, all 30 January months are examined, and the one judged most typical is selected to be included in the TMY. The other months of the year are treated in a like manner, and then the 12 selected typical months are concatenated to form a complete year. (Marion and Urban 1995)”

5.2 Processing

5.2.1 Sun Position

The key angles required for sun position include Solar Azimuth Angle, Solar Elevation Angle and Solar Zenith Angle. These equations, in addition to other necessary formulas, were derived from the National Oceanic and Atmospheric Administration’s Earth System Research Laboratory Sun Position Calculator, based off the book *Astronomical Algorithms* (Meeus 1991). In the performance and evaluation model, these equations are applied in 1 hour intervals (24 within a day) for every day of the year (365 days per year) for a total of 8760 data points.

5.2.2 Module Irradiance

Module irradiance I_{mod} , shown in Equation (1), is a summation of three components: beam, ground, and diffuse. The beam and diffuse components require a calculation of the angle of incidence, which varies depending upon the type of PV tracking system: fixed, 1-axis, and 2-axis.

$$I_{mod} = I_{beam} + I_{ground} + I_{diffuse} \quad (1)$$

5.2.2.1 Angle of Incidence

The AOI is based off angles of module tilt β , module azimuth γ , solar azimuth γ_{solar} , and solar zenith θ_{solar} . The equations vary depending on the type of tracking system (fixed, 1-axis, 2-axis), shown respectively in Equation (2) – Equation (4). A single, 1-axis tracker has a fixed tilt and follows the sun from east to west; thus, the module azimuth γ is now equivalent to the solar azimuth γ_{solar} . A dual, 2-axis tracker follows the sun from east to west (module azimuth $\gamma = \text{solar azimuth } \gamma_{solar}$) and the tilt follows the altitude angle (module tilt $\beta = \text{solar zenith } \theta_{solar}$), resulting in an angle of incidence of 0.

$$AOI_{fixed} = \cos^{-1}[\sin(\theta_{solar}) \cos(\gamma - \gamma_{solar}) \sin(\beta) + \cos(\theta_{solar}) \cos(\beta)] \quad (2)$$

$$AOI_{1-axis} = \cos^{-1}[\sin(\theta_{solar}) \cos(\gamma_{solar} - \gamma_{solar}) \sin(\beta) + \cos(\theta_{solar}) \cos(\beta)] \quad (3)$$

$$\begin{aligned} AOI_{2-axis} &= \cos^{-1}[\sin(\theta_{solar}) \cos(\gamma_{solar} - \gamma_{solar}) \sin(\theta_{solar}) \\ &+ \cos(\theta_{solar}) \cos(\theta_{solar})] = 0 \end{aligned} \quad (4)$$

5.2.2.2 Module Irradiance Beam Component

The module irradiance beam component I_{beam} is the product of the direct normal irradiance (DNI) and the cosine of the angle of incidence (AOI), as shown in Equation (5).

$$I_{beam} = DNI * \cos(AOI) \quad (5)$$

5.2.2.3 Module Irradiance Ground Component

The module irradiance ground component I_{ground} is simply the albedo coefficient, as shown in Equation (6), which is the portion of Global Horizontal Irradiance (GHI) reflected by the ground, or surface, in front of a tilted PV array (Andrews and Pearce 2013; Brennan, Abramase et al. 2014).

$$I_{ground} = ALB * GHI * \frac{1 - \cos(\beta)}{2} \quad (6)$$

The values range from 0, indicating a dark surface, up to 1, indicating a bright surface. Example values are provided in Table 14. For example, if the area in front of the PV array is grass, the albedo coefficient is 0.2. If the area in front of the PV array is fresh snow, the albedo coefficient is 0.82.

Table 14: Albedo values

0.08	Very dirty galvanized steel
0.12	Dry asphalt
0.20	Grass
0.26	Fresh grass
0.30	Concrete
0.33	Red tiles
0.35	New galvanized steel
0.60	Wet snow
0.74	Copper
0.82	Fresh snow
0.85	Aluminum

The albedo portion of the model has four assumptions/methods for dealing with snow. First, if snow depth is greater than 0 AND days since last snow fall equals 0, then fresh snow (0.82) will be applied. Second, if snow depth is greater than 0 AND days since last snow fall is greater than 0, then wet snow (0.6) will be applied. Third, if snow

depth equals 0, selected surface coefficient will be applied. Fourth, to ignore default snow assumptions (perhaps the snow is shoveled or plowed regularly), check appropriate box.

5.2.2.4 Module Irradiance Diffuse Component

The module irradiance diffuse component $I_{diffuse}$ is a result of scattered direct normal beam irradiance. There are many models available to estimate the diffuse component, however, an empirical study investigating the accuracy of six research accepted models (Isotropic model, Hay and Davies model, Perez model, Muneer model, Klucher model, and Reindl model) indicates that the Perez model (Perez, Seals et al. 1987; Perez, Ineichen et al. 1990) is the most efficient for predicting the POA diffuse component (Loutzenhiser, Manz et al. 2007). Thus, this model was chosen to predict the POA diffuse component, and is shown in Equations (7) through (13), given the diffuse horizontal irradiance (DHI), direct normal irradiance (DNI), angle of incidence (AOI), module tilt angle β , solar zenith angle θ_{solar} , air mass M_a , extraterrestrial radiation E_a , constant k (5.535×10^{-6} degrees), and f coefficients provided in Table 15.

$$I_{diffuse} = DHI * \left[(1 - F_1) \left(\frac{1 + \cos(\theta_{solar})}{2} \right) + F_1 \left(\frac{a}{b} \right) + F_2 \sin(\theta_{solar}) \right] \quad (7)$$

$$F_1 = \max \left[0, \left(f_{11} + f_{12} \Delta + \frac{\pi \theta_{solar}}{180^\circ} f_{23} \right) \right] \quad (8)$$

$$F_2 = f_{21} + f_{22} \Delta + \frac{\pi \theta_{solar}}{180^\circ} f_{23} \quad (9)$$

$$a = \max [0^\circ, \cos(AOI)] \quad (10)$$

$$b = \max [\cos (85^\circ), \cos(\theta_{solar})] \quad (11)$$

$$\varepsilon = \frac{\frac{DHI + DNI}{DHI} + k\theta_{solar}^3}{1 + k\theta_{solar}^3} \quad (12)$$

$$\Delta = \frac{DHI * AM_a}{E_a} \quad (13)$$

Table 15: Perez f coefficients

ε	f11	f12	f13	f21	f22	f23
0	0	0	0	0	0	0
1	-0.008	0.588	-0.062	-0.06	0.072	-0.022
2	0.13	0.683	-0.151	-0.019	0.066	-0.029
3	0.33	0.487	-0.221	0.055	-0.064	-0.026
4	0.568	0.187	-0.295	0.109	-0.152	-0.014
5	0.873	-0.392	-0.362	0.226	-0.462	0.001
6	1.132	-1.237	-0.412	0.288	-0.823	0.056
7	1.06	-1.6	-0.359	0.264	-1.127	0.131
8	0.678	-0.327	-0.25	0.156	-1.377	0.251

5.2.3 Module Temperature

There are five standard models used to estimate module temperature: Sandia (King, Boyson et al. 2004), Garcia (Garcia and Balenzategui 2004), Faiman (Faiman 2008), NREL – 3 Parameter (TamizhMani, Ji et al. 2003), and NREL – 5 Parameter (TamizhMani, Ji et al. 2003). These models estimate module temperature based off a

variety of factors including ambient temperature, plane-of-array irradiance, wind speed, wind direction, and humidity.

Table 16: Parameters associated with each module temperature model

Parameter	Garcia Model	Sandia Model	Faiman Model	NREL Model - 3 Parameter	NREL Model - 5 Parameter
POA Insolation [W/m ²]	X	X	X	X	X
Ambient Temperature [°C]	X	X	X	X	X
Wind Speed [m/s]		X	X	X	X
Humidity (%)					X
Wind Direction (degrees)					X

Note: X = parameter is used in model

A comparative analysis was applied to see which model best fit the actual data of a recently installed weather and solar irradiance monitoring station located in Keshena, WI, on the campus of the College of Menominee Nation. Data was assessed for a week's worth of 1 hour intervals for a total of 168 data points (24 hours x 7 days = 168 data points). Weather and solar irradiance was obtained, including day, time, module plane-of-array irradiance I_{mod} (W/m²), ambient temperature T_A (°C), module temperature T_M (°C), wind speed WS (m/s), wind direction WD (degrees), and humidity H (%). Table 16 shows the parameters applied in each module temperature model.

The results of a chi-square goodness-of-fit test indicate that all five models provide a statistically significant fit using an alpha value of 0.05. Additionally, the results of a paired sample dependent t-test indicate that all models are statistically similar to the

actual module temperature using an alpha value of 0.05. The results of the Pearson correlation, Table 17, indicate that the NREL Model – 3 Parameter provides the best correlation to the actual data. Thus, this model was chosen to predict module temperature.

Table 17: Module Temperature (Actual versus Model) Results of Pearson Correlation

	Garcia Model	Sandia Model	Faiman Model	NREL Model - 3 Parameter	NREL Model - 5 Parameter
Pearson Correlation	0.9671	0.9725	0.9792	0.9833	0.9830

The NREL Model – 3 Parameter is provided in Equation (14) and the coefficients are provided in Table 18.

$$T_M = w1 * T_A + w2 * POA + w3 * WS + cons \quad (14)$$

Table 18: Coefficients for NREL 3-Parameter Model

Technology	w1	w2	w3	cons
a-Si	0.943	0.026	-1.45	4.1
mono-Si	0.942	0.028	-1.509	3.9
poly-Si	0.926	0.03	-1.666	5.1
CIGS	0.96	0.029	-1.507	4
CdTe	0.943	0.028	-1.528	4.328

5.2.4 Module Performance

The module performance model is different for flat-plate versus cylindrical panels due to contrasting collector geometries.

5.2.4.1 Flat-Plate Panel

The flat-plate module performance equation is shown in Equation (15) given the system estimated AC power generation P_{mod} (W), module plane-of-array irradiance I_{mod} (W/m^2), STC solar irradiance I_0 (W/m^2), module rated maximum DC power P_{DC} (W), temperature coefficient γ ($\%/^{\circ}\text{C}$), module temperature T_M ($^{\circ}\text{C}$), and STC temperature T_0 ($^{\circ}\text{C}$).

$$P_{mod_i} = \frac{I_{mod}}{I_0} * P_{DC} * [1 + \gamma * (T_M - T_0)] \quad (15)$$

5.2.4.2 Flat-Plate Panel Model Verification

Data from Argonne National Laboratory were used to verify the module performance for flat-plate panels, including mono-crystalline silicon, poly-crystalline silicon, amorphous silicon, and cadmium telluride. The bright, cloudless day of 03-03-13 was used to demonstrate the model performance predictability of all four types of flat-plate panels with serial number. Table 19 and Table 20, respectively, crystalline silicon and thin-film technology, shows the expected performance, using the flat-plate panel model, in comparison to the actual panel performance.

Table 19: Crystalline Silicon Flat-Plate Panels: Expected vs Actual Power

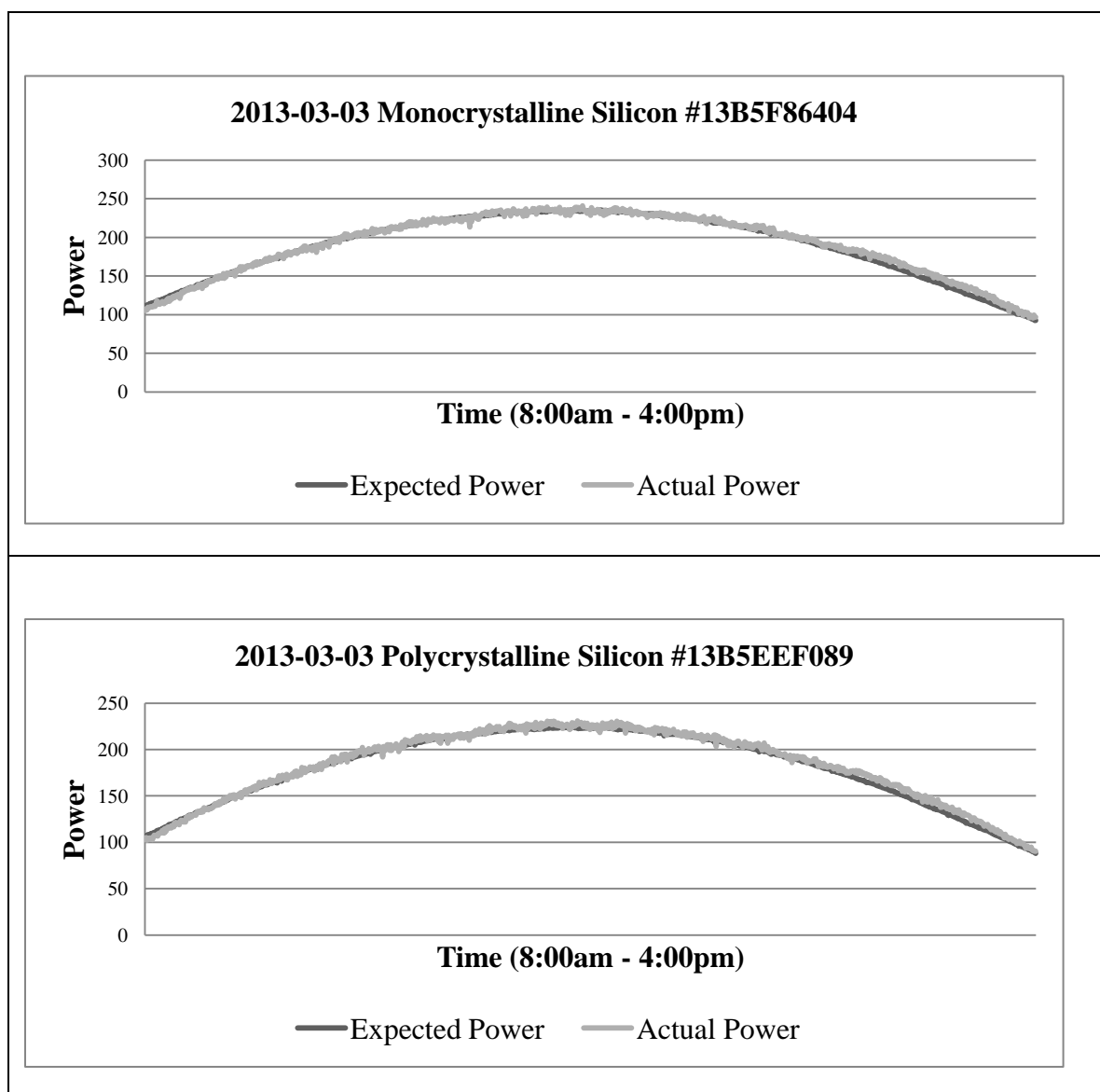
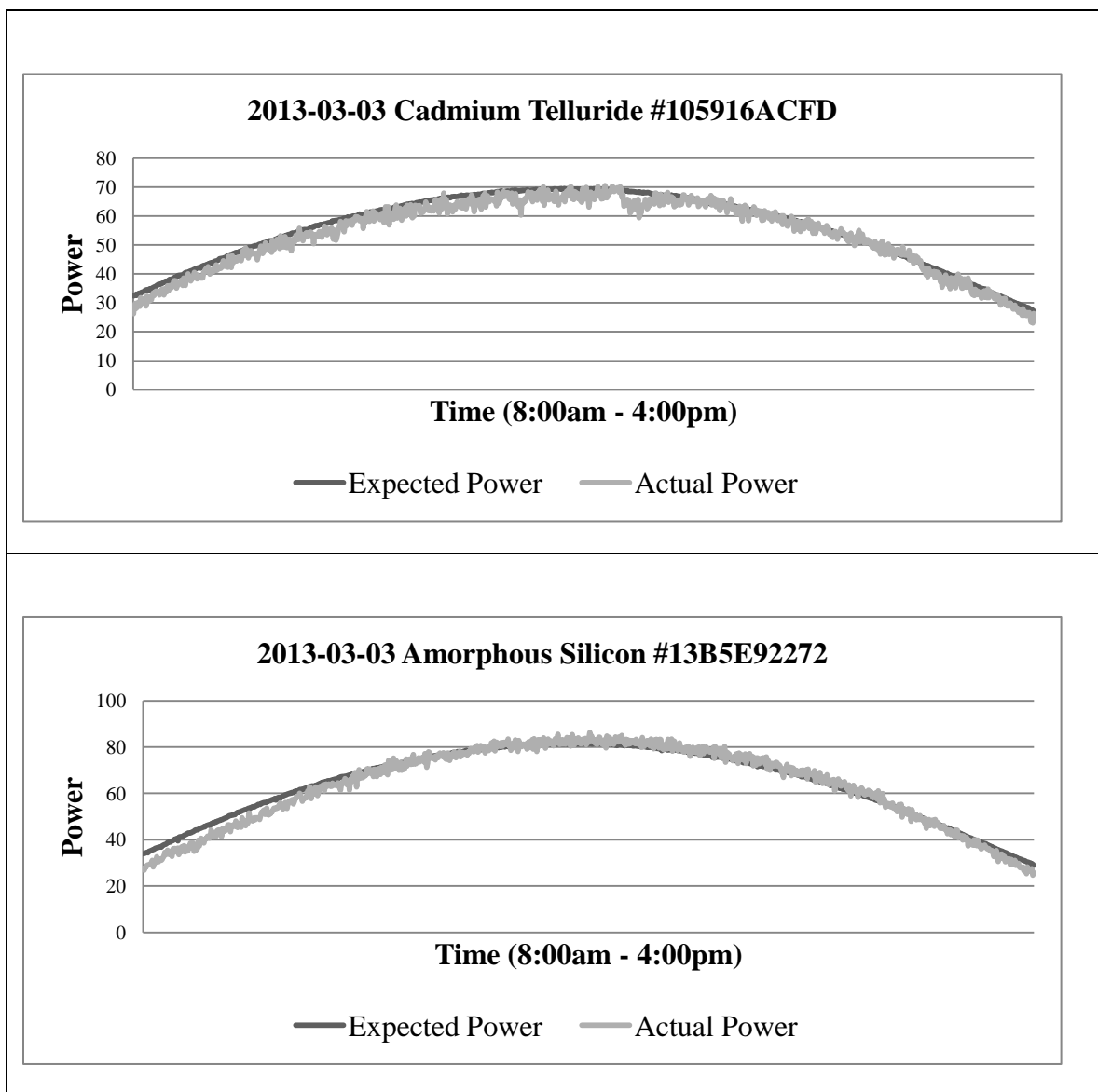


Table 20: Thin-Film Flat-Plate Panels: Expected vs Actual Power

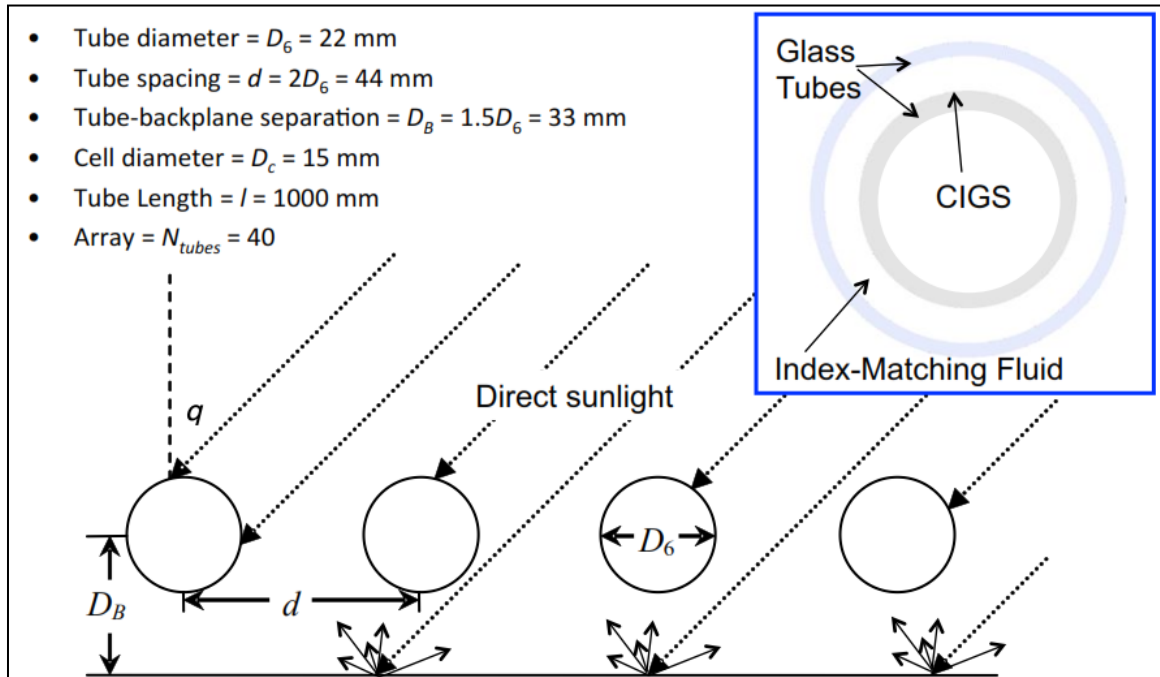


5.2.4.3 Cylindrical Panel

The unique design of cylindrical panels allows the modules to obtain more sunlight earlier and longer than the flat-plate panels, optimizing direct, diffuse, and reflected solar radiation (Koshel, Smestad et al. 2012). Currently, the only PV technology

incorporating the cylindrical panels is CIGS (copper indium gallium selenide). Characteristics of the cylindrical panel are shown in Figure 68.

Figure 68: Cylindrical Panel Characteristics (Koshel, Smestad et al. 2012)



In estimating the module performance of cylindrical panels in comparison to traditional flat-plate panels, there are two parameters of importance; the ratio of flat-plate area to cylindrical area, and the sun elevation angle at which the cylindrical panel performance diverges from the flat-plate panel performance.

First, the area of a flat-plate panel and comparably sized cylindrical panel can be calculated with basic math formulas as provide in Equations (16) and (17).

$$Area_{rectangle} = lw \quad (16)$$

$$Area_{cylinder} = 2\pi r^2 + 2\pi rh \quad (17)$$

However, cylindrical panels have capped ends and thus can only receive solar irradiance through the long sides and not through the tops and bottoms. Thus, the actual area of the cylindrical panel available to light becomes Equation (18). When looking from the top down onto both types of panels, the area of the rectangle length is the same as the area of the cylinder height. Furthermore, the area of the rectangle width is the same as the area of the cylinder radius. Thus, for the sake of fair PV technology comparison, height is substituted for length and diameter for width. Hence, the active surface area is shown in Equation (19).

$$Area_{cylinder} = 2\pi rh = \pi dh \quad (18)$$

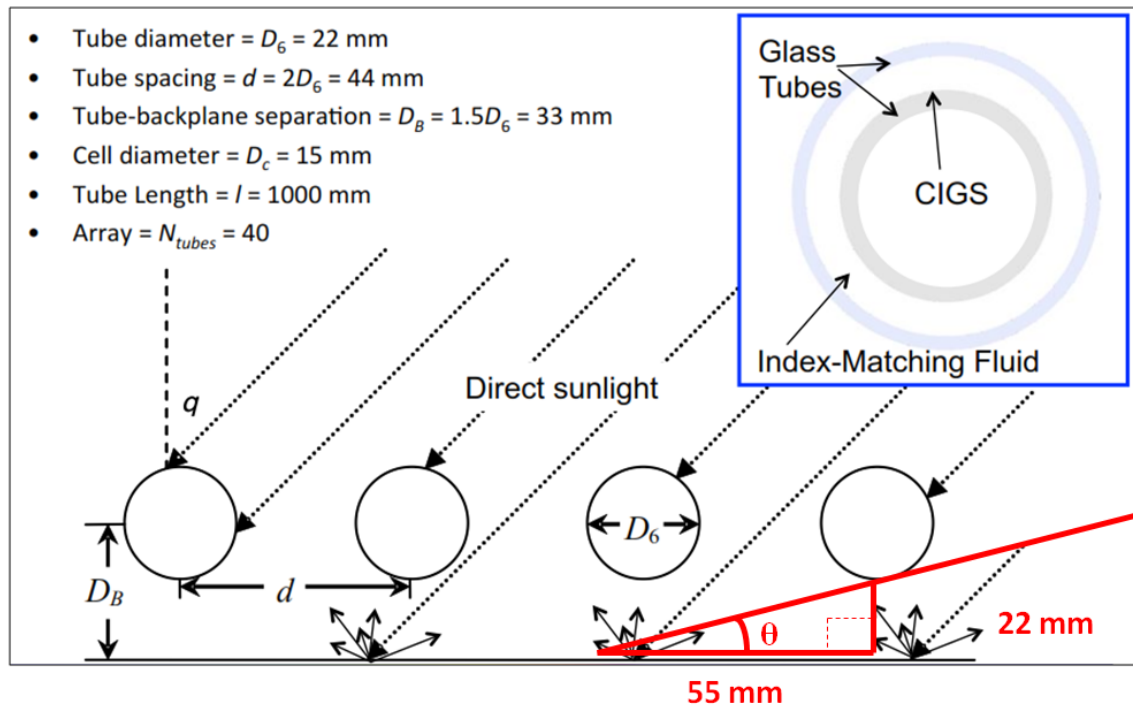
$$Area_{rectangle} = dh \quad (19)$$

The ratio of flat-plate area to cylindrical area is estimated to be 1: π , as shown in Equation (20). Furthermore, when estimating the performance as a whole, as shown in Equation (21), the proportion constant results in 0.759.

$$\frac{Area_{rectangle}}{Area_{cylinder}} = \frac{2rh}{2\pi rh} = \frac{1}{\pi} \quad (20)$$

$$\frac{1}{1 + \pi} = 0.759 \quad (21)$$

Second part of the cylindrical panel model is to determine the sun elevation angle at which the cylindrical panel performance diverges from the flat-plate panel performance. Using panel characteristics provided in Figure 68, the sun elevation angle is estimated to be 21.8° using basic laws of geometry as shown in Equation (22).



$$\theta = \tan^{-1} \frac{\text{opposite}}{\text{adjacent}} = \tan^{-1} \frac{22}{55} = 21.8 \quad (22)$$

The cylindrical panel module performance model is provided in Equation (23), with two parts. For solar elevation angles α_{solar} less than 21.8° , the model calculation is similar to the performance of flat-plate panels, because the sun covers a similar quantity of area. However, solar elevation angles α_{solar} greater than 21.8° , the model calculation takes into consideration the overall performance proportion of flat-plate to cylindrical with the factor of 0.759.

For solar elevation angle $\alpha_{\text{solar}} < 21.8^\circ$

$$P_{\text{mod}_i} = \frac{I_{\text{mod}}}{I_0} * P_{DC} * [1 + \gamma * (T_M - T_0)]$$

For solar elevation angle $\alpha_{\text{solar}} > 21.8^\circ$

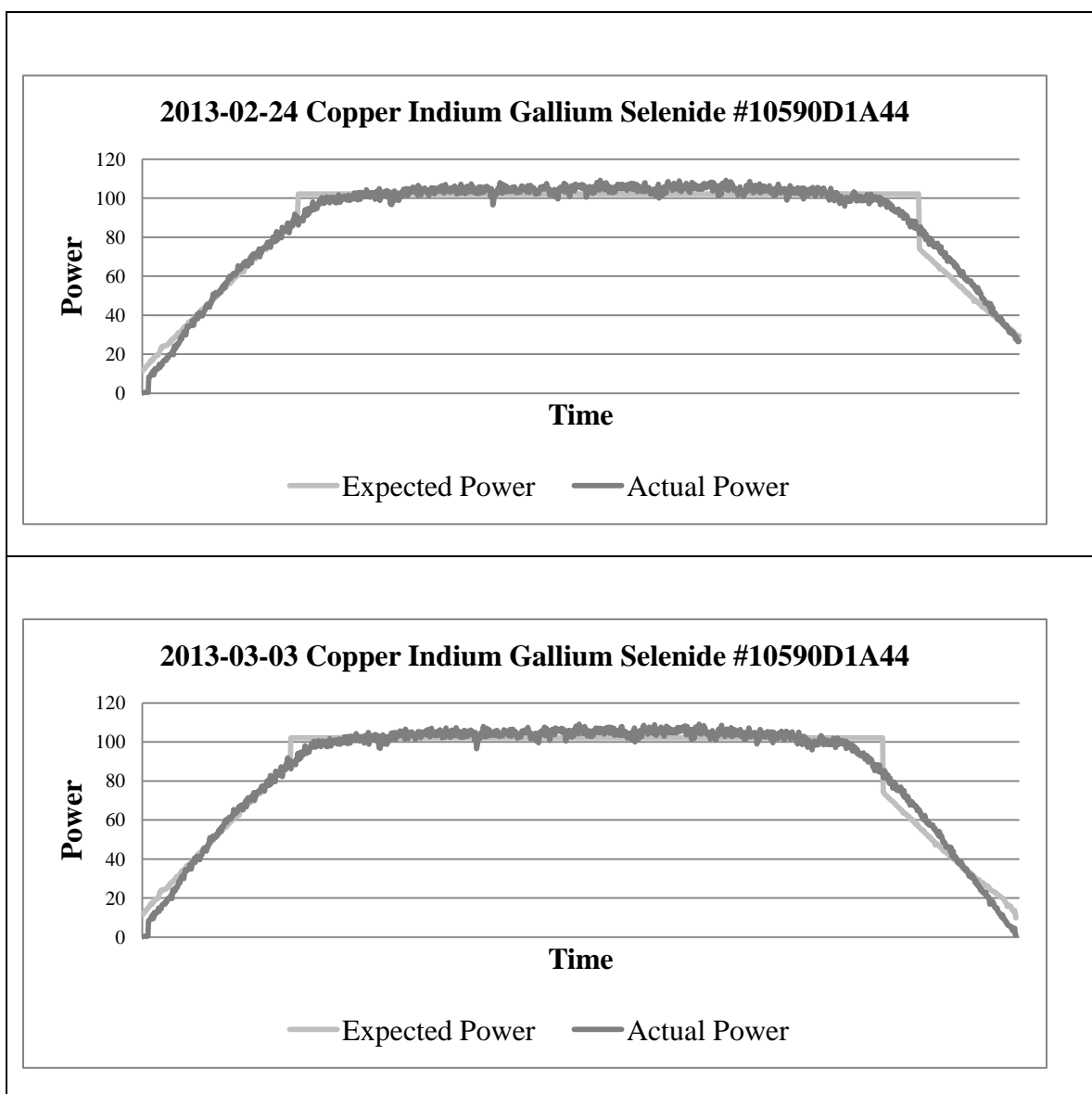
(23)

$$P_{\text{mod}_i} = \sum_{\alpha > 21.8}^{\alpha_{\text{max}}} \frac{\left[\frac{I_{\text{mod}}}{I_0} * P_{DC} * [1 + \gamma * (T_M - T_0)] \right] * 0.759}{n}$$

5.2.4.4 Cylindrical Panel Model Verification

Data from Argonne National Laboratory were used to verify the module performance for cylindrical panels, using the copper indium gallium selenide (CIGS) technology. The bright, cloudless days of 02-24-13 and 03-03-13 were used to demonstrate the cylindrical panel model performance predictability. Table 21 shows the expected performance, using the cylindrical panel model, in comparison to the actual panel performance.

Table 21: CIGS Cylindrical Panel: Expected vs Actual Power



5.2.5 System Degradation

System degradation, Δ_k , for a given year k is the product of the degradation associated with the applicable main system components (Rohouma, Molokhia et al. 2007), including PV array and inverter.

5.2.5.1 PV Array Degradation Component

The PV array degradation component Δ_{array} is the annual estimated performance loss due to PV module breakdown over time. It considers module rated maximum DC power P_0 , module rated DC upper power tolerance PTU_0 , module rated DC lower power tolerance PTL_0 , module rated warranty percent WP_0 , and module rated warranty quantity of years WY_0 (Vazquez and Rey-Stolle 2008). Since the module rated DC power tolerance allows for a +/- percentage, the PV array degradation component will result in three values: upper (+), average, and lower (-), shown respectively in Equations (24) - (26).

$$\text{For given year } k, \quad \Delta_{array+} = P_0 * (1 + PTU_0) * \left(1 - \frac{1 - WP_0}{WY_0} * k\right) \quad (24)$$

$$\text{For given year } k, \quad \Delta_{array} = P_0 * \left(1 - \frac{1 - WP_0}{WY_0} * k\right) \quad (25)$$

$$\text{For given year } k, \quad \Delta_{array-} = P_0 * (1 - PTL_0) * \left(1 - \frac{1 - WP_0}{WY_0} * k\right) \quad (26)$$

5.2.5.2 Inverter Degradation Component

The inverter degradation component $\Delta_{inverter}$ is the annual estimated loss due to inverter breakdown over time. It considers inverter rated efficiency INV_0 , inverter rated warranty percent INV_{WP} , and inverter rated warranty quantity of years INV_{WY} . The resulting value is provided in Equation (27).

$$\text{For given year } k, \quad \Delta_{inverter} = INV_0 * \left(1 - \frac{1 - INV_{WP}}{INV_{WY}} * k\right) \quad (27)$$

5.2.6 System Derate

The system derate is the monthly product of derate values attributed to inverter efficiency IE_j , DC and AC wiring W_j , module mismatch MM_j , shade Sh_j , soil So_j , snow Sn_j , and utility U_j .

$$\text{For given month } j, \delta_j = IE_j * W_j * MM_j * Sh_j * So_j * Sn_j * U_j \quad (28)$$

5.2.6.1 Inverter Efficiency

Inverter efficiency can be found on the manufacturer's technical data sheet. It is recommended to use the CEC-weighted efficiency for the derate value. However, a default value of 95.6% is provided, which is the average of all eligible inverter CEC-weighted efficiencies available through the Consumer Energy Center (<http://www.gosolarcalifornia.ca.gov/equipment/inverters.php>) as of May 8, 2014.

5.2.6.2 DC and AC Wiring

Energy losses due to DC and AC wiring are typically 2% or less on the DC side and 1% or less on the AC side (Solar Energy International 2013). Thus, the DC wiring derate default is 98% and the AC wiring derate default is 99%. The actual energy loss due to voltage drop can be accurately measured and verified by a certified electrician, however, it is recommended to apply the default values.

5.2.6.3 Module Mismatch

The module mismatch refers to losses due to manufacturing tolerances in a string inverter system. If one module's performance decreases, the combined performance of all

modules decrease. The default module mismatch derate is 100% minus the lower power tolerance, and it is recommended to apply the default value.

5.2.6.4 Shade

The default shade derate is 100%, as it is anticipated that solar modules will be installed in a location free of a shade. However, it is recommended that a shade analysis is completed, using a Solar Pathfinder or Solmetric SunEye, to verify potential monthly shading.

5.2.6.5 Soil

The default soil derate is 100%, as it is anticipated that any potential soil or dirt will be removed with rain. However, if the solar modules are located in a dry or dusty climate, or tilted at extremely low levels preventing rain from cleaning the modules, it is recommended that the soil derate factor is modified accordingly.

5.2.6.6 Snow

The default snow derate is based off the TMY2 weather data. Specifically, it takes the proportion of days per month of which the 'Days Since Last Snowfall' is greater than 0 (implying that it didn't snow that day). For example, if 26 days in January (total of 31 days) fits this profile, the default derate for the month of January is 84% ($26 \div 31$). It is recommended that the default snow derate factor is applied.

5.2.6.7 Utility

For a grid-tied PV system, the inverter will shut down if the grid is shut down, due to the legally required anti-islanding protection. The U.S. utility grid is extremely reliable, however, in the case of a natural disaster there is potential for the grid to be

down for several hours or days. The default utility derate is 100%, however, it is recommended that the utility derate factor is modified accordingly if the grid-tied PV system is located in an area associated with an unreliable grid access.

5.2.7 System Performance

The overall system performance model is provided in Equation (29).

$$P_{sys_{i,j,k}} = P_{mod_i} * \delta_j * \Delta_k \quad (29)$$

- $P_{sys_{i,j,k}}$ = system estimated AC power generation in Watts, for a given hour i , month j , and year k
- P_{mod_i} = module rated maximum DC power in Watts, for a given hour i
- δ_j = system derate factor, for a given month j
- Δ_k = system degradation factor, for a given year k

5.3 Output

5.3.1 Module Irradiance

The output provides the daily average solar irradiance ($\text{W}/\text{m}^2/\text{day}$) for each calendar month. The module irradiance I_{mod} is a summation of three components: beam, ground, and diffuse. This plane-of-array value varies depending on PV array location, azimuth, tilt, hourly sun position, and tracking system (fixed, 1-axis, 2-axis). These values may be useful when comparing the expected incoming module irradiance for different tilt configurations or different locations.

5.3.2 Derate Values

The output provides the monthly derate values, which are a product of derate factors and efficiencies related to inverter, DC wiring, AC wiring, module mismatch, shade, soil, snow, and utility. These values may be useful to for understanding losses throughout the year.

5.3.3 AC Energy Value

The output provides monthly AC energy value. This is the product of monthly system performance and the cost of electricity (\$/kWh), without considering degradation or maintenance. This value may be useful when comparing differing costs of electricity, either due to a commercial versus residential systems application, or for different locations and utility companies.

5.3.4 Hourly Expectations

The output provides hourly performance expectations, which will vary depending on the performance model selected (flat-panel versus cylindrical panel). The visual depiction provides values for the months of March, June, September, and December, to highlight changes due to sun position during peak solstice and equinox months.

5.3.5 Valuation

Insurance companies commonly use three different methods to value insurance claims: Replacement Cost, Actual Cash Value, and Depreciation.

To obtain an accurate Replacement Cost, it is advised to contact a local PV installer for a quote. This is important because PV system installation cost trends change

on a weekly basis. Furthermore, due to economies of scale, the price per watt of a larger installed system will be more cost effective than a smaller installed system. Thus, using a standard price per watt value will not be accurate.

The output does, however, provide Actual Cash Value and Depreciation. The Actual Cash Value (ACV) has a high and low range based on the module power tolerance. The high ACV uses the upper module power tolerance and the low ACV uses the rated module power. The annual ACV is a monthly sum of AC energy value minus maintenance costs (inverter replacement) and factoring in potential degradation due to PV and inverter warranties (useful life, age, and warranty performance percent). The cost of inverter replacement is assumed to be \$184/kW (pv.energytrend.com 05/24/2014).

The models for calculating the upper and lower ACV are shown in Equations (30) and (31), using PV module array warranty life WY_{Mod} , PV array warranty performance WP_{Mod} , PV module array age Age_{Mod} , inverter warranty life WY_{Inv} , inverter warranty efficiency WP_{Inv} , inverter age Age_{Inv} , module DC rated power P_0 , and module DC rated upper power tolerance PT_U .

$$ACV_{upper_k} = P_0 * (1 + PT_u) * \frac{1 - WP_{Mod}}{WY_{Mod}} k * \sum_{j=1}^{12} AC \text{ Energy Value}_k \quad (30)$$

for month = j and year = k (thru Age_{Mod})

*Note: If the Age_{inv} = MOD(k,0), add maintenance cost of \$184*P₀*

$$ACV_{lower_k} = P_0 * \frac{1 - WP_{Mod}}{WY_{Mod}} k * \sum_{j=1}^{12} AC \text{ Energy Value}_k \quad (31)$$

for month = j and year = k (thru Age_{Mod})

*Note: If the Age_{Inv} = MOD(k,0), add maintenance cost of \$184*P₀*

5.3.6 Comparison

The output allows the user to compare up to 3 different PV systems. The purpose is to easily compare system configurations, array tilts and azimuth, locations, cost of electricity, or any other number of changeable factors.

5.4 Feedback

5.4.1 Verification

Verification of the processing model was completed for several sub-model processes including sun position, module irradiance, module temperature, and module performance. The sun position model and equations were verified using several different calculators provided by reputable organizations including the National Oceanic and Atmospheric Administration's Earth System Research Laboratory Solar Calculator (<http://www.esrl.noaa.gov/gmd/grad/solcalc/>) and the United States Naval Observatory Astronomical Applications Department Sun Altitude/Azimuth Table (<http://aa.usno.navy.mil/data/docs/AltAz.php>). The module irradiance and module temperature model and equations were verified using data obtained from the College of Menominee Nation. The module performance models (flat-plate and cylindrical panels) were verified using data obtained from Argonne National Laboratory. Due to the more ambiguous and complicated nature of system derate and system degradation, logic and reasoning was used to quantify the potential effects of derate and degradation.

5.5 Novel PVSysCo Decision Support System

The new solar energy evaluation tool, PVSysCo, is displayed in Figure 69 and Figure 70. The three scenarios are as follows: (1) Green Bay, WI, with default information; (2) Green Bay, WI, with adapted information for the College of Menominee Nation Solar Initiative, and (3) Honolulu, HI, with default information.

To verify the accuracy of the new PVSysCo solar energy system performance and evaluation tool, a comparison was made with PVWatts for 50 days worth of actual hourly data collected from the College of Menominee Nation (CMN) Solar Initiative facility. CMN's solar energy system, located nearest to the Green Bay weather station, is a 3.0 kW system comprising of crystalline silicon solar panels, installed on a steel roof. It is south facing, 26 degree in tilt, a temperature coefficient of $-0.45\%/^{\circ}\text{C}$, and is partially shaded in the morning due to a nearby water tower. Each of the 12 panels uses Enphase microinverters, for the purpose of converting the energy from DC to AC, with a CEC rating of 0.965.

The total energy generation over the 50-day period was 695.25 kWh, hence an average daily energy generation of 13.91 kWh/day. Since this actual data was used to compare the predicted (expected) power generated using PVSysCo and PVWatts, both of which use typical model year (TMY) solar irradiation and weather data, total (for the period), the average daily power generation data as well as the calculated Mean Square Error values were used as indicators of model accuracy. The results are provided in Table 22, and the actual data is provided in Table 23 and Table 24.

Figure 69: PVSysCo Example Screen 1 of 2

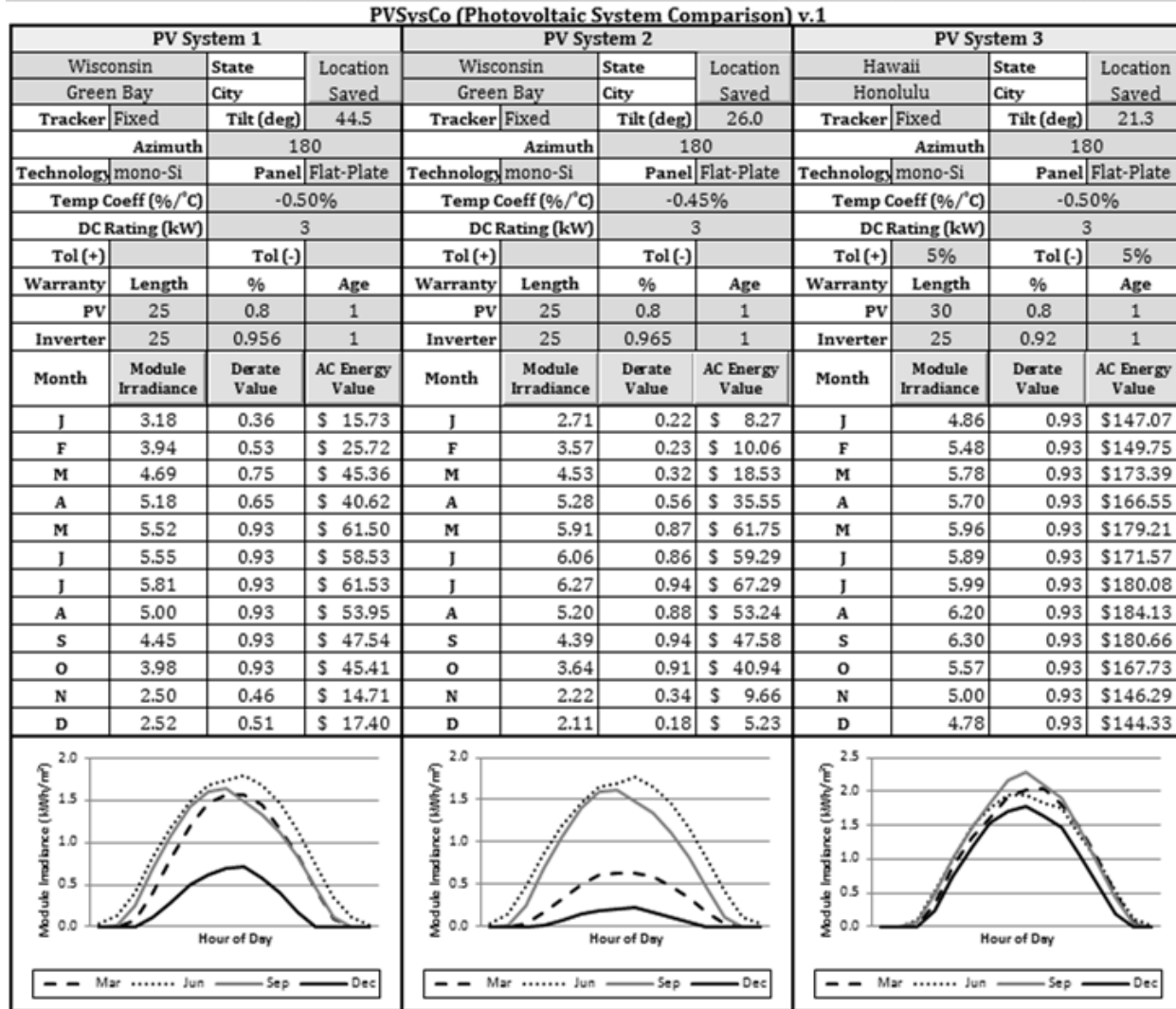


Figure 70: PVSysCo Example Screen 2 of 2

PVSysCo (Photovoltaic System Comparison) v.1											
PV System 1				PV System 2				PV System 3			
Year	ACV (No OEM)	ACV w/ OEM (Upper)	ACV w/ OEM (Lower)	Year	ACV (No OEM)	ACV w/ OEM (Upper)	ACV w/ OEM (Lower)	Year	ACV (No OEM)	ACV w/ OEM (Upper)	ACV w/ OEM (Lower)
1	\$488	\$488	\$488	1	\$417	\$417	\$417	1	\$1,991	\$2,090	\$1,991
2	\$484	\$484	\$484	2	\$414	\$414	\$414	2	\$1,978	\$2,076	\$1,978
3	\$480	\$480	\$480	3	\$411	\$411	\$411	3	\$1,964	\$2,062	\$1,964
4	\$476	\$476	\$476	4	\$407	\$407	\$407	4	\$1,951	\$2,049	\$1,951
5	\$472	\$472	\$472	5	\$404	\$404	\$404	5	\$1,938	\$2,035	\$1,938
6	\$468	\$468	\$468	6	\$401	\$401	\$401	6	\$1,924	\$2,021	\$1,924
7	\$465	\$465	\$465	7	\$397	\$397	\$397	7	\$1,911	\$2,007	\$1,911
8	\$461	\$461	\$461	8	\$394	\$394	\$394	8	\$1,898	\$1,993	\$1,898
9	\$457	\$457	\$457	9	\$391	\$391	\$391	9	\$1,885	\$1,979	\$1,885
10	\$453	\$453	\$453	10	\$387	\$387	\$387	10	\$1,871	\$1,965	\$1,871
11	\$449	\$449	\$449	11	\$384	\$384	\$384	11	\$1,858	\$1,951	\$1,858
12	\$445	\$445	\$445	12	\$381	\$381	\$381	12	\$1,845	\$1,937	\$1,845
13	\$441	\$441	\$441	13	\$377	\$377	\$377	13	\$1,832	\$1,923	\$1,832
14	\$437	\$437	\$437	14	\$374	\$374	\$374	14	\$1,818	\$1,909	\$1,818
15	\$433	\$433	\$433	15	\$371	\$371	\$371	15	\$1,805	\$1,895	\$1,805
16	\$429	\$429	\$429	16	\$367	\$367	\$367	16	\$1,792	\$1,881	\$1,792
17	\$426	\$426	\$426	17	\$364	\$364	\$364	17	\$1,778	\$1,867	\$1,778
18	\$422	\$422	\$422	18	\$361	\$361	\$361	18	\$1,765	\$1,853	\$1,765
19	\$418	\$418	\$418	19	\$357	\$357	\$357	19	\$1,752	\$1,839	\$1,752
20	\$414	\$414	\$414	20	\$354	\$354	\$354	20	\$1,739	\$1,826	\$1,739
21	\$410	\$410	\$410	21	\$351	\$351	\$351	21	\$1,725	\$1,812	\$1,725
22	\$406	\$406	\$406	22	\$347	\$347	\$347	22	\$1,712	\$1,798	\$1,712
23	\$402	\$402	\$402	23	\$344	\$344	\$344	23	\$1,699	\$1,784	\$1,699
24	\$398	\$398	\$398	24	\$341	\$341	\$341	24	\$1,686	\$1,770	\$1,686
25	\$394	-\$158	-\$158	25	\$337	-\$215	-\$215	25	\$1,672	\$1,204	\$1,120
								26	\$1,659	\$1,742	\$1,659
								27	\$1,646	\$1,728	\$1,646
								28	\$1,632	\$1,714	\$1,632
								29	\$1,619	\$1,700	\$1,619
								30	\$1,606	\$1,686	\$1,606
Total	\$ 11,029	\$10,477	\$ 10,477	Total	\$ 9,433	\$8,881	\$ 8,881	Total	\$ 53,950	\$56,096	\$ 53,398
	Cost of Electricity (\$/kWh) \$ 0.1319				Cost of Electricity (\$/kWh) \$ 0.1319				Cost of Electricity (\$/kWh) \$ 0.3734		

Table 22: Results of comparing actual to predicted for Days 1-50

Results	CMN Actual Energy Produced (kWh)	PVSysCo Default (kWh)	PVSysCo Adjusted (kWh)	PVWatts Default (kWh)	PVWatts Adjusted (kWh)
Total (kWh)	695.25	724.99	721.98	599.01	730.43
Avg (kWh/day)	13.91	14.5	14.44	11.98	14.61
MSE	n/a	22.79	21.96	30.1	27.34

Once the actual data was collected, the energy generation performance was estimated using default values, for both PVSysCo and PVWatts, applying a system location of Green Bay and system size of 3.0kW. The PVSysCo default resulted in a total of 724.99 kWh and an average daily energy generation of 14.51 kWh/day. The PVWatts default resulted in a total of 599.01 kWh and an average daily energy generation of 11.98 kWh/day, the furthest value from the actual CMN daily average.

Next, the PVSysCo adjusted value was estimated by adjusting the (1) albedo value to 0.35, to account for the new galvanized steel roof and to account for snowfall in April, (2) temperature coefficient to account for the lower value of $-0.45\%/^{\circ}\text{C}$, (3) monthly shading derate to account for the changing values due to sun position in the months of April, May, and June, (4) fixed tilt value to 26 degrees, (5) inverter efficiency value to the microinverter CEC rating of 0.965, and (6) the mismatch derate to 100% to account for limited losses because of the microinverters. The PVSysCo adjusted resulted in a total of 721.98 kWh and the average daily energy generation was 14.44 kWh/day, the closest value to the actual CMN daily average.

Finally, the PVWatts adjusted value was estimated by adjusting the (1) fixed tilt to 26 degrees, (2) inverter efficiency derate to 0.965, and (3) shading derate of 0.933. Furthermore, in an attempt to correctly compare PVSysCo to PVWatt, the PVWatt derate values of mismatch, diodes and connections, soiling, and system availability were respectively set to 0.995, 0.997, 0.995, and 0.995 (the max value allowed). The overall derate factor was 0.857, resulting in a PVWatts adjusted total of 730.43 kWh and the average daily energy generation was 14.61 kWh/day.

Table 23: Data comparison for Days 1-25

Day	Date	CMN Actual Energy Produced (kWh)	PVSysCo Default (kWh)	PVSysCo Adjusted (kWh)	PVWatts Default (kWh)	PVWatts Adjusted (kWh)
1	4/25/2014	12.74	13.85	12.23	15.84	18.19
2	4/26/2014	13.44	14.01	12.43	16.03	18.55
3	4/27/2014	4.62	12.9	11.52	14.87	17.27
4	4/28/2014	4.86	10.47	9.34	12.39	14.38
5	4/29/2014	3.17	6.41	5.84	6.8	8.46
6	4/30/2014	5.14	5.03	4.62	5.17	6.53
7	5/1/2014	6.82	6.59	5.94	7.29	8.65
8	5/2/2014	6.69	9.63	9.61	7.5	9.17
9	5/3/2014	13.87	12.8	12.7	10.17	12.17
10	5/4/2014	21.17	13.89	13.88	11.33	13.61
11	5/5/2014	11.82	17.75	17.41	14.61	17.15
12	5/6/2014	19.77	16.95	16.74	13.98	16.41
13	5/7/2014	5.46	8.45	8.57	6.19	7.88
14	5/8/2014	8.21	18.6	18.44	14.95	17.74
15	5/9/2014	11.2	8.68	8.73	6.61	8.13
16	5/10/2014	20.87	14.55	14.53	11.83	14.24
17	5/11/2014	13.11	11.15	11.31	8.66	10.79
18	5/12/2014	3.35	13.81	13.75	11.05	13.44
19	5/13/2014	10.83	14.07	14.07	11.46	13.96
20	5/14/2014	17.19	17.48	17.38	13.99	16.83
21	5/15/2014	9.24	16.72	16.74	13.5	16.3
22	5/16/2014	11	16.51	16.53	13.51	16.3
23	5/17/2014	14.74	18.08	18.14	14.7	17.7
24	5/18/2014	14.78	9.27	9.07	6.8	8.67
25	5/19/2014	11.35	8.56	8.47	6.25	7.95

Table 24: Data comparison for Days 26-50

Day	Date	CMN Actual Energy Produced (kWh)	PVSysCo Default (kWh)	PVSysCo Adjusted (kWh)	PVWatts Default (kWh)	PVWatts Adjusted (kWh)
26	5/20/2014	11.7	17.73	17.73	14.67	17.53
27	5/21/2014	20.38	18.11	18.05	14.61	17.68
28	5/22/2014	13.14	9.68	9.94	7.24	9.21
29	5/23/2014	20.38	20.63	20.8	16.29	19.98
30	5/24/2014	20.84	14.91	15.38	11.88	14.94
31	5/25/2014	20.86	19.03	19.16	15.08	18.43
32	5/26/2014	14.76	20.15	20.28	16.1	19.71
33	5/27/2014	13.43	11.64	11.96	9.16	11.55
34	5/28/2014	17.23	15.34	15.49	12.35	15.09
35	5/29/2014	20.83	19.74	20.2	15.45	19.23
36	5/30/2014	20.37	19.8	20.1	15.63	19.22
37	5/31/2014	20.57	18.33	18.56	14.55	17.82
38	6/1/2014	9.11	14.25	14.45	11.47	13.91
39	6/2/2014	9.98	16.62	16.69	13.29	16.35
40	6/3/2014	16.4	17.13	17.26	13.72	16.78
41	6/4/2014	20.29	16.46	16.67	13.27	16.27
42	6/5/2014	16.55	19.6	19.8	15.62	19.31
43	6/6/2014	12.73	8.23	8.38	5.97	7.65
44	6/7/2014	11.53	17.96	18.32	14.34	17.89
45	6/8/2014	21.33	19.68	20.1	15.41	19.32
46	6/9/2014	18.52	18.15	18.39	14.4	17.87
47	6/10/2014	15.14	10.52	10.8	7.73	10.15
48	6/11/2014	16.11	21.29	21.59	16.77	20.9
49	6/12/2014	15.96	15.14	15.28	12.19	15.04
50	6/13/2014	21.18	8.67	8.65	6.33	8.12

Chapter 6

6.0 Conclusion

This chapter concludes with research contributions, research limitations and recommendations for future research.

6.1 Contributions

The research and development of PVSysCo, a novel PV performance and evaluation decision support system, is important for several reasons. First, dependency upon energy resources (primarily non-renewable energy sources) has created global challenges related to climate change, wars over energy supplies, famine, poverty, and cycles of deforestation concerns (Bradford 2006), thus making solar energy a top priority in the U.S. and many other countries. Second, in 2010, the U.S. Department of Energy announced the SunShot Initiative, which aims to reduce the total installation cost of solar technologies by 75% between 2010 and 2020. This dissertation research focused on creating a model to better understand the performance and reliability of photovoltaic (PV) energy systems over time. The resulting decision support system, PVSysCo, can be used to analyze, predict, and evaluate the performance of PV systems, and thus, cost and savings implications over time. Third, PVSysCo, fitted with an elaborate Graphic User Interface, overcomes several limitations of current evaluation tools, identified in Table 2, and reiterated in Table 25.

PVSysCo allows for multiple system configurations, offers a monthly derate option with enhanced defaults and more detailed recommendations. The tool considers

degradation from a systems perspective, allows entry of panel specific characteristics including cell type and temperature coefficient. It allows monthly albedo coefficient inputs for varying reflective surface types (in front of the panel), provides model adjustments based upon inverter selection and has the capability to view and compare up to 3 different PV system options all at one time and on one screen. Using PVSysCo, accurate estimates of actual cash value taking into consideration replacement of PV system components and component degradation based on warranty and age can be obtained.

Table 25: Limitations of current PV performance and evaluation tools

Limitation	Performance and Evaluation Tool								
	[1]	[2]	[3]	[4]	[5]	[6]	[7]	[8]	[9]
System Configuration								Gray	Black
Monthly Derate Factor	Gray	Gray	Gray	Gray	Gray	Gray	Gray	Gray	Black
Annual Degradation by Component	Gray	Gray	White	Gray	Gray	Gray	Gray	Gray	Black
PV Module Selection	Gray	Gray	White	White	White	White	Black	Black	Black
Cylindrical Panel Performance	White	White	White	White	White	White	White	White	Black
Albedo Coefficient	White	White	White	White	White	White	Gray	Gray	Black
Inverter Selection	White	White	Gray	White	White	White	Gray	Gray	Black
Project Comparison	White	White	White	White	White	White	Gray	White	Black
Various Valuation Techniques	White	White	White	White	White	Gray	Gray	Gray	Black
<p>Note (1): [1] 5-Parameter Array Performance Model, [2] Sandia Array Performance Model, [3] Sandia Inverter Performance Model, [4] PVWatts, [5] Solar Estimate, [6] PV Value, [7] Solar Advisor Model, [8] RETScreen Photovoltaic Project Model, and [9] PVSysCo</p> <p>Note (2): Black = Full coverage, Gray = Partial coverage, White = No coverage</p>									

6.1.1 Contribution 1: System Configuration

In general, there are two main types of PV systems, systems that are tied to the utility grid and systems that are not tied to the grid. Off-grid systems can function regardless of whether the utility grid is up and running. However, grid-tied systems can only function when the grid is up and running, due to anti-islanding policies. The PVSysCo application provides the opportunity to include system components depending upon system configuration. For example, an off-grid DC direct system only has 1 major component: PV array. Thus, the system efficiency will be calculated differently in comparison to a grid-tied battery system, which will have 3 major components: PV array, inverter, and battery.

The laws of system efficiency indicate that an increase in individual system components is likely to lower overall system performance. Similarly, a decrease in individual system components is likely to improve overall system performance. As such, it is important to consider the type of PV system configuration because the quantity of components will increase the probability of system degradation or likelihood of a system failure.

6.1.2 Contribution 2: Monthly Derate Factor

Current PV system performance tools make an effort in considering system inefficiencies by providing the derate factor parameter. However, there is limited information about the range values or recommendations on how the value should be assigned. Furthermore, the derate factor lacks an overall systems perspective. Finally, the derate factor considers the potential of shading, soil, and snow, yet, it does not allow for

monthly changes. For example, shading varies depending on time of year, due to the position of the sun. Additionally, snow and other potential soiling also varies depending on time of year. The PVSysCo application accounts for these deficiencies by offering a monthly derate option with enhanced defaults and more detailed recommendations.

6.1.3 Contribution 3: Annual Degradation by Component

The PV systems overall efficiency refers to the reliability of the solar technology over time, taking into consideration the degradation associated with the module and system components over their service time. Stability, or degradation, of solar energy technologies is extremely complex due to the large quantity of components and variety of system configurations. Failures can occur at different levels of analysis, including system, array, panel, module, or cell levels, and, furthermore, the degree (or probability) of a failure depends on the type of solar material used and the environmental conditions.

Many PV system performance tools make reference to the derate factor of Age, however, Age is considered constant for all system components, which is rarely the case. PVSysCo considers degradation from a systems perspective, considering the potential degradation factors associated with all system components.

6.1.4 Contribution 4: PV Module Specific Characteristics

There are many different types of PV modules available on the market including crystalline silicon based modules and thin-film modules (see Figure 13). Crystalline silicon modules include mono-crystalline silicon and poly-crystalline silicon; thin-film modules include amorphous silicon, cadmium telluride, and copper indium gallium selenide.

In general, advantages of crystalline silicon technologies (in comparison to thin-film) include higher conversion efficiency, established longevity, robustness, and maturity. On the other hand, Thin-Film technologies have a superior temperature coefficient, meaning that they hold up better under warmer temperatures. Also, the different Thin-Film materials allow them to be lightweight, versatile, and flexible. For example, a-Si is what is used for solar powered calculators. Lastly, thin-film PVs have better shade tolerance, meaning that they are less sensitive to shade received from buildings, trees, or cloud coverage.

Setting aside the type of materials, specific module performance attributes vary depending upon model and manufacturer (even when using the same type of material). These module specific characteristics include conversion efficiency, temperature coefficient, power tolerance, and panel type.

Many PV system performance tools only consider crystalline silicon PV modules and make assumptions about these specific module characteristics. However, it is important for a PV performance tool to go beyond one type of PV technology, to increase inclusiveness to market available thin-film modules. More importantly, a PV performance tool should allow the user to modify performance parameters such as efficiency, temperature coefficient, power tolerance, and panel type to gain an understanding of how the PV module affects the overall system performance. PVSysCo overcomes this limitation by allowing specific input of these characteristics to show how these straightforward, individualized module parameters can greatly influence energy generation.

6.1.5 Contribution 5: Albedo Coefficient

The albedo coefficient is the portion of Global Horizontal Radiation reflected by the ground, or surface, in front of a tilted PV array. Similar to PV module-specific characteristics, mentioned above, many PV system performance tools make assumptions about the albedo coefficient. PVSysCo overcomes this limitation by allow monthly inputs for the albedo coefficient, depending on the surface type in front of the array.

6.1.6 Contribution 6: Inverter Selection

The purpose of the inverter is to convert DC electricity, generated by the PV array, into AC electricity required by the utility grid and most household appliances. Inverters can be used in both off-grid and utility grid-tied configurations, however, the requirements for grid-direct inverters are more stringent due to safety concerns for if and when the grid shuts down. Grid-tied inverters must be equipped with anti-islanding protection, an automatic shut-off for when the grid goes down, and ultimately preventing utility lineman from being electrocuted by a distributed generation source. There are two general types of inverters use in PV systems, which include string or central inverters, and microinverters.

Taking into consideration overall PV system efficiency, the central inverter is likely to produce differing operating efficiencies in comparison to its more expensive counterpart, the microinverter. First, with respect to shading, a string inverter allows shading on one module to impact the output for all modules. However, a microinverter limits the effects of shading to the specific module. Second, if a central inverter fails, the entire system goes down, however, if a microinverter fails, only that particular portion of the system goes down. Third, microinverters are sensitive to temperature and as such, the

operating temperature increases when the microinverter is mounted underneath the PV array leading to lower efficiency and life span.

Many PV system performance tools were developed based on the traditional central inverter technology. However, PVSysCo overcomes this deficiency by allowing for inverter selection and corresponding model adjustments based on the type of inverter used.

6.1.7 Contribution 7: Comparison

Research and comparison is an important requirement of any purchasing decision, especially for long-term investing in solar energy. Unlike current PV system performance tools, PVSysCo has the capability to view 3 different PV system options all at one time and on one screen. This capability allows ease in understanding the potential difference, for example, in deciding to place solar panels on your primary residence in Chicago, IL, versus the lake house in northern Wisconsin versus the summer home in Aspen, CO; in deciding to place solar panels on the garage roof with a 35 degree tilt versus the house roof with a 45 degree tilt versus the shed with a 25 degree tilt; in deciding to purchase flat-plate panels versus cylindrical-plate panels; or in understanding the potential impact of any input factors related to the performance of the PV system installation.

6.1.8 Contribution 8: Differing Valuation Techniques

Accurate insurance and appraisal evaluation is important for homebuyers to correctly assess the value of the PV system in the event of an unexpected natural disaster. Two important valuation techniques include replacement value (current cost to replace the original PV system) and actual cash value (which takes into consideration

depreciation and degradation). Unlike current PV system performance tools, PVSysCo has the capability to estimate actual cash value, taking into consideration AC energy value, the potential replacement of PV system components, and component degradation based on warranty standards and age.

6.2 Assumptions and Limitations of Research

The PVSysCo model has many contributions, however, with this follows various research limitations. First, due to data accessible through Argonne National Laboratory, the PVSysCo model is inclusive of several PV technologies including crystalline silicon (mono-crystalline silicon and poly-crystalline silicon) and thin-film (amorphous silicon, cadmium telluride, and copper indium gallium selenide), however, there are some emerging technologies (organic and dye-sensitized solar cells) that were not considered in this research. Second, PV performance models use historical weather and solar irradiance data, assuming that the past is a reliable prediction for the future. This is commonly done through the use of Typical Meteorological Data (TMY), which enables the determination of typical weather patterns. However, this provides a limitation for better solar predictions during extreme weather and natural disasters, which could potentially result in extended utility downtime (and thus, PV system downtime). Furthermore, TMY data does not consider the impacts of climate change, which can greatly impact energy consumption, load combinations, and heating/cooling peak loads in both residential and commercial buildings (U.S. Department of Energy 2008). Third, the actual cash value assumes an inverter replacement value of \$184/kW (pv.energytrend.com 05/24/2014), however, inverter prices continue to decrease and vary

depending on location and economies of scale. Thus, to overcome this potential future limitation, it is recommended to update this value regularly.

6.3 Future Research

PV technology is still emerging and there is still a wealth of uncertainties, growth opportunities, and future research related to this viable renewable energy technology. First, future research will incorporate the hourly analysis of inverter efficiency. Inverter research has shown that as power output increases, inverters become more efficient (Ransome and Funtan 2005; Notton, Lazarov et al. 2010), thus it would be beneficial to incorporate the hourly changes into the PV system performance model. Second, future research will incorporate the performance and valuation of currently manufactured thin-film PV technologies and the verification of other emerging PV technologies including organic and dye-sensitized solar cells. Third, future research will require performance studies related to other solar technology, outside of photovoltaics (PV), such as solar thermal energy and concentrated solar power. Fourth, future research would benefit from better understanding the needs and abilities of potential performance and valuation tool users, such as home appraisers, realtors, insurance underwriters, solar contractors and utility companies.

Chapter 7

7.0 References

- Aleo Solar AG (2011). Solar Module Aleo S_18 ULR, Power Classes: 225, 230, 235W.
- Andrews, R. W. and J. M. Pearce (2013). "The effect of spectral albedo on amorphous silicon and crystalline silicon solar photovoltaic device performance." *Solar Energy* 91(0): 233-241.
- Austech Forums. (Jan 2008). "Solar Installations." from www.austech.info/home-energy-improvements/21589-solar-installations-2.html.
- Bartholomew County REMC. (Obtained 07/01/2013). "Time-of-Use Rates." from <http://www.bcremc.com/tou/>.
- Beazley, D. M. (2009). *Python Essential Reference*, 4th Edition, Addison-Wesley.
- Bosco, N. (2010). *Reliability Concerns Associated with PV Technologies*, National Renewable Energy Laboratory.
- Bradford, T. (2006). *Solar Revolution: The Economic Transformation of the Global Energy Industry*, SPI Publisher Services.
- Brennan, M. P., A. L. Abramase, et al. (2014). "Effects of spectral albedo on solar photovoltaic devices." *Solar Energy Materials and Solar Cells* 124(0): 111-116.
- Browning, A. (2011). "Finding PV's Next Big Cost Reductions " renewableEnergyWorld.com.
- California Energy Commission (2001). *A Guide to Photovoltaic (PV) System Design and Installation*. E. Engineering.

- Carus, F. (2013). "PV module costs to fall to 36c per watt by 2017: GTM Research." PV Tech.
- Clean Energy Decision Support Centre (2004). Clean Energy Project Analysis: RETScreen Engineering and Cases Textbook, Natural Resources Canada.
- Clean Energy Decision Support Centre (2005). RETScreen Software Online User Manual Photovoltaic Project Model, Natural Resources Canada.
- CPS Solar (Retrieved 07/01/14). "Comparison: Centralized Inverter System and Micro-Inverter."
- Curthoys, A. (2012). Solar Energy Generation Potential of Tompkins County.
- DeSoto, Klein, et al. (2006). "Improvement and Validation of a Model for Photovoltaic Array Performance." Solar Energy 80(1): 71-80.
- Duluk, S., H. Nelson, et al. (2013). Comparison of Solar Evaluation Tools: From Learning to Practice, University of Oregon.
- Enecsys Micro Inverters. (Retrieved 06/28/2013). "Micro inverter technology." from <http://www.enecsys.com/products/micro-inverter-technology/#!prettyPhoto>.
- Energy Matters LLC (2009). Solar and Wind Estimator Assumptions and System Sizing Result Comparisons, Solar-Estimate.org.
- Faiman (2008). "Assessing the outdoor operating temperature of photovoltaic modules." Progress in Photovoltaics 16(4): 307-315.
- Garcia, M. C. A. and J. L. Balenzategui (2004). "Estimation of photovoltaic module yearly temperature and performance based on Nominal Operation Cell Temperature calculations." Renewable Energy.

- Green Alchemy. (Retrieved 07/06/2013). "Green Alchemy Farm Solar Power." from <http://greenalchemyfarm.com/solar.asp>.
- Hall, Prairie, et al. (1978). Generation of Typical Meteorological Years for 26 SOLMET Stations. SAND78-1601, Albuquerque, NM: Sandia National Laboratories.
- Hesmondhalgh, S., W. Zarakas, et al. (2012). Approaches to setting electric distribution reliability standards and outcomes.
- Home Power. (2013). "Tracker Types & Features." from <http://www.homepower.com/tracker-types-features>.
- Honsberg, C. and S. Bowden. (Obtained 01/21/2014). "Solar Radiation on a Tilted Surface." <http://pveducation.org/pvcdrom/properties-of-sunlight/solar-radiation-on-tilted-surface>.
- Hren, R. (2011). "Understanding PV Module Specifications." Home Power.
- Infinigi Infinite Energy Solutions. (2013). "Wattsun AZ-225 Solar Tracker for 12 Kyocera 200 Modules." from <http://www.infinigi.com/wattsun-az225-solar-tracker-for-12-kyocera-200-modules-p-2389.html>.
- Jordan, D. C., R. M. Smith, et al. (2010). Outdoor PV degradation comparison. Photovoltaic Specialists Conference (PVSC), 2010 35th IEEE.
- Juda, C. (2013). "5 Ways to Track Your Solar Tracker." from <http://blog.pepperl-fuchs.us/blog/bid/253098/5-Ways-to-Track-Your-Solar-Tracker>.
- King, Boyson, et al. (2004). Photovoltaic Array Performance Model, Sandia National Laboratories: Albuquerque, New Mexico.
- King, Gonzalez, et al. (2007). Performance Model for Grid-Connected Photovoltaic Inverters, SAND2007-5036, Sandia National Laboratories, Albuquerque, NM.

- Klise, Johnson, et al. (2013). "Valuation of Solar Photovoltaic Systems Using a Discounted Cash Flow Approach." *The Appraisal Journal*.
- Koshel, Smestad, et al. (2012). *Cylindrical and Flat Solar Collector Geometry Theory and Experiment*. OSA Solar 2012 - Eindhoven, The Netherlands.
- Loutzenhiser, Manz, et al. (2007). "Empirical validation of models to compute solar irradiance on inclined surfaces for building energy simulation." *Solar Energy* 81: 254-267.
- Marion and Urban (1995). *Users Manual for TMY2s Typical Meteorological Years*, National Renewable Energy Laboratory.
- Meeus, J. (1991). *Astronomical Algorithms*, Willmann-Bell.
- Mehos and Mooney (2005). *Performance and Cost Model for Solar Energy Technologies in Support of the Systems-Driven Approach*, NREL/CP-550-37085, National Renewable Energy Laboratory, Golden, CO.
- Mermoud, A. and B. Wittmer (2014). *PVSYST User's Manual PVSYST6*.
- National Renewable Energy Laboratory (2014). *System Advisor Model (SAM) Help System, Version 2014.1.14*.
- Notton, G., V. Lazarov, et al. (2010). "Optimal sizing of a grid-connected PV system for various PV module technologies and inclinations, inverter efficiency characteristics and locations." *Renewable Energy* 35(2): 541-554.
- Osterwald, C. R. and T. J. McMahon (2009). "History of accelerated and qualification testing of terrestrial photovoltaic modules: A literature review." *Progress in Photovoltaics: Research and Applications* 17(1): 11-33.

- Perez, Ineichen, et al. (1990). "Modeling daylight availability and irradiance components from direct and global irradiance." *Solar Energy* 44(5): 271-289.
- Perez, Seals, et al. (1987). "A new simplified version of the Perez diffuse irradiance model for tilted surfaces." *Solar Energy* 39(3): 221-232.
- Pham, H. (2003). *Handbook of Reliability Engineering*, Springer.
- PV Powered (2009). PVP1100 to PVP5200 String Inverters: Proven Reliability - Now With an Integrated AC and DC PV System Disconnect Listed to the UL 98 Standard.
- pv.energytrend.com. (05/24/2014). "Price Quotes - Energy Trend PV."
- Ransome and Funtan (2005). Why hourly averaged measurement data is insufficient to model PV system performance accurately. Twentieth European PVSEC, Barcelona.
- Ristow, Begovic, et al. (2008). "Development of a Methodology for Improving Photovoltaic Inverter Reliability." *IEEE Transactions on Industrial Electronics* 5(7).
- Rhouma, W. M., I. M. Molokhia, et al. (2007). "Comparative study of different PV modules configuration reliability." *Desalination* 209(1-3): 122-128.
- RS Components (2005). *Solar Panels Data Sheet*.
- Schwartz, J. (2002). *Go Configure: Configuring Your PV Array*. Home Power. 87, February/March.
- Schwartz, J., I. Woofenden, et al. (2013). "DIY or Pro? Practical Advice for Homeowners." *Home Power*.

- Shahan, Z. (2013). "Solar PV Module Prices Have Fallen 80% Since 2008, Wind Turbines 29%." Clean Technica.
- SNE Research (2009). "Global PV Market Perspective." Markest Insight.
- Solar Energy International (2013). Solar Electric Handbook: Photovoltaic Fundamentals and Applications, Pearson Learning Solutions.
- solarenergyfallacies.com (Retrieved 06/28/2013). "Solar Energy Fallacies: Misunderstood Facts and Economic Realities."
- SolarWorld. (Obtained 06/27/2013). "Roof mount multicrystalline photovoltaic solar panel." from <http://www.directindustry.com/prod/solarworld-ag/roof-mount-multicrystalline-photovoltaic-solar-panels-54786-441838.html>.
- TamizhMani, G., L. Ji, et al. (2003). Photovoltaic Module Thermal/Wind Performance: Long-term Monitoring and Model Development for Energy Rating. NCPV and Solar Program Review Meeting 2003.
- Ton and Bower (2005). Summary report on the DOE high-tech inverter workshop, U.S. Department of Energy . [Online]. Available: http://www1.eere.energy.gov/solar/pdfs/inverter_II_workshop.pdf.
- U.S. Department of Energy (2008). Climate Change Impacts on Residential and Commerical Loads in the Western U.S. Grid, PACIFIC NORTHWEST NATIONAL LABORATORY.
- U.S. Department of Energy: Energy Efficiency & Renewable Energy. (Last Updated 06/18/2013). "Photovoltaic System Configurations." from http://www1.eere.energy.gov/tribalenergy/guide/pv_configs.html.

U.S. Energy Information Administration (2011). 2010 Annual Review, Table 10.1 Renewable Energy Production and Consumption by Primary Energy Source, 1949-2010.

U.S. Energy Information Administration (2012). "U.S. Energy Consumption by Energy Source (Preliminary 2011 Data)." Monthly Energy Review March 2012.

Vazquez, M. and I. Rey-Stolle (2008). "Photovoltaic Module Reliability Model Based on Field Degradation Studies." Progress in Photovoltaics: Research and Applications 16: 419-433.

Wilcox, S. and W. Marion (2008). Users Manual for TMY3 Data Sets, Technical Report NREL/TP-581-43156, National Renewable Energy Laboratory.

www.powertripenergy.com. "Power Trip Energy Corp." from <http://www.powertripenergy.com/Projects-2006.htm>.

www.powertripenergy.com. (2006). "Power Trip Energy Corp." from <http://www.powertripenergy.com/Projects-2006.htm>.

Ye, Z., R. Walling, et al. (2004). Study and development of anti-islanding control for grid-connected inverters, National Renewable Energy Laboratory.

Zielnik, A. (2009). PV Durability and Reliability Issues. Photovoltaics World Magazine. Nov/Dec, Vol 1, Iss 5.

CURRICULUM VITAE

Lisa Bosman

Place of birth: Wisconsin

Education

B.S., Milwaukee School of Engineering, May 2003

Major: Industrial Engineering

M.S., Clemson University, December 2007

Major: Industrial Engineering

Dissertation Title: A Decision Support System to Analyze, Predict, and Evaluate Solar Energy System Performance: PVSysCo (Photovoltaic System Comparison)

Affiliations:

Institute of Industrial Engineers (IIE)

Institute for Operations Research and the Management Sciences (INFORMS)

Teaching Experience:

University of Wisconsin-Milwaukee (Intro to Engineering, Intro to AutoCAD)

College of Menominee Nation (Intro to Engineering, Statistics, Trig/Pre-Calc)

Milwaukee School of Engineering (Lean Manufacturing)

Clemson University (Statistics, Management Information Systems)

Research Experience:

2014-2017 NASA Innovations in Climate Education (NICE) Grant; National Aeronautics and Space Administration (NASA). \$413,423

2014-2015 AIHEC/TCU Stem Student Success Collaborative Project; National Science Foundation (NSF). \$23,000

2013-2014 National Partnership for Environmental Technology Education (PETE) Mini-Grant; National Science Foundation (NSF). \$3,000

2013-2014 Tribal ecoAmbassador Grant; Environmental Protection Agency. \$60,000

2011-2012 Growing Tribal Climate Change Education Leaders; National Council for Science and the Environment (NCSE), the Council of Environmental Deans and Directors, (CEDD) and the American Indian Higher Education Consortium (AIHEC). \$10,000

Awards and Honors:

2014 IIE Annual Doctoral Research Colloquium Poster Competition. 3rd Place

2014 Mellon TCU Faculty Career Enhancement Fellowship; Mellon Foundation. \$40,000

2013 Blanchard Pre-Dissertation Faculty Grant; American Indian College Fund. \$3,000

2012 Blanchard Pre-Dissertation Faculty Grant; American Indian College Fund. \$2,500

Publications:

- Henry, R. and L.B. Bosman. 2013. "Strategic Management and Social Media: An Empirical Analysis of Electronic Social Capital and Online Fundraising," Book Chapter in "Social Media and Management"
- Bosman, L.B. and T. Zagenczyk 2011. "Revitalize Your Teaching: Creative Approaches to Apply Social Media in the Classroom," Book Chapter in "Social Media Tools and Platforms in Learning Environments: Present and Future"

Presentations:

- Bosman, L. and W. Otieno. "PVSysCo: PV System Comparison of Solar Energy System Performance and Evaluation," Industrial and Systems Engineering Research Conference, Montreal, Canada, May 2014
- Bosman, L. and W. Otieno. "College of Menominee Nation: Solar Energy Initiative," Council of Energy Research and Education Leaders Conference, Argonne National Laboratory, November 2013
- Bosman, L., W. Otieno, S. Darling, E. Forsyth. "Comparative Investigation of Solar Module Performance for the Midwest Market," Industrial and Systems Engineering Research Conference, San Juan, Puerto Rico, May 2013
- Bosman, L. and W. VanLopik. "Shifting Seasons: Tribal Communities Fostering Resilience to Climate Change," Association for Environmental Studies and Sciences, Santa Clara, CA, June 2012
- Bosman, L. and W. VanLopik. "Integrating Climate Change into the Tribal College Curriculum - Case of the College of Menominee Nation" Council for Environmental Deans and Directors, San Jose, CA, June 2012
- Bosman, L. and W. VanLopik. "Climate Change and Tribal Colleges" A webinar presentation for www.CAMELClimateChange.org, May 2012
- Bosman, L. and W. Otieno. "A framework to Model the Performance and therefore Reliability of Dye-Sensitized Solar Cells," Industrial and Systems Engineering Research Conference, Orlando, FL, May 2012

Industry Experience:

- Oshkosh Corporation, Contract Industrial Engineer
- Deere & Company, Industrial Engineer
- Harley-Davidson Motor Company, Manufacturing Engineer
- Plastics Engineering Company, Intern Industrial Engineer